# The role of telomeric DNA damage, mitochondria biogenesis and mTOR signalling in cellular senescence

FRANCISCO MARQUES

Thesis submitted to Newcastle University for the degree of Doctor of Philosophy

Institute for Cell & Molecular Biosciences

Newcastle University Institute for Ageing

School of Biomedical Sciences

Faculty of Medical Sciences

Newcastle University

Newcastle-upon-Tyne - the United Kingdom

November 2014

Supervisor: Dr. João Passos

*“O que hoje não sabemos, amanhã saberemos”*

Garcia de Orta, 1563

## INDEX

## FIGURES AND TABLES

## ABBREVIATION INDEX

ADP – adenosine diphosphate

APS – ammonium Persulfate

Atg5 – autophagy related gene 5

ATM – ataxia telangiectasia mutated

ATP – adenosine-5'-triphosphate

ATR – ataxia telangiectasia and Rad3 related

AU – arbitrary unit(s)

BAT – brown adipose tissue

BCA – bicinchoninic acid

BrdU – bromodeoxyuridine

CDK – cyclin-dependent kinase

CDKI – cyclin-dependent kinase inhibitors

ChIP – chromatin immuno-precipitation

COX – cytochrome c oxidase

CPD – cell population doubling

CR – caloric restriction

DAPI – 4',6-diamidino-2-phenylindole

DDF – DNA damage foci

DDR – DNA damage response

DEN – N-Nitrosodiethylamine

DHE – dihydroethidine

DHR – dihydrorhodamine 123

DMEM – Dulbecco's modified Eagle's medium

DMSO – dimethyl sulfoxide

DN – dominant-negative

DNA – deoxyribonucleic acid

DNA-SCARS – DNA segments with chromatin alteration reinforcing senescence

DNP – dinitro-phenol

DOX – doxycycline

DR – dietary restriction

DSB – double strand break

ECM – extracellular matrix

ETC – electron transport chain

FACS – fluorescence activated cell sorter

FC – fold-change

FCCP – carbonilcyanide *p*-triflouromethoxyphenylhydrazone

FCS – foetal calf serum

FISH – fluorescent *in situ* hybridisation

FSC – forward scatter

GFP – green fluorescent protein

GTP – guanosine triphosphate

GDP – guanosine diphosphate

Gy – Gray

$H_2O_2$ – hydrogen peroxide

HEK – human embryonic kidney cells

HR – homologous recombination

HSC – haematopoietic stem cells

hTERT – human telomerase reverse transcriptase (catalytic subunit)

ICC – Immunocytochemistry

IR – irradiation / irradiated

KCl – potassium chloride

KD – knockdown

KO – knockout

MAPK – mitogen-activated protein kinase

MEF – mouse embryonic fibroblasts

MitoQ – 10-(6′-ubiquinonyl) decyltriphenylphosphonium bromide

MMP – mitochondrial membrane potential

MSHE – mannitol, sucrose, HEPES-KOH, EDTA buffer

Mt – mitochondria

mtDNA mitochondrial deoxyribonucleic acid

mTOR – mammalian target of rapamycin

mTORC1 – mammalian target of rapamycin complex 1

mTORC2 – mammalian target of rapamycin complex 2

NAC – N-acetyl-L-cysteine

NAO – 10-n-nonyl-acridine orange

NCS – neocarcinostatin

NF-κB - nuclear factor of kappa light chain gene enhancer in B-cells

NHEJ – non-homologous end joining

NRF – nuclear respiratory factor

NT – non-treated

$O_2$ – oxygen

OIS – oncogene-induced senescence

OXPHOS – oxidative phosphorylation

PBGT – phosphate-buffered saline gelatin Triton X

PBN – N-tert-butyl-α-Phenylnitrone

PBS – phosphate-buffered saline

PD – population doubling

PFA – paraformaldehyde

PGC-1 – peroxisome proliferation activated receptor γ co-activator 1

PML – Promyelocytic leukemia nuclear bodies

PPAR – peroxisome proliferation activated receptor γ

PROL – proliferation/proliferating

Pyr – sodium pyruvate

RAP(A) – rapamycin

RB – retinoblastoma

RISC – Rieske iron sulphur protein

ROS – reactive oxygen species

RT-PCR – reverse transcriptase Polymerase chain reaction

s.e.m. – standard error mean

SAHF – senescence- associated heterochromatin foci

SASP – senescence-associated secretory phenotype

SA-β-Gal – senescence-associated β-galactosidase

SCR – scrambled

SD – standard deviation

SDS – sodium dodecyl sulphate

SFM – serum free medium

shRNA – short-hairpin ribonucleic acid

SIPS – stress-induced premature senescence

siRNA small interference Ribonucleic acid

SMS – senescence-messaging secretome

SOD – superoxide dismutase

SSB – single strand break

SSC – sodium chloride, sodium citrate

ssDNA – single-stranded deoxyribonucleic acid

TAF – telomere-associated foci

TBST – Tris-Buffered Saline and Tween 20 solution

TCA – tricarboxilic acid cycle

TE – Tris-EDTA buffer

TEM – transmission emission microscopy/micrograph

TEMED – Tetramethylethylenediamine

TERC/TR – RNA component of telomerase

TERT – telomerase reverse transcriptase

TIF – telomeric induced foci

TMRM – tetramethylrhodamine

TRF2 – TTAGGG repeat binding factor 2

Trolox – 6-Hydroxy-2,5,7,8-tetramethylchromane-2-carboxylic acid

UCP – uncoupling protein

UV – ultraviolet

WB – western blot

WT – wild type

## THESIS ABSTRACT

Cellular senescence is a state of enduring cell-cycle arrest characterised by a persistent DNA damage response, elevated Reactive Oxygen Species (ROS), mitochondrial dysfunction and a senescence-associated secretome. Senescence impacts *in vivo* not only by acting as a tumour suppressor mechanism but also hindering tissue repair and regeneration. Senescent cells build-up with age in many tissues from humans, baboons and mice, and clearance of senescent cells in mice has been demonstrated to ameliorate age-related pathologies.

The mTOR (mechanistic target of rapamycin) is a primeval and conserved pathway among eukaryotes. Inhibition of the mTOR pathway has been shown to extend lifespan of model organisms, to be beneficial against cancer progression and to ameliorate several age-related diseases. While reports suggest that mTOR plays a role in cellular senescence, it is still incompletely understood how it contributes to the phenotype.

Mitochondria sit on the crossroad of many cell fate decisions including apoptosis, differentiation and metabolism. Despite requirement for the aforementioned processes, the role of this organelle in cellular senescence has not been fully elucidated.

In this thesis, I describe potential mechanisms by which mTOR may impact on cellular senescence, given its roles in regulating the DNA damage response and mitochondrial homeostasis. Additionally, I inspect the role of mitochondrial biogenesis during induction and maintenance of cellular senescence. Finally, I study the impact of mTOR inhibition by rapamycin and, the effects of compromised mitochondrial biogenesis in liver senescence with age in mice.

## THESIS GRAPHICAL ABSTRACT

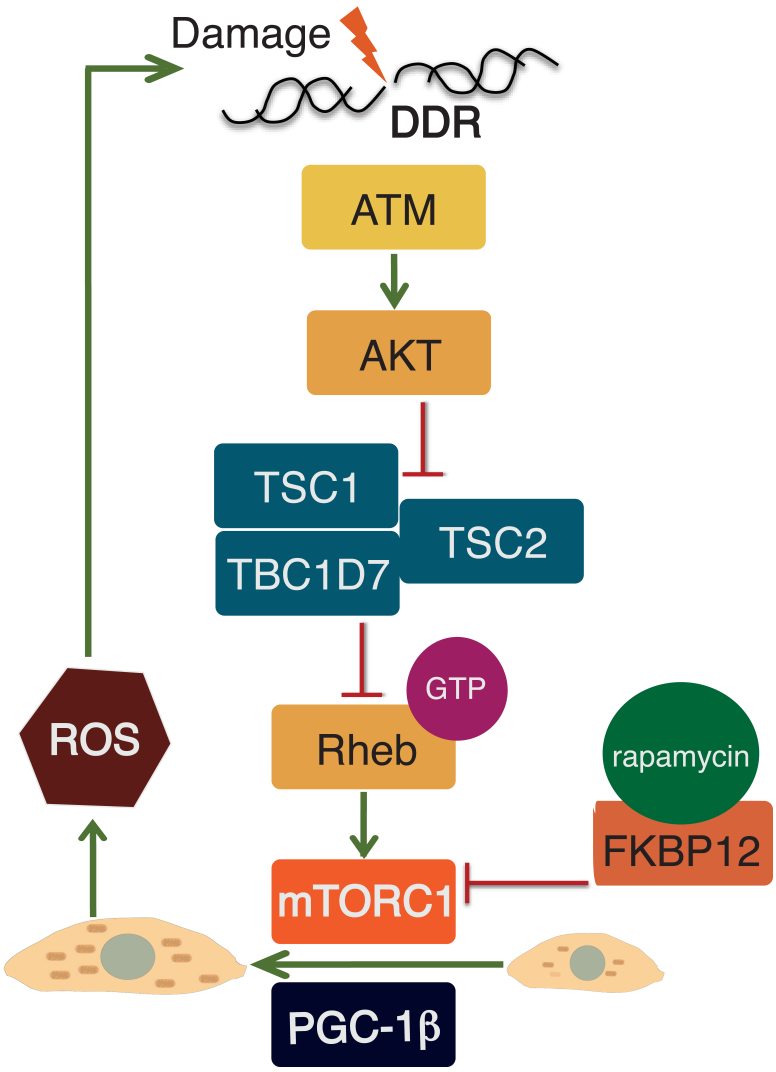

# CHAPTER 1 – INTRODUCTION

## What is cellular senescence?

Senescent cells show a long-lasting inability to resume proliferation being commonly barred at $G_1$ and $G_2$/M [1]. This enduring cell cycle arrest is caused by mutiple inducers. These incude oncogene (in)activation, tumour suppressors loss, persistant DNA and telomeric damage, chronic mitogenic signalling, chromatin changes, oxidative-, epigenetic-, nucleolar-, mitotic checkpoint- and spindle-stresses and $BRAF^{V600E}$ metabolic changes [2-7, 8{Schmidt, 2010 #51, 9-11] which limits cells' replicative capacity. Cellular senescence was first observed in 1961 by Hayflick and Moorhead [12]. They found that human fibroblasts cultured for a long time arrested after a fixed number of passages - this process was coined as replicative senescence. Senescent cells undergo multiple phenotypic changes, which are collectively known as the senescent phenotype. Although many molecular markers have been described in senescent cells, currently it is impossible to specify a universal marker to identify these cells. The difficulty to pinpoint a sole marker has to do with the fact that during the development of the senescent phenotype, markers can be expressed at different times, not being expressed at all, or are not present simultaneously. One example of this is the sequential and temporal expression of the senescent inflammatory secretome [13]. Eventually, not all cells senesce equally and there could be perhaps different types of senescence.

Phenotypically, senescent cells are morphologically and metabolically distinct from young cells and other non-proliferating cells [14, 15] and, are less prone to apoptosis [16]. Furthermore, senescent cells are hypertrophic by exhibiting increased cellular volume and a flattened cytoplasm [1]. Senescent cells are commonly believed to be insensitive to either growth factors or mitogens [17].

Senescent cells display changes in nuclear structure and increased nuclear area, loss of chromatin and altered gene expression [18, 19]. Furthermore, depending on the original senescence stimuli, some senescent cells can present nuclear inclusions namely PML (promyelocytic leukemia nuclear)

bodies, SAHF (senescence-associated heterochromatin foci) and DNA-SCARS (DNA segments with chromatin alteration reinforcing senescence) [20, 21].

Senescent fibroblasts have been shown to secrete growth factors, cytokines, extracellular matrix, and degradative enzymes, which have been collectively called the "senescence-associated secretory phenotype" (SASP) or "senescence-messaging secretome" (SMS) [22, 23]. It is believed that the main function of secreted factors is to allow inter- and intra-cellular communication. In fact, senescent cells have been shown to impact on their surrounding environment in different ways: firstly, senescent cells can induce senescence in neighbouring young cells [24, 25]; secondly, senescent cells have been shown to induce hyper-proliferation of cancer cells, neoplastic transformation and tissue damage [26, 27]; finally, this senescence secretome is able to reinforce and stabilise senescence via autocrine loops [22]. Not only secreted proteins have been shown to play a role in this cell-to-cell communication. Elevated ROS production, which is also characteristic of senescent cells, has also been implicated in paracrine senescence though gap junction-mediated cell-cell contact [24] and in the stability and re-enforcement of the senescent phenotype [28].

Below we detail how high reactive oxygen species (ROS) generation, mitochondrial dysfunction and loss of telomere homeostasis contribute together to the onset and stability of cellular senescence.

## What makes cells senescent?

### ▪ The role of telomeres in cellular senescence

Since Hayflick's discovery, the phenomenon of cellular senescence has intrigued scientists and has been the object of various studies aiming to uncover its underlying mechanisms. A major breakthrough occurred when it was theoretically suggested that telomere shortening could function as a

counter of the number of cell divisions and, ultimately contribute to replicative senescence [29, 30]. Nearly all organisms have in their chromosome ends a series of repetitive TTAGGG DNA sequences ending on a 3' protruding ssDNA 50-400 bases long overhang, called telomeres [31, 32]. Telomeres are protected by a protein-complex denominated shelterin that halts telomere recombination preventing top-to-top chromosome fusions [33]. Additionally, telomeric sequences cannot be entirely replicated mainly due to the inability of the DNA replication machinery, specifically the DNA polymerase, to synthesise in a 3'-5' direction leading to the incomplete replication of the lagging strand. This leads to a progressive loss of telomere repeats with each cell division. Only in the 1990s, it was experimentally validated that not only cell division contributed to gradual telomere shortening and was associated with cellular senescence [34] but also, that ectopic expression of telomerase (an enzyme specialised in telomere length maintenance) extended the replicative lifespan of human fibroblasts in culture [35]. Telomere shortening has been hypothesised to destabilise these telomere loops (t-loops) structures [36], thereby contributing to telomere uncapping, *i.e.* loss of the protective shelterin components.

Only recently we have begun to understand the mechanisms underlying the recognition of telomeres by cells undergoing senescence. Damaged telomeres, whether by inhibition of shelterin components or telomere shortening, activated the same DNA damage response (DDR) pathways as do double-strand breaks (DSB) [37-39]. This DDR is regarded as a core mechanism by which cells prevent replication of damaged DNA and allow enough time for its repair [40]. If the DNA damage turns out to be irreparable, then the arrest becomes permanent.

Several reports described that telomeres are sources of senescence signals whether the damage was triggered by uncapped telomeres or genotoxic stress [3, 4]. Indeed telomeres, via shelterin components, are widely known to thwart the majority of the repair pathways in order to prevent chromosomal instability [41]. Structurally, telomeres have high presence of guanines, which can be highly prone to oxidation [6, 42]. Moreover, tandem oxidative lesions have been shown to contribute to the displacement of shelterin components

(TRF1 and TRF2) from telomeres [43]. Besides telomeric shortening, recently our group has also observed that DNA damage can physically occur at long telomeres and, that these lesions seem to be irreparable [3]. We named this phenomenon - Telomere-associated foci (TAF). Based on the fact that that TAF are induced by ionising irradiation or by hydrogen peroxide, we hypothesised that oxidative stress is involved in this type of telomere dysfunction [3]. TAF are bigger and more enduring than other genomic damage, again suggesting reparability problems [3].

Mechanistically, shelterin components prevent telomeres from being recombined and to be repaired, working therefore as a barrier for genomic instability [32],[44, 45],[46, 47]. Shelterin component TRF2 stops non-homologous end-joining (NHEJ) by inhibiting ligase IV activity avoiding therefore chromosomal top-to-top fusions [44-47]. Finally, replicative senescent cells with long telomeres and still containing TRF2, have been shown to also to co-localise with DDR proteins [48].

Besides the presence of persistent DSB at telomeres, also single strand breaks (SSB) remain unrepaired for long periods of time after treatment with hydrogen peroxide at telomeres [6]. Moreover, damage at telomere regions can be a consequence of acute hyper-proliferation, replication forks stalling and aleatory completion of telomere DNA replication during the initial stages of oncogene-induced senescence (OIS) [49].

*In vivo*, DNA damage can be also observed at long telomeres in hepatocytes and in enterocytes from mice [3]. These telomere-associated damage (TAF) build-up with age in mice liver and intestine and, do not correlate with telomere length [3]. Due to its irreparability, we proposed that TAF can be a robust marker for senescence *in vivo* [3]. Indeed, TAF can qualitatively be a predictor of mean and maximum lifespan of short- and long-lived mice cohorts [50]. Other groups have shown previously that in non-proliferating baboons' skin fibroblasts and neurons, telomeres can be targets of DNA damage [3, 4, 51]. In humans, TAF are observed in melanocytes of benign- and dysplastic-*neavi*, in epithelial cells of precursor lesions to breast- and colon- cancers, but are absent in melanoma, colon- and breast carcinoma [49]. Overall this data

can pinpoint TAF as biomarkers for senescence, but not necessarily a marker for cancerous lesions. Finally, more work needs to be conducted in order to understand if only the shortest of telomeres are the sole inducers of a DDR in tissues and, which degree of telomere uncapping functions as threshold to elicit a DDR during senescence [39].

The role of telomeres as inducers of accelerated ageing has been supported by studies involving genetically modified mice. Loss of telomere integrity has been shown to impact on organismal ageing. Late generation mTERC$^{-/-}$ mice, which carry a homozygous deletion of the RNA component of telomerase, show a generation-dependent telomere shortening [52]. This mouse model of acute telomere shortening, are short-lived and present early onset of ageing traits such as stem cell exhaustion, loss of regenerative capacity, cell cycle arrest and apoptosis [53]. Moreover, ablation of p21 in mTERC-null mice rescued regenerative capacity and extended lifespan [54].

In summary, telomeres seem to be hotspots for irreparable DSB and SSB and, therefore, they may act as sentinels to oxidative damage within cells and tissues, contributing to the senescence *in vivo*.

- **Mitochondrial dysfunction via oxidative stress stimulates and reinforces senescence**

As previously stated, telomeres are more sensitive to ROS-derived damage than the rest of the genome. Consistent with this idea several studies have shown that oxidative stress can accelerate telomere shortening *in vitro*. A variety of interventions, including treatment with free radical scavengers [55], overexpression of antioxidant enzymes [56], low ambient oxygen concentrations [57, 58], and mild mitochondrial uncoupling [59] have been shown to delay telomere shortening, thereby extending the replicative lifespan of cultured cells. On the other hand, mild oxidative stress has been shown to accelerate telomere shortening and lead to premature senescence [60].

Several lines of evidence demonstrate that activation of several signalling pathways known to impact on cellular senescence can increase ROS levels in

cells. Activation of a DDR either by telomere uncapping or genotoxic stress [28], overexpression of oncogene $BRAF^{V600E}$ [10], over-expression of activated RAS [61], p53 [62], p21 [63] and p16 [64] have all been shown to result in elevated ROS generation. The use of antioxidants in the majority of those conditions has been shown to prevent or postpone senescence, suggesting an essential role for ROS in the process. Altogether, this evidence strongly supports the idea that ROS act as signalling molecules during senescence, and are not merely the outcome of time-dependent "wear-tear". Indeed, recent evidence has demonstrated that ROS are simultaneously mitogenic-hyperproliferative and DNA damaging molecules during OIS [65]. These ROS are produced via a cascade involving $H\text{-}Ras^{V12}$-Rac1-Nox4 (a NADPH oxidase) [65].

Mechanistically, the links between the DDR efector pathways (p53-p21 and p16-Rb) and ROS generation are not yet fully clear. Firstly, the p16-Rb axis has been connected with ROS production via PKCδ [64], most likely through action of this protein kinase onto NADPH oxidases [66]. New data from the Hara group puts forward a model in which both the Rb and AKT signalling activation halts mitochondrial superoxide dismutase (SOD2) expression, – enzyme responsible for transforming superoxide into hydrogen peroxide – leading to ROS accumulation [67]. Additionally, antioxidant defence enzymes activity have shown to increase in senescent fibroblasts when compared to young proliferating controls [68].

Besides an outcome of a DDR, high ROS is proposed to be a switch that maintains a stabilises the DDR during cellular senescence [28, 67]. Indeed, also down-regulation of p53 or p21 reduces ROS either in telomere-dependent and –independent senescence [28]. p21 (a cyclin-dependent kinase inhibitor responsible for the $G_1$ arrest) mediates an increase in ROS generation that damages the DNA and activates the DDR, maintaining and stabilising therefore, a positive feed-back loop that keep cells in senescence [28]. Moreover, ROS can also exert effects on the DDR by promoting activation of ataxia-telangiectasia mutated (ATM) by dimerization through an oxidised bisulfide-bond [69]. In addition, p21 has been shown to impact on the TGF-β and MAPK pathways, which have then been demonstrated to

contribute to ROS generation [28, 70, 71]. In settings of lung fibrosis, chemical inhibition of NOX4, decreased ROS, p16 and p21 levels [72]. Finally, SASP is also connected to ROS production via IL-1–TGF-β–Nox4, thus promoting senescence in a paracrine fashion [73].

Mitochondria are thought to have evolved from symbiotic α-proteobacteria. These organelles reside within cells and, one of their major function is the production of energy in ATP form [74]. Despite evidence suggesting a causal role for ROS (particularly originated from external sources) in senescence, we still do not really understand the role of intrinsic ROS levels in cellular senescence. It was proposed that the majority of cellular ROS are originated in mitochondria [75]. In cellular senescence, production of high ROS, low mitochondrial membrane potential and decreased ATP production– mitochondrial dysfunction – are key features [59, 76]. Additionally to the loss of energy levels either in oncogene- or replicative- senescence, metabolic inefficacy (activation of AMPK) and high mitochondrial ROS that oxides DNA have been observed [59, 76-79]. Also, markers of macromolecule oxidation such as protein carbonyls and lipofuscin have been shown to be present in senescent cells [80, 81].

Direct intereference on mitochondrial functions either silencing of components of the electron transport chain (ETC) (such as the Rieske iron sulphur protein (RISC)) or, by pharmacollogical inhibition of oxidative phosphorylation (using rotenone or oligomycin) promotes proliferation arrest and SA-β Gal activity [76]. Once more, this data points out a role of high ROS and ATP shortage in senescence. Chronic use of high concentrations of the uncoupler FCCP also prompts cell cycle arrest and, induces cellular senescence in primary fibroblasts via increased ROS generation and telomere dysfunction [82].

Although ROS have been extensively shown to play a role in senescence, its functions in organismal ageing are less clear with numerous conflicting results mostly obtained from animal models in which mitochondrial function, oxidative stress or the DDR have been modulated [83]. *In vivo*, mechanisms known to play a role in cellular senescence have been shown to impact on mitochondrial function and ROS generation. For instance, $p53^{-/-}$ mice show

defects on complex IV due to reduced expression of Sco2 cytochrome c oxidase assembly factor [84]. In late generation mTERC$^{-/-}$ mice, activation of p53 represses the promoters of mitochondrial biogenesis genes PGC-1α and PGC-1β, thereby reducing mitochondrial function [85]. Moreover, mTERC$^{-/-}$ mice have more oxidative damage in intestinal crypts and brain and this is dependent on p21 [28]. Another example of the relation between oxidative stress and senescence *in vivo* comes from the SOD2-null mice's skin, in which senescent cells have been shown to accumulate [86]. Finally, mice with chronic inflammation (*nfkb1* KO mice) have elevated ROS levels, which drive senescence and impair regeneration in liver and in intestinal crypts. Furthermore, the authors demonstrate that antioxidant BHA rescues cellular senescence and liver regeneration in *nfkb1* KO mice [50]. Finally, besides inflammation, cellular senescence has been associated to a metabolic syndrome with enhanced mitochondrial tricarboxylic acid (TCA) cycle usage and, in which PDK1 works as a tumour suppression mechanism perhaps via ROS increase [10].

## Mitochondria dynamics and homeostasis in cellular senescence, disease and ageing

Within organs in the human body, mitochondria exhibit distinct morphology, different fuel preferences and biosynthetic abilities. For instance, skeletal-muscle mitochondria are proficient at oxidizing fatty acids, brain mitochondria are competent for ketone oxidation, while adrenal mitochondria are prone to biosynthesize steroid hormone [87]. Despite mitochondria having organ specific adaptations, overall they share about 75% of their molecular components [88].

Regardless the existing mitochondrial heterogeneity within cells and tissues, we can identify core regulatory mechanisms such as: mitochondrial biogenesis [89, 90], mitophagy [91], fission and fusion [92], and movement [93]. Many of these processes of mitochondrial quality control have been implicated in processes such as cancer, degenerative diseases and ageing [94, 95]. Moreover, several lines of evidence suggest that disruption of this

equilibrium can contribute to cellular senescence. An example of this is the knock-down of the mitochondrial fission protein 1 (Fis1), that has been shown to induce senescence via increased ROS generation and activation of a DDR [96].

Knock-down of several core-autophagy genes (Atg7, Atg12 and LAMP2) have been shown to contribute to mitochondrial dysfunction (higher mitochondrial mass, lower mitochondrial membrane potential, and higher endogenous superoxide levels) and increased Sen-β-Gal activity [97]. Atg5 loss in macrophages, T-lymphocytes and mouse embryonic fibroblasts (MEF) leads to increased mitochondrial mass [98, 99]. Additionally, $Atg5^{-/-}$ MEF have higher mitochondrial DNA copies, higher mitochondrial superoxide levels and increased secretion of IFN-γ [98]. This data seems to be in disparity with Young *et al.*, which showed increased autophagy in OIS, that Atg5 and Atg7 silencing delayed the expression and secretion of inflammatory cytokines IL-6 and IL-8 and, decreased SA-β-Gal activity [100].

Mitochondrial biogenesis is a process by which cells maintain, increase and divide their pre-existing mitochondria. The core regulator of this process is the PGC-1 family, which comprises PGC-1α, PGC-1β and PPRC1 [101]. In a variety of cell types over-expression of PGC-1α and PGC-1β increases mitochondria biogenesis and enhances respiration, proposing that both co-activators are the limiting factors for mitochondrial gene expression program [101]. Increasing mitochondrial biogenesis via expression of PGC-1α has been shown to speed the rate at which senescence occurred in human diploid fibroblasts [102]. Additionally, higher PGC-1α expression increased in senescent fibroblasts concomitant with an increase in mitochondrial mass [103].

In a broader context, PGC-1α does not only impact on cellular senescence, but also has multiple effects in pathological settings such as renal fibrosis [104], cardiomyopathy [105], and diabetes [106]. This later study, reports that endothelial PGC-1α overexpression induced multiple diabetic phenotypes that encompassed blunted wound healing, reduced blood flow after hindlimb ischemia and aberrant re-endothelialization following carotid injury [106].

The exact role of mitochondrial biogenesis during ageing is a controversial topic [107]. Whilst Nisoli and colleagues associated the beneficial effects of caloric restriction (CR) to enhanced mitochondrial content (which shaped the concept that impaired mitochondrial biogenesis represented a loss of function during ageing)[108], more comprehensive analyses using quantitative proteomic approaches have failed to support such findings [107, 109, 110]. Lanza and co-workers have shown by large-scale proteomic analysis and whole-genome expression profiling, less mitochondrial protein synthesis under CR was coupled with improved antioxidant capacity [110].

## What is the role of cellular senescence in organismal ageing, disease and cancer?

Senescence is thought to play a role on cellular physiology within living tissues. Senescent cells increase with age in a variety of mammalian tissues [111-113] and may represent more than 15% of the cell population in aged baboons' skin [114]. Accumulation of senescent cells is also associated to age-related pathologies like osteoarthritis, atherosclerosis and diabetes [115-117].

In cancer, senescence is thought to block tumour growth *in vivo* and, antagonistically, it leads to decreased tissue regeneration and the decrease of repair mechanisms with age [118-121].

Consistent with this pleiotropic view, senescent cells can also stimulate and confer a suitable environment for cancer progression [27]. Undeniably, senescent cells are observed in mouse and human tissues in pre-malignant lesions [122], in lung adenomas, in prostatic intraepithelial neoplasia, in pancreatic intraductal neoplasia, and in melanocytic *naevi* [123-126]. However, in settings of malignant lesions – lung carcinoma, prostrate carcinomas, pancreatic ductal adenocarcinomas and melanomas – senescence is heavily abolished (perhaps suggesting that elimination of senescent cells weakens the anti-tumourigenic barriers) [124, 126, 127]. More examples of the impact of cellular senescence on pathologies was broadly revised recently [128]

Upon liver damage, hepatic stellate cells divide and secrete extracellular matrix (ECM) leading to fibrotic scar formation [129]. Sequentially, senescent stellate cells build-up a secretory response leading to pro-inflammatory molecules and matrix metalloproteinases secretion, damaging the ECM components. Inhibiting the normal activity of these senescent cells lead to the aggravation of fibrosis and liver damage, reflecting therefore the importance of senescent cells in wound-healing [129]. CCN1 (an extracellular matrix protein) induces senescence in fibroblasts – by activating ROS generation via NOX1 that culminates on activation of the DDR (p53 and p16) – limits fibrosis and resolves skin wound healing [130]. In addition, damaged hepatocytes release CCN1 that promotes HSC senescence [131]. Finally, the SASP is complex, highly context and microenvironment dependent phenomenon, that can be an example of antagonistic pleiotropy, once not all those secreted factors are pro-tumorigenic in liver [132].

Recent evidence indicates that senescent cells may be cleared by the immune system both *in vitro* and *in vivo* (for instance by natural killer cells) [129]. Immune surveillance is a mechanism that not only detects and eliminates invading pathogens, but also is able to perceive, locate and displace senescent cells within tissues due to SASP secretion [133, 134]. Finally, immune surveillance of senescent cells appear to be a fine tuned mechanism since *naevi* can remain for decades without signs of malignant transformation [125].

In senescent cells, $p16^{Ink4a}$ expression increases during ageing and has a role on the development of age-related human diseases [135]. Baker and colleges reported that clearance $p16^{Ink4a}$ positive senescent cells delays appearance of cataracts and kyphosis in mice, strengthens muscle fibbers and make BubR1 hypomorphic-mice fitter for exercise [136]. Besides this, there is a decrease of senescent traits such as SA-β-Gal, IL-6 and metalloproteinase enzymes upon p16-positive cells clearance [136].

Albeit the fact senescence is widely connected to loss of organ function and tumour suppression, senescence plays a part during normal cellular development and differentiation, for instance during terminal differentiation of

megakaryocytes [137]. Briefly, very recently studies identified also senescent cells during embryonic development [138, 139]. Finally, the authors propose that senescence, alike apoptosis is programmed [138].

From the aforementioned studies, it is clear that senescence plays an important role *in vivo* during organismal development, ageing and disease. Increasing data suggests that de-regulation of nutrient-sensing pathway mTOR and cellular metabolism can contribute to these processes and modulate cellular senescence and organismal longevity [10, 140].

## The mTOR pathway – the cells' survival kit

mTOR (mammalian/mechanistic target of rapamycin) is an ancient and conserved pathway among eukaryotes. It is a key signalling pathway that integrates multiple cellular inputs and outputs, channelling those into two major mTOR kinase complexes – mTORC1 and mTORC2 [141]. Besides the serine-threonine mTOR kinase, each complex share common subunit proteins namely Deptor, mLST8 and TTI1-TEL2; while mTORC1 has Raptor and PRAS40 as specific associates, mTORC2 contains Rictor, Protor and mSIN1 [141]. These two complexes are modulated by numerous stimuli as amino acids, growth factors and glucose among others. In turn, these basic blocks are put into varied cellular anabolic processes that include protein synthesis, energy generation or lipids biosynthesis, contributing to cell growth, survival and division [141]. Upstream of the mTOR complexes we find the IGF-1–PI(3)K–Akt axis. Downstream of Akt, there is the TSC-TBC complex (composed from TSC1 (hamartin), TSC2 (tuberin) and TBC1D7) that negatively impacts on mTORC1 activity. In more detail, this effect is mediated by a GTPase-activating protein (GAP) domain within tuberin,that accelerates conversion of Rheb-GTP to Rheb-GDP. From the two known mTOR complexes, mTORC1 is by far the best studied to date in respect to downstream cellular functions. For instance, mTORC1 coordinates messenger RNA translation and protein synthesis through the phosphorylation status of ribosomal protein S6 kinase 1 (S6K1) and the 4E-BP protein [142]. mTORC1 activity is measured by the phosphorylation status

of S6K1 at T389, or by phosphorylation of S6 at S235/S236 [143]. mTORC1 activity can be blunted by amino-acid starvation or using rapamycin. Rapamycin or sirolimus, is a drug first found and isolated from the bacteria *Streptomyces hygroscopicus* from Easter Island, also known as Rapa Nui [144]. This chemical compound has anti-proliferative properties, is commonly used to prevent organ transplantation rejection and, itself and its analogues have been used in several clinical trials [145]. Although rapamycin is known to selectively interfere with some mTORC1 processes for more than two decades, it remains to be elucidated how rapamycin mechanistically modulate mTORC1 functions [146]. On reverse, deletion of either TSC1 or TSC2, or use of a mutant Rheb allows a high constitutively active mTORC1 [147]. **FIGURE 1** depicts in summary the mTOR pathway.

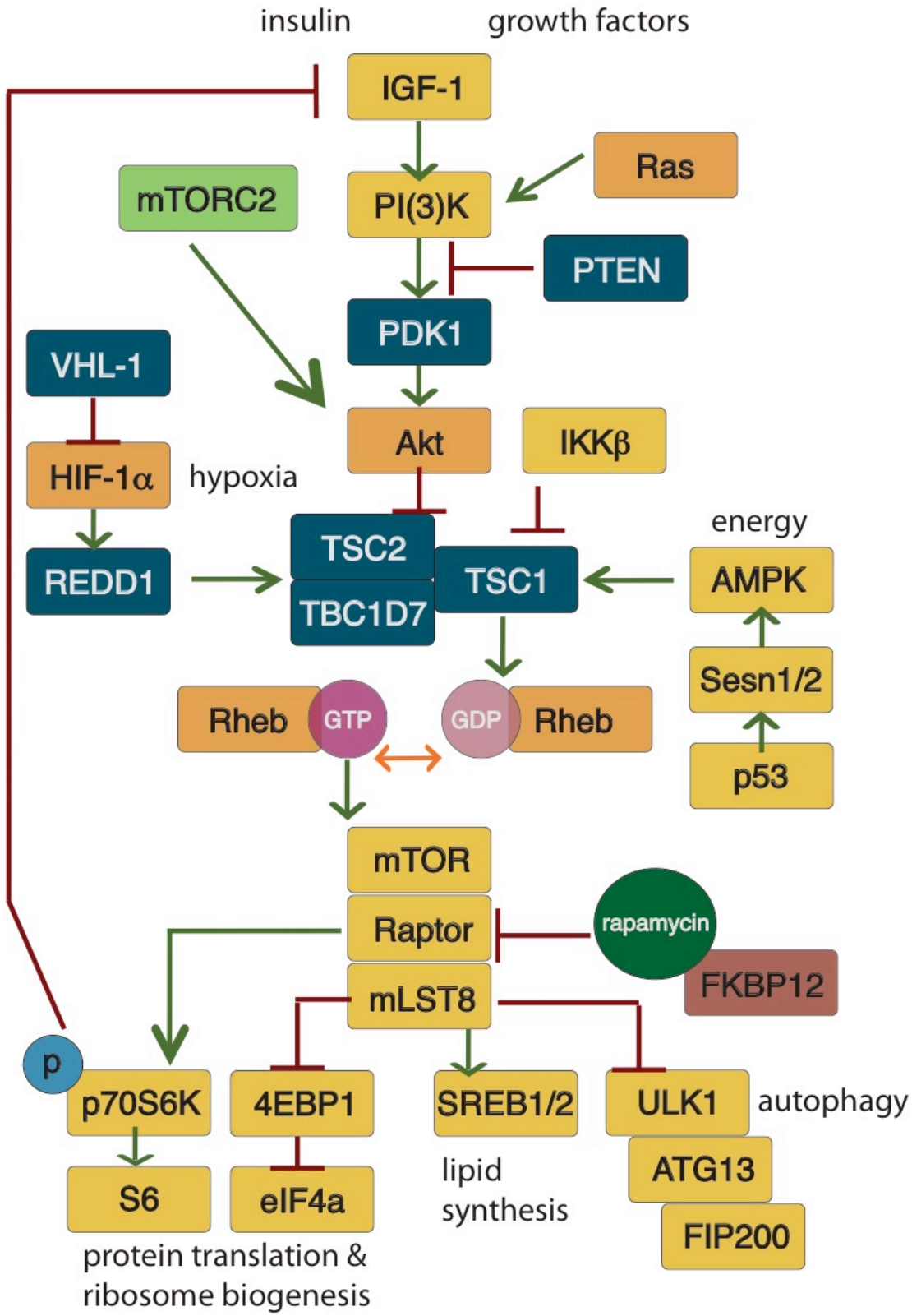


**FIGURE 1| The mTOR pathway.**

**mTOR impacts on organismal ageing**

Genetic studies have highlighted the role of mTOR as a master regulator of lifespan and ageing in yeast, worms, flies and mice [140, 148-153]. Additionally, dietary restriction (DR) acts through the mTOR pathway [149]. Other mark of mTOR involvement in ageing is the extension of mice lifespan when rapamycin is administered, being therefore the first known evidence that mTOR inhibition effects and increases lifespan in mammals [140]. Rapamycin supplemented diet ameliorate health span and lifespan of several cancer mice models [154-159]. mTOR inhibition by rapamycin besides attenuating disease progression [160], it also was beneficed health span of a mouse model of mitochondrial disease (Leigh syndrome) [161].

Stem cells exhaustion is one of the features that accompany organismal ageing. mTOR impacts on cell stemeness tuning the *Wnt* signalling (critical rheostat for stem cell renewal and proliferation) [162-164] and, by promotion pluripontency genes expression (Oct4, Sox2, Nanog and Telomerase)[165].

Besides ageing, the mTOR pathway could be linked to cellular senescence via the DNA damage and mitochondrial dysfunction (aim and discussed throughout this dissertation).

# OBJECTIVES

- Investigate the impact of mTOR on mitochondrial dysfunction during cellular senescence;
- Evaluate the relative contribution of mitochondrial homeostatic mechanisms such as autophagy and mitochondrial biogenesis to the development of the senescent phenotype;
- Examine the impact of mTOR dependent mechanisms on the maintenance of a DNA damage response during cellular senescence;
- Analyse the impact of mTORC1 inhibition using rapamycin and mitochondrial biogenesis in senescence *in vivo*.

# CHAPTER 2 – METHODS

## Cell culture

Human embryonic lung MRC5 fibroblasts, human foreskin BJ fibroblasts (CRL-2522™), MRC5 fibroblasts transfected with the catalytic subunit of telomerase (MRC5-hTERT)[166], MRC5 fibroblasts bearing a fluorescent 53BP1 fusion protein - AcGFP-53BP1c [167] were grown in Dulbecco's modified Eagle's medium – high glucose (DMEM, Sigma D5796, Dorset, UK) supplemented with 10% heat inactivated foetal calf serum (FCS)(Sigma©-Aldrich, Ayrishire, UK), Penicillin/Streptomycin and 2mM glutamine under atmospheric oxygen conditions (air plus 5% $CO_2$). All fibroblasts used in all experiments were between PD20 and PD30 unless they were immortalized.

Replicative senescent MRC5 cells were generated by continued passaging (2 to 3 months) until the population doubling was lower than 0.1. Once cultures were in deep-senescence state, Ki-67 staining was conducted to verify lack of proliferation. Cells' media was replaced two times per week.

Human embryonic kidney cells HEK293, human breast cancer MCF7 (CRL-2351™), human primary glioblastoma U87 (HTB-14™), human colon carcinoma cells HCT116 (ATCC CCL-247™), HeLa (CCL-2™) cells and human fibrosarcoma T19 cells -containing a stably integrated dominant negative $TRF2^{\Delta B \Delta M}$ expression cassette under the control of a Tet-off promoter doxycycline inducible was a gift from Titia de Lange, Rockefeller University, NY [44] - were cultured in similar conditions as those used for fibroblasts.

Mouse embryonic fibroblasts (MEFs) were obtained from C57BL/6 wild-type mice. MEFs from autophagy-related protein 5 (Atg5)-deficient - $Atg5^{-/-}$ (kind gift from Dr. Viktor Korolchuk and Dr. Noboru Mizushima [168]), PGC-$1\beta^{-/-}$ (kind gift from Dr. Antonio Vidal-Puig) and respective matched wild-type, were cultured in Advanced DMEM/F-12 (Invitrogen #12634) plus 10% FSC, Penicillin/Streptomycin and 2mM glutamine at 3% oxygen in a 3-gas cell culture incubator (Zapf Instruments, Sarstedt, Germany).

In order to inducible knockdown of TSC1 or TSC2, HEK293 cells were first transduced with lentivirus encoding the doxycycline/tetracycline-sensitive tTR-KRAB repressor and a DsRed reporter. Afterwards, cells were transduced with lentivirus encoding the specific shRNA and a GFP reporter (pLVTH vector), both under the control of tTR-KRAB. Expression of shRNA was induced by treating cells with 2µg/mL doxycycline for 3 days. Target sequences of shRNA: TSC1 shRNA 1 (5'- GACACACAGAATAGCTATG-3'), TSC2 (5'-CGACGAGTCAAACAAGCCAAT-3'), and non-targeting scramble shRNA (5'- TGGTTTACATGTCGACTAA-3'). Cells were a kind gift from Dr. Kathrin Thedieck.

### Cell fixation

Media was aspirated from a 12 well plate with a Pasteur pipette connected to a vacuum pump. Next a brief wash with 1xPBS was done. After removing the PBS, cells were fixed using 1mL of 2% PFA for each well. After ten minutes incubation at room temperature, PFA was aspirated. Coverslip were covered with 400µl PBS and store at -80°C until use further use.

### Cells storage

Cells were centrifuged at 1200 rpm for 3 minutes. After removal of the media, cells were re-suspended in FBS with 10% DMSO HYBRI-MAX© (D2650 - Sigma©-Aldrich). Afterwards, cells were aliquoted in cryotubes and placed in a Cryo-Freezer previously thawed. Vials were put at -80$^{o}$C and then stored into a liquid nitrogen tank - Biorack 6000 (Statebourne Cryogenics, Washington, UK).

### Tissue culture treatments

### X-ray irradiation

Stress-induced senescence in MRC5 fibroblasts was induced by X-ray irradiation with 20Gy (unless stated otherwise). Mouse embryonic fibroblasts and HEK293T cells were X-ray irradiated with 10Gy. All cancer cells and T19 cells were irradiated with 20Gy X-ray radiation. The cell X-radiator (X-Rad

225, Precision X-Ray INC, N-BRANFORD, CT USA) was used for every cell line/experiment. Following irradiation all culture medium was refreshed.

### Chemical treatments

Cells were stimulated with neocarzinostatin (80ng/ml) (Sigma-Aldrich N9162) and $H_2O_2$ (400μM) in serum free media for 1 hour. Following treatment, culture medium was refreshed. Immediately after irradiation, medium was replaced by fresh DMEM containing the drug of choice. Cells treated with etoposite (50 μM) were continuously treated every 3 days for 10 days after irradiation. ATM (Ataxia telangiectasia mutated) kinase was inhibited using 2-morpholin-4-yl-6-thianthren-1-yl-pyran-4-one (Ku55933) (Pfizer S1092) at 10μM one day post-X-ray radiation. mTORC1 activity was inhibited using rapamycin (Sigma-Aldrich #R8781). All experiments were conducted using rapamycin at 100nM unless stated otherwise. N-acetyl-cysteine (NAC) (Sigma A9165) was used as antioxidant at 2.5nM for 24 hours. A 250μM Trolox (6-Hydroxy-2,5,7,8-tetramethylchromane-2-carboxylic acid) (Sigma 238813) solution was made in water and filter sterilized. Samples were treated with Trolox one day prior to analysis. A 1M sodium pyruvate solution was made. After filtration (0.45μm filter), working solutions were prepared by dissolving the pyruvate solution in full DMEM media at 10 or 50mM.

### Microscopy

### Live-cell imaging

For live cell time-lapse microscopy, cells were plated in Iwaki glass bottomed dishes (Iwaki) and imaged on an inverted Zeiss LSM510 equipped with a Solent incubator (Solent Scientific) at 37$^{o}$C with humidified 5% $CO_2$, using a 40x 1.3 NA oil objective. Autofocus was performed at each time point prior to capturing z-stacks to ensure the whole cell was captured (1.65μm pinhole every 1.5μm over 4.5μm total z range). Cells and AcGFP-53BP1c foci were tracked manually using ImageJ (http://rsb.info.nih.gov/ij/).

### Telomere PNA probes incorporation

Incorporation of telomere specific PNA probe by glass beads was performed as described [169]. Cy-3 labelled telomere specific $(C_3TA_2)_3$ peptide nucleic acid (PNA) probe (Panagene) was dissolved in 80mM KCl, 10mM $K_2PO_4$, 4mM NaCl, pH 7.2, to a final concentration of 1μM. Mouse embryonic fibroblasts (MEFs) were grown in glass bottomed dishes and PNA probe was pipetted onto the culture. 0.12g of 75μm alkali washed glass beads (Sigma) were carefully and evenly sprinkled onto the surface of the dish.

### Transmission electron microscopy (TEM) analysis

Transmission electron microscopy was performed at the Electron Microscopy Research Services – Newcastle University. Mitochondrial volume fraction, mitochondrial area and mitochondria number were tracked manually using Image J (http://rsb.info.nih.gov/ij/). Results presented consist of data from 3 rapamycin-fed and 3 control male C57BL/6 mice 16 month old, 20 electron micrographs, 2000 mitochondria per animal were analysed.

### Western blot

Western blotting was performed using conventional techniques. Mitochondrial protein abundance was determined by western blotting using antibodies against mitochondrial proteins TOMM20, VDAC, NDUFB8, SDHA, UQCR2, MT-CO1 and MT-CO2 (**Table 2.1**).

| Protein | Species | Host | Dilution | Reference/ Manufacturer |
|---|---|---|---|---|
| p21 | Human | Rabbit monoclonal | 1:1000 | #2947 - Cell signalling |
| p21 | Human<br>Mouse | Rabbit polyclonal | 1:1000 | ab7960 - Abcam |
| PGC-1α | Human<br>Mouse | Mouse monoclonal | 1:1000 | ST1202 - EMD Millipore |

| | | | | |
|---|---|---|---|---|
| PGC-1β | Human<br>Mouse | Rabbit polyclonal | 1:1000 | ab61249 - Abcam |
| NDUFB8 | Human<br>Mouse | Mouse monoclonal | 1:1000 | ab110242 - Abcam |
| UQCRC2 | Human<br>Mouse | Mouse monoclonal | 1:1000 | ab14745 - Abcam |
| MT-CO1 | Human<br>Mouse | Rabbit monoclonal | 1:250 | ab14705 - Abcam |
| MT-CO2 | Human | Mouse monoclonal | 1:1000 | ab110258 - Abcam |
| SDHA | Human<br>Mouse | Mouse monoclonal | 1:1000 | ab14715 - Abcam |
| TOMM20 | Human<br>Mice | Mouse monoclonal | 1:1000 | ab56783- Abcam |
| VDAC1/Porin | Human<br>Mouse | Mouse monoclonal | 1:1000 | ab14734 - Abcam |
| SOD2 | Human<br>Mouse | Rabbit | 1:500 | 806-984 - Millipore |
| S6 | Human<br>Mouse | Rabbit monoclonal | 1:1000 | #2217- Cell signalling |
| S6(Ser235/236) | Human<br>Mouse | Rabbit monoclonal | 1:1000 | #4858- Cell signalling |

| | | | | |
|---|---|---|---|---|
| p70S6K | Human<br>Mouse | Rabbit polyclonal | 1:1000 | #9202 - Cell signalling |
| p70S6K(Thr389) | Human<br>Mouse | Rabbit polyclonal | 1:1000 | #9205 - Cell signalling |
| TSC2 | Human<br>Mouse | Rabbit monoclonal | 1:1000 | #4308 - Cell signalling |
| β-tubulin | Human<br>Mouse | Rabbit polyclonal | 1:2000 | #2146 - Cell signalling |
| α-tubulin | Human<br>Mouse | Mouse monoclonal | 1:2000 | T9026 Sigma Aldrich |
| GAPDH | Human<br>Mouse | Rabbit monoclonal | 1:5000 | #5174 - Cell signalling |
| FLAG | - | Mouse monoclonal | 1:1000 | F3165 - Sigma Aldrich |
| Atg5 | Human<br>Mouse | Mouse monoclonal | 1:1000 | A2859 - Sigma Aldrich |

| **Secondary antibodies** | **Dilution** | **Reference/Manufacturer** |
|---|---|---|
| Goat anti-rabbit IgG -HRP conjugated | 1:5000 | A0545 - Sigma-Aldrich |
| Rabbit anti-mouse IgG -HRP conjugated | 1:5000 | A2554 - Sigma-Aldrich |

**TABLE 2.1| Primary and secondary antibodies used for Western Blot**

### ROS - cellular superoxide levels (FACS)

Cellular superoxide levels were measured using 10μM of dihydroethidium – DHE - (Molecular Probes, D-1168). Cells were stained in serum-free media (SFM) for 30 minutes at 37$^{o}$C in the dark, red (FL3 channel) median fluorescence intensity was measured by flow cytometry (30,000 cells were analysed per condition).

### Mitochondrial mass - cellular cardiolipin levels (FACS)

In order to measure mitochondrial mass, cells were stained with the fluorescent dye 10-n-nonylacridine orange – NAO (Molecular Probes – A1372). Cells were re-suspended in 1 ml of DMEM containing 10μM of NAO. After incubation for 10 minutes at 37°C in the dark, NAO fluorescence intensity was measured by flow cytometry. Green (FL1 channel) fluorescence was recorded.

### Mitochondrial mass – MitoTracker Green staining (microscopy)

Cells were plated at a suitable density on coverslips avoiding confluence during the experiments. MitoTracker Green FM (Invitrogen M7514) was diluted 1 in 1000. Add 200μl MitoTracker Green and 30μl (100μg/ml) Hoechst 33342 (Invitrogen) to 2.8ml SFM. After incubation at 37°C for half an hour, dyes were removed and cells washed. Mount in PBS and image immediately and for no longer than 25 to 30 minutes.

### Mitochondria membrane potential - Tetramethylrhodamine methyl ester (TMRM) staining (microscopy)

Cells were plated at a suitable density on coverslips avoiding confluence during the experiments. MitoTracker Green FM (Invitrogen M7514) and TMRM (Invitrogen) 1:1000. 1μl TMRM working solution, 200 μl MitoTracker Green FM and 30μl (100μg/ml) Hoechst 33342 (Invitrogen) were added to 2.8 ml serum free media. Cells were incubated at 37°C for 30 minutes. After dyes removal, cells were washed, mounted in PBS and imaged immediately and for no longer than 25-30 minutes.

### Lysogeny broth (LB)

Ten grams of tryptone, 5g of yeast extract and 10g of NaCl were weighed and suspended in 800 ml of distilled/deionized water. After homogenisation, further water was added to make a total volume of 1L. Media was sterilised by autoclaving it at 121°C for 20 minutes. For plates, 15g of agar was added to the media. When media cooled down, (before solidification) the antibiotic resistance advised for selection was added.

### *E. coli* transformation by heat shock

Prepare the water bath to 42°C. Add 1µg plasmid (in TE or water) into 150µl chemical competent cells. Incubate the mixture on ice for 30 minutes. Heat-shock the mixture on 42°C bath for 45 seconds. Bring the tube back in ice for 2 minutes. Add 250µl of S.O.C medium. Incubate the tube at 37°C for 1 hour. Spin down cells 10.000g. Remove 300µl of the supernatant and re-suspend the pellet. Plate cells in LB agar plates containing 100µg/ml ampicillin. Incubate the plates overnight at 37°C (12-16 hours). Pick a satellite colony and incubate in 5ml LB medium with the adequate antibiotic (1:1000 dilution). Incubate at 37°C and 200 rpm at least 6 to 8 hours (until media start to become opaque). The next day take 1ml of the grown culture and inoculate 200ml of LB medium with antibiotic resistance overnight.

### *E. coli* glycerol stock

Take 1 ml of the 10 ml of overnight culture (37°C and 200 rpm) and add 500µl of 50% glycerol. Store at -80°C.

**Plasmid isolation – Pure Yield™ Plasmid Miniprep System** (Promega – A2492)

Centrifuge the overnight culture for fifteen minutes at 4000 rpm. Afterwards re-suspend pelleted bacterial cells in 400µl Cell Resuspension Solution. Add 400µl Cell Lysis Solution and gently invert the tube four to six times to mix. Add 400µl Neutralization Solution and invert the tube immediately but gently four to six times. The solution should become cloudy. Centrifuge for ten minutes at 10000x *g*. Thoroughly mix the resin and add 1ml to each

Minicolumn/syringe assembly. Carefully transfer the supernatant to the resin in each assembly. Open stopcocks of the vacuum manifold. Apply vacuum to pull the liquid through the column. Release vacuum when all the liquid has passed the column. Add 2ml Column Wash Solution (containing ethanol, avoid leaving the bottle opened for long time) and apply vacuum again. Continue vacuum for about thirty seconds to dry the resin. Transfer mini-column to an Eppendorf and dry the column by centrifugation. Transfer the mini-column to a new micro-centrifuge tube, add 50µl 70°C deionised water and wait for one minute (for plasmids bigger than 10Kb use 80°C deionised water). Centrifuge at 10000x *g* for one minute. Remove and discard mini-column. Lastly, measure DNA concentration on the Nanodrop.

### Restriction enzyme digestion

One microgram of PGC-1β was digested using 0.3µl of BamHI and/or EcoRV enzymes. Digestion mixture was incubated at 37°C for three hours. DNA-digestion product was verified by agarose gel electrophoresis.

### DNA gel electrophoresis

Prepare your 1% agarose-gel by taking 100ml of 1x TAE-buffer in a 200ml Erlenmeyer flask. Weigh one gram agarose and add to the TAE-buffer. Add Ethidium Bromide-solution to the agarose gel in a final concentration of 0.5µg/ml when it is hand warm. Poor the gel and put a comb in the electrophoresis unit. After hardening of the agarose-gel, pull out the comb. Load the samples using 6x concentrated DNA-loading buffer. Use 5µl of the 1Kb Plus DNA Ladder (Invitrogen) as a MW marker. Run the gel on 80-100V for 30 to 45 minutes.

**Cell transfection** (using Lipofectamine 2000$^{TM}$ Invitrogen and GunJ – Glyn Nelson)

For each well prepare 1µg of your plasmid (DNA) and add the transfection reagent at a ratio of 2:1 from the volume of DNA in 100µl Opti-MEM (Invitrogen - 31985-062). Mix gently by flicking the Eppendorf tube. Incubate at room temperature thirty minutes. Add this mixture dropwise to the cells.

### Plasmids

For overexpression of activated Rheb both HeLa cells and MEFs were transduced with empty vector or pcDNA3-flag-Rheb-N153T (Addgene #19997). Overexpression of PGC-1β was conducted using pcDNAf:PGC-1β (Addgene #1031).

### Immunofluorescence

Take a new 12 well plate and transfer the 19 mm cover slips with the help of forceps (cells always facing up). Wash twice in PBS for 5 minutes. Then permeabilize cell membranes using 1ml PBG-Triton X for 45 minutes. This step should be done at room temperature and with slightly shake. Remove solution and add 400µl of primary antibody in PBG-Triton X per cover-slip. Alternatively, add 60µl droplet into PARAFILM® and placed the coverslip with the cells facing the diluted primary antibody. Incubate at room temperature 2 hours. In lieu of this, incubation with the primary antibody can be done overnight at 4°C. Wash twice in PBGT for 5 minutes. Incubate samples with the secondary antibody (Alexa Fluor® 594 or Alexa Fluor® 488) (Invitrogen) at room temperature 45 minutes in dark (wrap the 12 well plate with aluminium foil). Put samples to shake slightly. Aspirate secondary antibody and wash three times with PBS (10 minutes each wash). Incubate each sample in 400 µl DAPI for 10 minutes. Remove DAPI and wash three more times with PBS (10 minutes each wash). Prepare clean slides and label them. Add 10 µl anti-fade (DABCO or Vector) mounting medium on the middle of the slides. Flip-flop coverslip, put cells facing the mounting medium. Let it dry and protect slides from light. Examine slides under the fluorescence microscope. A complete list of primary antibodies used in all experiments is depicted in **Table 2.2**.

| Protein | Species | Host | Dilution | Reference/Manufacturer |
|---|---|---|---|---|
| Ki67 | Human<br>Mouse | rabbit polyclonal | 1:250 | ab15580 - Abcam |

| | | | | |
|---|---|---|---|---|
| γH2A.X(Ser139) | Human | Mouse | 1:2000 | AB10022 - Upstate Millipore |
| 53BP1 | Human<br>Mouse | rabbit polyclonal | 1:200 | NB100-305 - Novus Biologicals |
| 53BP1 | Human | Rabbit polyclonal | 1:500 | #4937 - Cell signalling |
| p21 | Human<br>Mouse | rabbit polyclonal | 1:200 | ab7960 - Abcam |
| SDHA | Human<br>Mouse | Rabbit monoclonal | 1:1000 | #11998- Cell signalling |
| FLAG | - | Mouse monoclonal | 1:1000 | F3165 - Sigma Aldrich |
| Atg5 | Human<br>Mouse | Mouse monoclonal | 1:1000 | A2859 - Sigma Aldrich |

**TABLE 2.2| Primary antibodies used for Immuno-fluorescence stainings**

### Immuno-FISH in cells

Immuno-FISH were performed as described [59]. Briefly, cells grown on sterile coverslips were fixed with 2% paraformaldehyde and γ-H2A.X (Upstate Biotechnology) or 53BP1 (Cell Signalling) immuno-staining for 1h at room temperature was performed as described above. After application of the secondary antibody, cells were washed with PBS and FISH was performed. 20µl of Cy-3 labelled telomere specific $(C_3TA_2)_3$ peptide nucleic acid (PNA) probe (4ng/µl) (Panagene) was applied to the cells followed by co-denaturation at 80°C and hybridisation for 2 hours at room temperature in the dark. Cells were then washed 3 times for 10 minutes with wash buffer made from 70ml Formamide (70%) 30ml SSC 2% (3ml stock SSC 20% + 27ml $H_20$)

and 3 times for 5 minutes with TBS-Tween 0.05%. Cells were incubated with DAPI, mounted and imaged using a Leica DM5500B fluorescence microscope. In depth Z stacking was used (Images were captured as stacks separated by 0.247µm with 100×objective) followed by Huygens (SVI) deconvolution.

### Immuno-FISH in paraffin embedded tissues

For Immuno-FISH in formalin-fixed paraffin embedded liver mice sections, following antibody incubations, sections were incubated with avidin–DCS (diluted to 1:500; Vector Lab) for 30 min. Subsequently, tissue sections were washed 3 times in PBS and fixed in 4%PFA for 20 min and dehydrated with 70%, 90%, 100% ethanol for 3 min each. Sections were air dried and then denatured for 10 min at 80°C in hybridization buffer [70% formamide (Sigma), 25mM $MgCl_2$, 1M Tris pH 7.2, 5% blocking reagent (Roche, Welwyn, UK)] containing 25µg/ml Cy-3 labeled telomere specific (CCCTAA) peptide nuclei acid probe (Panagene), followed by hybridization for 2 hours at room temperature in the dark. The slides were washed for 10 minutes with 70% formamide in SSC 2%, following by a 10 minutes wash in SSC 2% and a final wash in PBS for 10 minutes. Nuclei were stained by DAPI for 10 minutes, mounted and imaged in a Leica DM5500B fluorescence microscope. In depth Z stacking was used (a minimum of 40 optical slices with 63×objective) followed by Huygens (SVI) deconvolution.

### Clonogenic assay

Colony assay of wild-type and PGC-1β$^{-/-}$ MEF grown at 3% or 21% $O_2$ (normoxia) were followed for three weeks after seeding 10.000 cells. Cells were re-seeded and counted every three to four days. After PFA fixation and a brief wash with PBS1x cells were stained in Crystal violet solution. After a thorough wash in water, cells were solubilized in methanol and optical absorbance was monitored at 540nm using FLUOstar Omega reader (BMG-Labtech).

### Senescence-associated β-Galactosidase (SA-β-Gal) staining

For senescence-associated β-galactosidase staining, cells were fixed with 2% formaldehyde in PBS for 5 minutes and stained as described in [170, 171]. Briefly, following fixation, cells were washed once with PBS and incubated at 37°C for 16 hours in freshly prepared senescence-associated β-galactosidase staining solution containing 2mM magnesium chloride, 150mM sodium chloride, 40mM citric acid, 12mM sodium phosphate dibasic, 5mM potassium ferrocyanide, 5mM potassium ferricyanide and 1mg/l – 1-5-bromo-4-chloro-3-inolyl-β-d-galactoside (X-Gal) enzyme at pH 6.0. Following staining, nuclei were counterstained with DAPI and randomly chosen fields were imaged (20x objective). For *in vivo* liver and fat Sen-β-Gal assay, tissues were fixed in 4% PFA one day at room temperature. Next, tissues were rinsed in PBS 1X trice for ten minutes. After preparing the same Sen-β-Gal solution described above, tissues were incubated overnight at 37ºC. Next day, tissues were rinsed extensively in 1xPBS solution. For primary MEF and mouse tissues Sen-β-Gal pH was adjusted to 5.5 [172].

### DNA isolation

DNA was extracted using DNeasy 96 Blood & Tissue Kit (Qiagen # 69581) kit and guidelines.

### RNA isolation

Total RNA was extracted using the RNeasy minikit (Qiagen). Complementary DNA was generated using Superscript II (Gibco).

### Quantitative RT-PCR

PCR reactions were performed on an Opticon 2 (Bio-Rad) using SYBR Green PCR Master Mix (Applied Biosystems) and TaqMan Universal PCR Master Mix (Applied Biosystems). Expression was normalized to GADPH expression. Primers used are depicted in **Table 2.3**.

| Gene | Species | | Sequence |
|---|---|---|---|
| PGC-1β | Human | Forward | 5’ AGTCAACGGCCTTGTGTTAAG 3’ |
| | | Reverse | 5’ ACAACTTCGGCTCTGAGACTG 3’ |
| PGC-1α | Human | Forward | 5’ TGAGAGGGCCAAGCAAAG 3’ |
| | | Reverse | 5’ ATAAATCACACGGCGCTCTT 3’ |
| GAPDH | Human | Forward | 5’AAATCCCATCACCATCTTCC 3’ |
| | | Reverse | 5’ GACTCCACGACGTACTCAGC 3’ |
| PGC-1β | Mouse | Forward | 5’ CGCTCCAGGAGACTGAATCCAG 3’ |
| | | Reverse | 5’ CTTGACTACTGTCTGTGAGGC 3’ |
| PGC-1α | Mouse | Forward | 5’ AATCAGACCTGACACACG 3’ |
| | | Reverse | 5’ GCATTCCTCAATTTCACCAA 3’ |
| CXCL1 | Mouse | Forward | 5’ GACTCCAGCCACACTCCAAC 3’ |
| | | Reverse | 5’ TGACAGCGCAGCTCATTG 3’ |
| IL-6 | Mouse | Forward | 5’ CTACCAAACTGGATATAATCAGGA 3’ |
| | | Reverse | 5’ CCAGGTAGCTATGGTACTCCAGAA 3’ |
| p16 | Mouse | Forward | 5’ TTGCCCATCATCATCACCT 3’ |
| | | Reverse | 5’GGGTTTTCTTGGTGAAGTTCG 3’ |
| β-actin | Mouse | Forward | 5’ TAAGGCCAACCGTGAAAAG 3’ |
| | | Reverse | 5’ ACCAGAGGCATACAGGGACA 3’ |

**TABLE 2.3| Primer sequences for Real-time PCR**

### mtDNA copy number assay

Ratio between mitochondrial ND1 and a nuclear reference gene (ND5 or B2M - β2- microglobulin) was measured in human and mouse fibroblasts, and HEK293T cells by RT-PCR (primers in **Table 2.4**).

| Gene | Species | | Sequence |
|---|---|---|---|
| B2M | Human | Forward | 5’ CCAGCAGAGAATGGAAAGTCAA 3’ |
| | | Reverse | 5’ TCTCTCTCCATTCTTCAGTAAGTCAACT 3’ |
| ND1 | Human | Forward | 5’ CCCTAAAACCCGCCACATCT 3’ |
| | | Reverse | 5’ GAGCGATGGTGAGAGCTAAGGT 3’ |
| ND1 | Mouse | Forward | 5’ ACACTTATTACAACCCAAGAACACAT 3’ |
| | | Reverse | 5’ TCATATTATGGCTATGGGTCAGG 3’ |
| ND5 | Mouse | Forward | 5’ CCACGCATTCTTCAAAGCTA 3’ |
| | | Reverse | 5’ TCGGATGTCTTGTTCGTCTG 3’ |

**TABLE 2.4| Primer sequences used for mtDNA copy number assay**

### MICE

- **Ageing cohort** (used in Chapter 3)

Three male C57BL/6 mice per age group - 3, 12, 22, 36 and 42 months old were sacrificed. Tissues were immediately perfusion fixed. Formalin-fixed paraffin embedded 3 μm sections were prepared from liver and gut.

- **Short-time rapamycin treatment** (from 12 until 16 months of age)

C57/BL6 male mice at 12 months of age were divided into 2 groups (N=10/group), matched for body mass, food intake and age. Mice were both fed with control diet or rapamycin for four months starting at twelve months of age and sacrificed at 16 months of age.

- **Life-long rapamycin treatment** (from 3.5 months of age until 15.5 months of age)

C57/BL6 male mice at 3.5 months of age were divided into multiple groups (n=6-11/group), matched for body mass, food intake and age. Mice were both

fed with control diet or rapamycin for three, six or twelve months. Mice were sacrificed at 6.5, 9.5 and 15.5 months of age.

- **Rapamycin diet**

Control and Rapamycin diet was purchase from TestDiet - Control diet: 5LG6/122 PPM EUDRAGIT 3/8 #1814831 (5AS0) and Encapsulated Rapamycin diet: 5LG6/122 PPM ENCAP RAP 3/8 #1814830 (5ARZ). Mice were fed *ad libitum* and weight and food intake was monitored weekly.

- **PGC-1β$^{-/-}$ mice**

Wild-type and PGC-1β$^{-/-}$ C57/BL6 mice were sacrificed at 7 and 18 months of age. Tissues were either paraformaldehyde-fixed paraffin embedded or frozen in liquid nitrogen and stored at -80$^{o}$C for biochemical analysis. Professor Antonio Vidal-Puig and Dr. Sergio Cuenca-Rodriguez are the holders of the PGC-1β$^{-/-}$ mice colony in the University of Cambridge - Metabolic Research Laboratories, Wellcome Trust-MRC Institute of Metabolic Science, Addenbrooke's Hospital, Cambridge, UK.

### Ethics statement

Animal procedures were performed in accordance with the UK Home Office regulations and the UK Animal Scientific Procedures Act [A(sp)A 1986]. The project was approved by the Faculty of Medical Sciences Ethical Review Committee, Newcastle University. Project license number 60/3864.

### Statistical analyses

We conducted One-Way ANOVA, Student Two-Tailed t-test, linear and non-linear regression analysis and Gehan-Breslow test using Sigma Plot 11.0. Wilcoxon-Mann-Whitney tests were conducted using IBM SPSS Statistics 19.

# CHAPTER 3 – TELOMERES ARE FAVOURED TARGETS OF A PERSISTENT DNA DAMAGE RESPONSE (DDR) IN STRESS-INDUCED SENESCENCE AND AGEING

## INTRODUCTION

Telomeres are found at the end regions of chromosomes and they are known to shorten in each replication cycle [29, 30, 34]. Once telomeres become critically eroded, they trigger a DNA damage response that elicits cellular senescence [37-39].

In mice, senescence is unanimously regarded as being telomere independent [174], once telomeres in these animals are extremely long and, in order to reach a critical size to engage on senescence, it would take multiple replication rounds [175].

It is generally believed that cells treated with high concentrations of hydrogen peroxide stress, do not exhibit telomere length shortening however, under mild oxidative conditions, telomeres can be damaged, accumulating single strand breaks (SSB) that, combined with cellular division, accelerates telomere shortening [6, 42].

Besides SSB at telomeres caused by oxidative stress, the loss of telomere protective capacity, in other words, lost of shelterin components, can lead to telomere induced damage foci (TIF)[38]. TIF have been reported in multiple human primary cells that engage DDR pathways [37, 176] and in cancer cell lines [177]. Additionally, damaged telomeres are thought to be unable to retain their normal conformational architecture (e.g. their *t-loop*) and, also, are incapable of keep enough TRF2 to halt non-homologous end-joining (NHEJ) fusions [177].

Finally, previous observation in senescent cells, induced either by X-ray irradiation or by $H_2O_2$ treatment, has evidenced that certain DNA damage foci are persistent [178]. Despite this observation, the nature and location of these lesions is not known.

## AIMS

- Are persistent DNA damage foci (DDF) located at telomeres during stress-induced senescence?
- Are telomere-associated foci (TAF) present *in vivo* in mice liver and small intestine and, do they change with age?

## RESULTS

Senescent cells can be characterised by having an unresolved DNA damage response [37] (**FIGURES 3.1a** and **3.1d**). Upon induction of senescence using X-ray ionising radiation, human MRC5 fibroblasts display high number of γH2A.X damage foci that gradually become repaired with time (**FIGURES 3.1a**). Interestingly, after several days, double stranded lesions labelled by γH2A.X or 53BP1 are still present within the nucleus (**FIGURES 3.1a, 3.1d, 3.2c** and **3.2e**). Similarly, this feature was seen in mouse embryonic fibroblasts (MEF) following X-ray radiation treatment, suggesting that this process is common across species upon induction of senescence by genotoxic stress (**FIGURES 3.1b-3.1e**). Moreover, increasing doses of X-ray radiation lead to a linear increase of DNA damage foci number in both human and mouse fibroblasts (**FIGURES 3.1d, 3.1e,** and **3.2a**),
Overall this unrepaired damage foci may be important for the induction of the senescent phenotype. Finally, also replicative senescent MRC5 fibroblasts show persistent DNA damage foci [178].

Based on the existing literature that telomere binding proteins impede proper DNA repair at telomeres, we hypothesized that unrepaired DNA damage foci could specifically be located at telomeres.

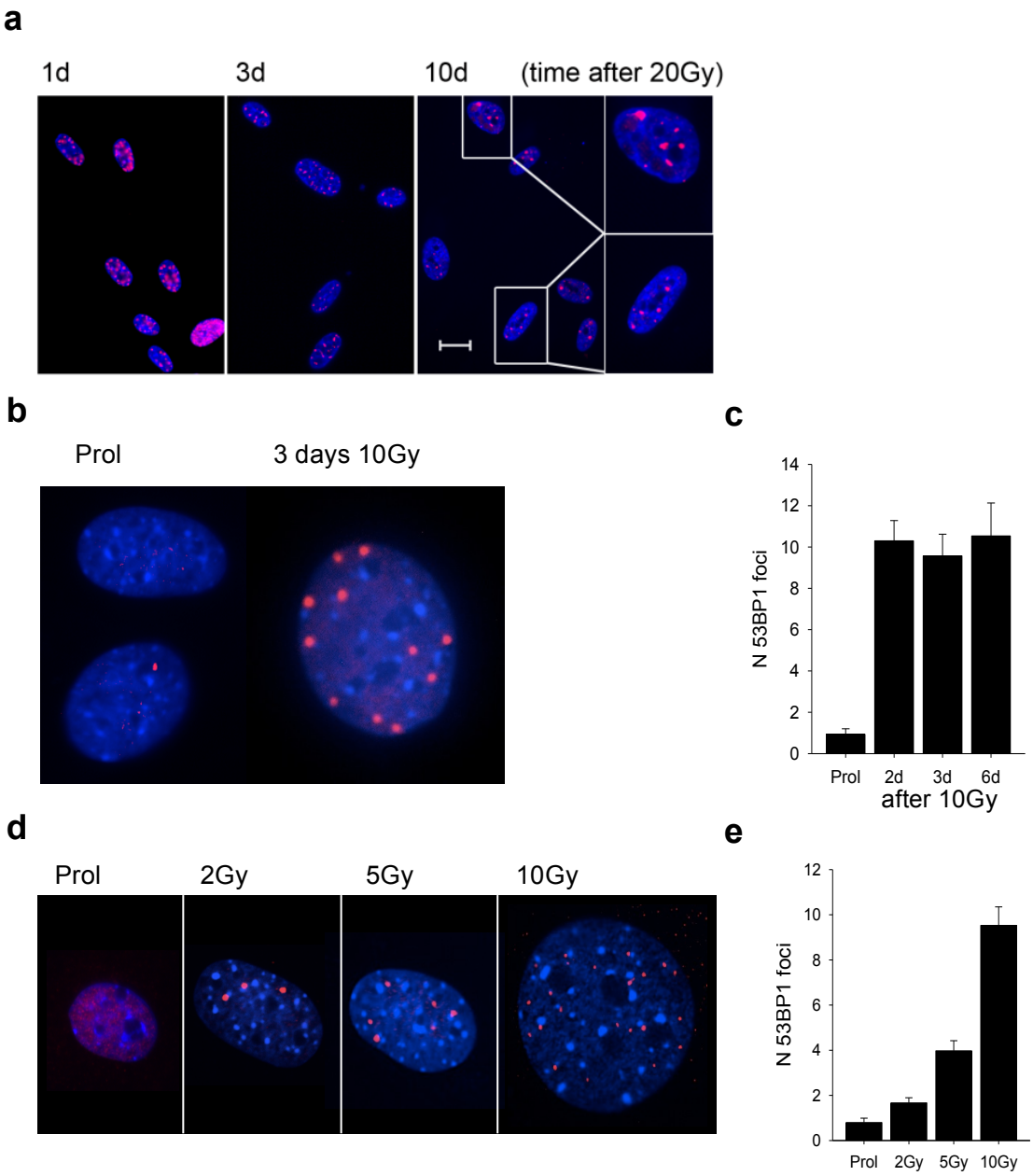


**FIGURE 3.1| Human and mouse fibroblasts have a chronic DDR in senescence**

**a)** γH2A.X-labelled double strand breaks (DSB) are seen in senescent MRC5 treated with 20Gy. Data are mean ± s.e.m. of *n*=15. Scale bar=10 μm; **b)** Representative image of 53BP1 damage foci in MEF in stress-induced senescence; **c)** Quantification of number of 53BP1 foci in MEF up to six days following ionising radiation (n=4,4,6,1 experiments); **d)** 53BP1 damage foci increase with increasing doses of DNA damage in MEF at day 3 post-irradiation (representative image); **e)** Quantification of number of 53BP1 foci 3 days following 10Gy. Data are mean ± s.e.m. of *n*=50-120 cells per condition. Prol – proliferating/proliferation.

To address this hypothesis, telomere labelling by FISH together with γH2A.X staining was performed after induction of senescence by ionising radiation. We saw that young cells barely had any γH2A.X foci or telomere-associated foci (TAF) (**FIGURES 3.2a, 3.2b** and **3.2e**). After increasing doses of X-ray radiation, more damage foci were located at telomeric regions and, furthermore, the percentage of cells harbouring telomere-associated foci (TAF) increased with time (**FIGURES 3.2b-3.2d**). Finally, once cells are senescent (9 days after irradiation) a mixture of TAF and non-TAF are present in these cells (**FIGURE 3.2e**).

To verify that DSB lesions signalled by phosphorylated H2A.X were preferentially enriched at telomeres ten days after 20Gy, we collaborated with Dr. Jelena Mann and conducted ChIP for γH2A.X along the short-arm of chromosome 12. This was then followed by a real-time PCR method for telomeric repeats previously described and validated for replicative senescent cells [179]. While distal regions from telomeres had very few γH2A.X associated to chromatin in senescence, sub-telomeric and telomeric repeats were highly enriched with phosphorylated histone H2A.X (**FIGURES 3.2f** and **3.2g**). Besides ionising radiation, also acute oxidative stress (induced by hydrogen peroxide) or treatment with DNA damaging drug neocarzinostatin induced TAF in MRC5 fibroblasts and consequently senescence (data not shown).

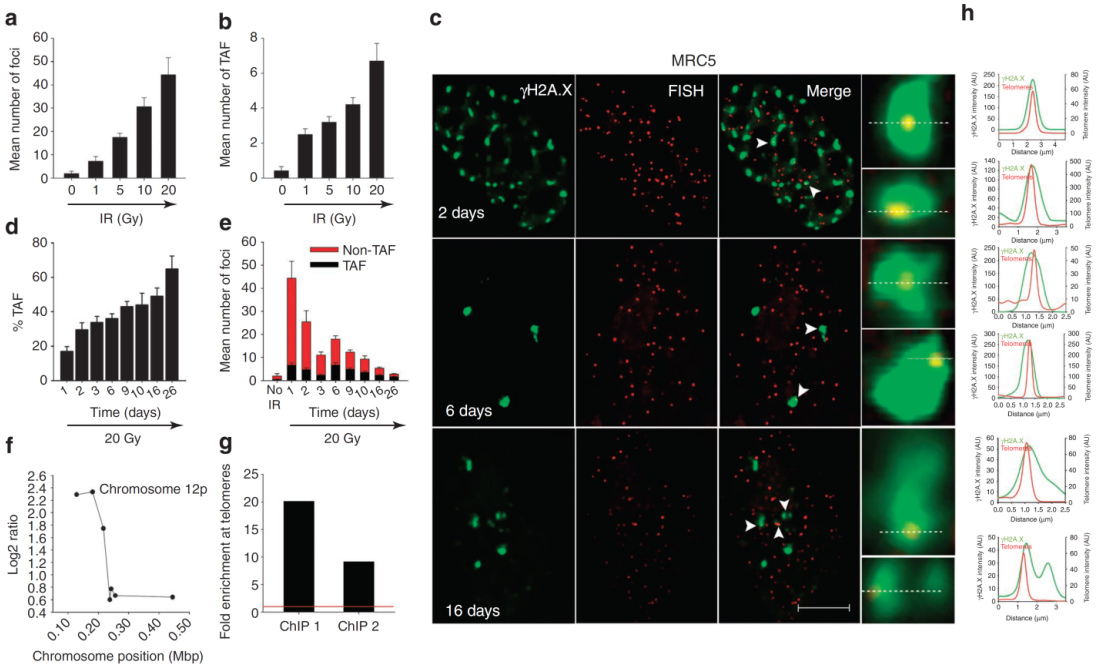


**FIGURE 3.2| DDF occur at telomeres in stress-induced senescent human fibroblasts**

**a)** γH2A.X foci numbers increase linearly with increasing doses of ionising radiation (1, 5, 10, 20Gy). Data are mean ± s.e.m. of *n*=15; **b)** Total number of telomeric colocalizing γH2A.X foci (TAF) 1 day post ionising radiation (1, 5, 10, 20Gy). Data are mean ± s.e.m. of *n*=15; **c)** Representative images of TAF in MRC5 fibroblasts 2, 6 and 16 days post 20Gy. Scale bar = 10 μm; **d**) Percentage of TAF up to 26 days after 20 Gy ionising radiation. Data are mean ± s.e.m. of *n*=15; **e)** Mean number of TAF (black) and non-TAF (red) up to 26 days after 20Gy ionising radiation. Data are mean ± s.e.m. of *n*=15; **f)** γH2A.X is enriched at sub-telomeric regions of chromosome 12p after 10 days 20Gy ionising radiation. Each PCR reaction was conducted trice and the data are mean of two independent ChIP experiments; **g)** γH2A.X protein is enriched at telomere repeats after 10 days 20Gy ionising radiation; red line denotes the non-irradiated control; **h)** Graphs represent quantification of γH2A.X (green) and telomere signals (red) in selected regions of interest (dotted lines **c)**).

Telomerase is a key enzyme that synthesises and elongates telomeric sequences. Moreover, telomerase prevents cells to enter replicative senescence and extends their replicative potential [35]. Telomere shortening has previously been shown to be responsible for triggering a DDR when cells reach the end of their replicative lifespan. In order to test whether TAF were generated independently of telomerase presence and possibly telomere shortening, we over-expressed hTERT in MRC5 fibroblasts [166] and characterised these cells in terms of TAF presence and other senescence markers following treatment with X-ray irradiation (**FIGURE 3.3**). MRC5-hTERT exhibited TAF after induction of senescence by ionising radiation likewise parental MRC5, TAF number was constant with time following irradiation and the majority of foci generated by ionising radiation were non-telomeric and gradually became repaired (**FIGURES 3.3a-3.3c**). MRC5-hTERT after X-ray ionising radiation still arrested irreversibly did not exhibit the Ki67 proliferation marker and were positive for Sen-β-Gal activity (**FIGURE 3.3d**).

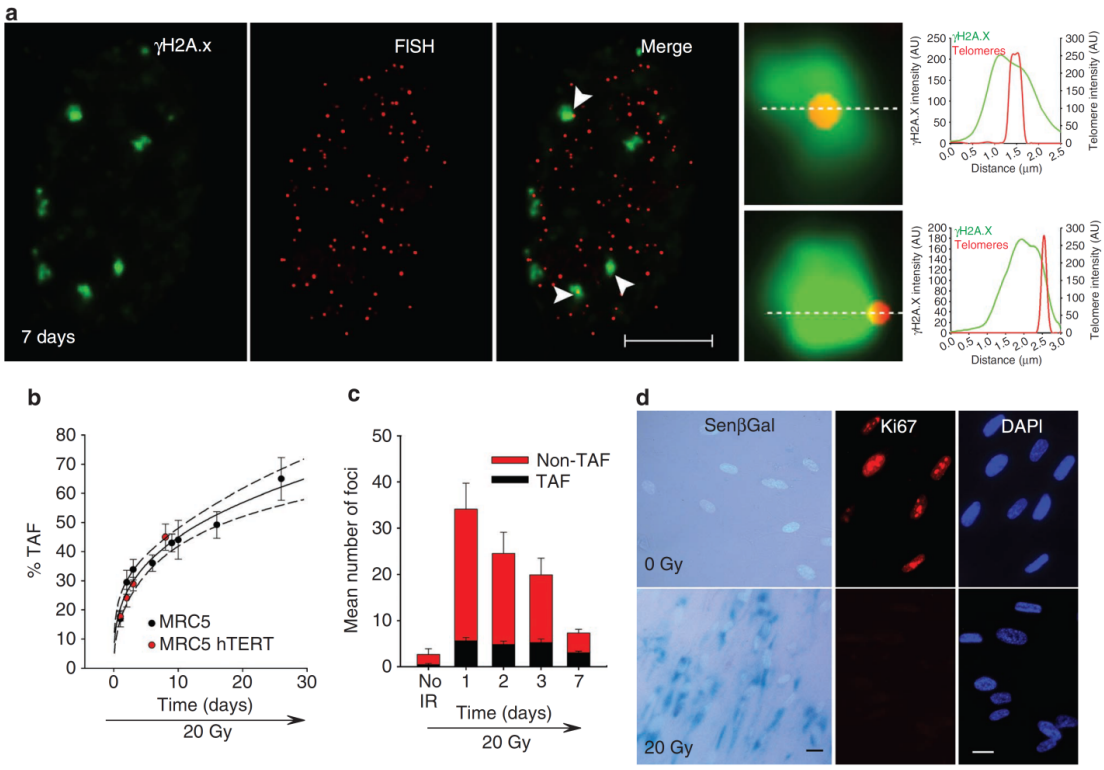


**FIGURE 3.3| TAF occur in stress-induced senescence in MRC5 fibroblasts over-expressing telomerase (hTERT)**

**a)** Representative images of TAF in MRC5 fibroblasts over-expressing hTERT seven days after 20Gy. γH2A.X foci (green), telomeres (red), white arrows indicating colocalizing foci are magnified in the right panel. Graphs represent quantification of γH2A.X (green) and telomere signals (red) in selected regions of interest (dotted lines). Scale bar=10 μm; **b)** Comparison between percentage of TAF in MRC5 with or without telomerase overexpression. Power curve (solid line) and 95% CI (dotted lines) (R=0.977, *p*=0.0001). Data are mean ± s.e.m. of *n*=15; **c)** Mean number of TAF and non-TAF in MRC5-hTERT fibroblasts up to seven days after 20Gy ionising radiation. Data are mean ± s.e.m. of *n*=15; **d**) Representative images of staining for Sen-β-Gal activity (DAPI – light blue, Sen-β-Gal activity – cytoplasmic darker blue) and proliferation (DAPI – blue, Ki67 – red). Scale bar=20 μm.

To better understand the nature of telomere-associated foci, mouse embryonic fibroblasts were transfected using AcGFP-53BP1c [167] and, upon the initiation of a DDR, foci dynamics were monitored using live-cell microscopy (**FIGURE 3.4**). In order to scrutinise DDF at telomeres we conducted microbead-mediated incorporation of a fluorescently labelled telomere PNA probe. Due to their stability, PNA probes form PNA/DNA heteromultiplexes that are suitable for visualisation of telomeres over several hours [169].

Comparable to what we observed by ImmunoFISH in human fibroblasts fibroblasts, TAF were induced and their numbers remained fairly constant over time in MEF following ionising radiation (**FIGURE 3.4a**). Additionally, 53BP1 foci repair kinetics in MEF was similar to γH2A.X foci repair kinetics in human MRC5 and, MEF equally presented an unresolved DDR (TAF and non-TAF) in senescence (**FIGURES 3.4b** and **3.4c**). In order to assess TAF persistence and reparability, live-cell imaging was performed three days post ionising radiation and foci-lifespan and their colocalization with telomeres was traced manually (**FIGURE 3.4d**). We observed that TAF were stable structures that remained present during the whole or the vast majority of the experiment (**FIGURES 3.4d-f**). In this experiment we calculated that on average TAF had a half-life of 90±11.9 minutes and about 50% of TAF survived more than six hours. Furthermore, the data highlights that non-TAF are the short-lived damage focus which have a half-life of 48±3.5 minutes and a maximal lifespan of about three hours (**FIGURES 3.4d-f**).

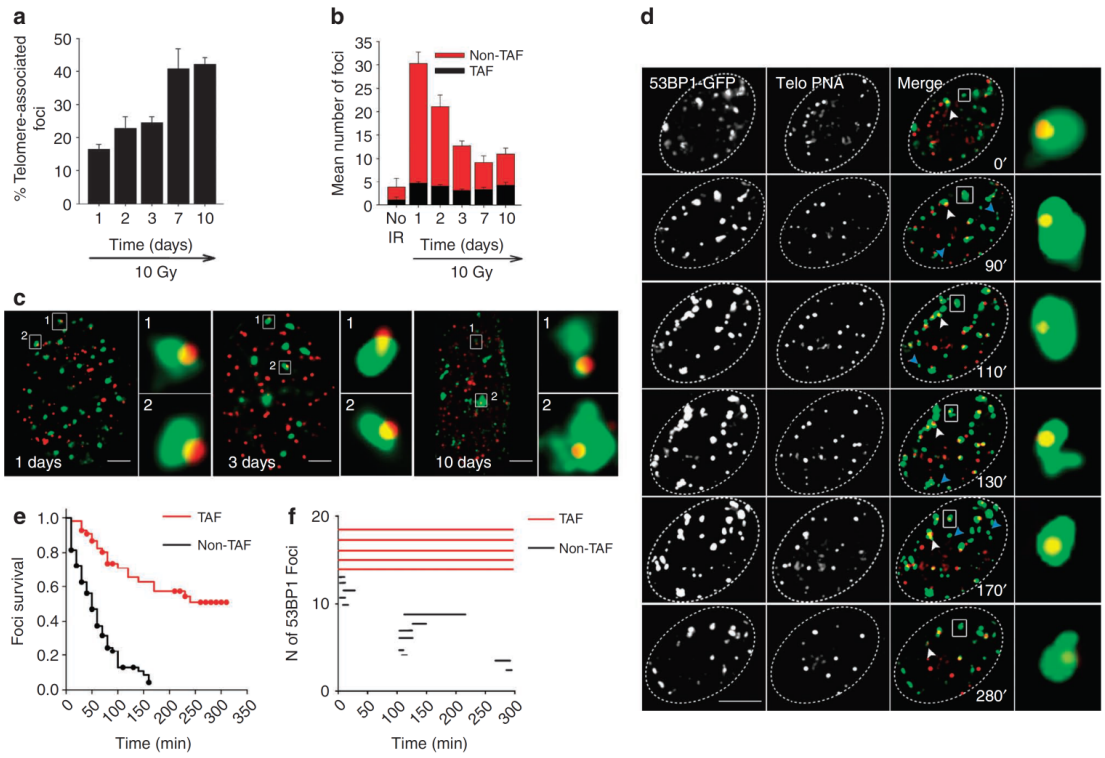


**FIGURE 3.4| TAF are long-lived while non-TAF are transient**

**a)** 53BP1 TAF percentage increases with time in MEF following 10Gy ionising radiation; **b)** Mean number of TAF and non-TAF in MEF up to ten days after ionising radiation (20Gy); **c)** Telo-FISH representative images of MEFs 1, 3 and 10 days following 10Gy irradiation. 53BP1 (green), telomeres (red) and yellow outline co-localisation (TAF). White boxes denotes TAF and image on the right portraits at a higher magnification of a single Z plane; **d)** Confocal life cell imaging of MEFs expressing AcGFP:53BP1 together with a PNA Cy5-labeled telomere probe three days post-irradiation at indicated times (minutes). Images are maximum intensity projections. The white arrows indicate TAF which were persistent during the entire time series (white boxes and magnified image on the right), blue arrows represent short-lived non-TAF; **e)** Kaplan-Meyer survival curves for AcGFP:53BP1 TAF and non-TAF. Two hundred foci were followed belonging to 8 cells, $p<0.001$ – Gehan-Brelow test; **f)** Representative AcGFP:53BP1 foci tracking during 6h in MEF three days post-irradiation. Each line represents one single focus identified at the indicated time interval. TAF (red) and non-TAF (black).

Following the *in vitro* observations, we asked if telomere associated foci would also be present *in vivo* in mouse organs and, if they would accumulate randomly with age. The reasons why we used mice has to do with: 1) the view that telomeres do not play an active role in mouse senescence [174] and, 2) due to the fact that mouse telomeres are extremely long [175].

To address this, we performed immuno-FISH in liver (**FIGURE 3.5g**) and small intestine (**FIGURE 3.5h**) from a mice cohort ranging from 3 to 42 months of age. In both organs we observed that TAF mean numbers per cell increased exponentially with age (**FIGURES 3.5a. and 3.5c**). Additionally, the percentage of foci co-localising with telomeres per cell (% TAF) also increased linearly on hepatocytes and on the small gut of mice with age (**FIGURES 3.5b and 3.5d**). Whilst the number of TAF increased significantly, damage located elsewhere in the genome (non-TAF) increased with age but not significantly (**FIGURES 3.5e and 3.5f**). Telomere shortening has been proposed as one source of telomere damage. Despite the fact that mice have huge telomeres [175], we analysed telomere length and tested whether TAF were preferentially at shorter telomeres. To test this, we used mean telomere intensity as readout for mean telomere length in both TAF and non-TAF. In the 36 months old intestinal crypts no significant alteration on telomere length was observed between TAF and non-TAF, whereas in hepatocytes, we saw a mild preferential location of TAF at telomeres with increased mean length (**FIGURE 3.5i**).

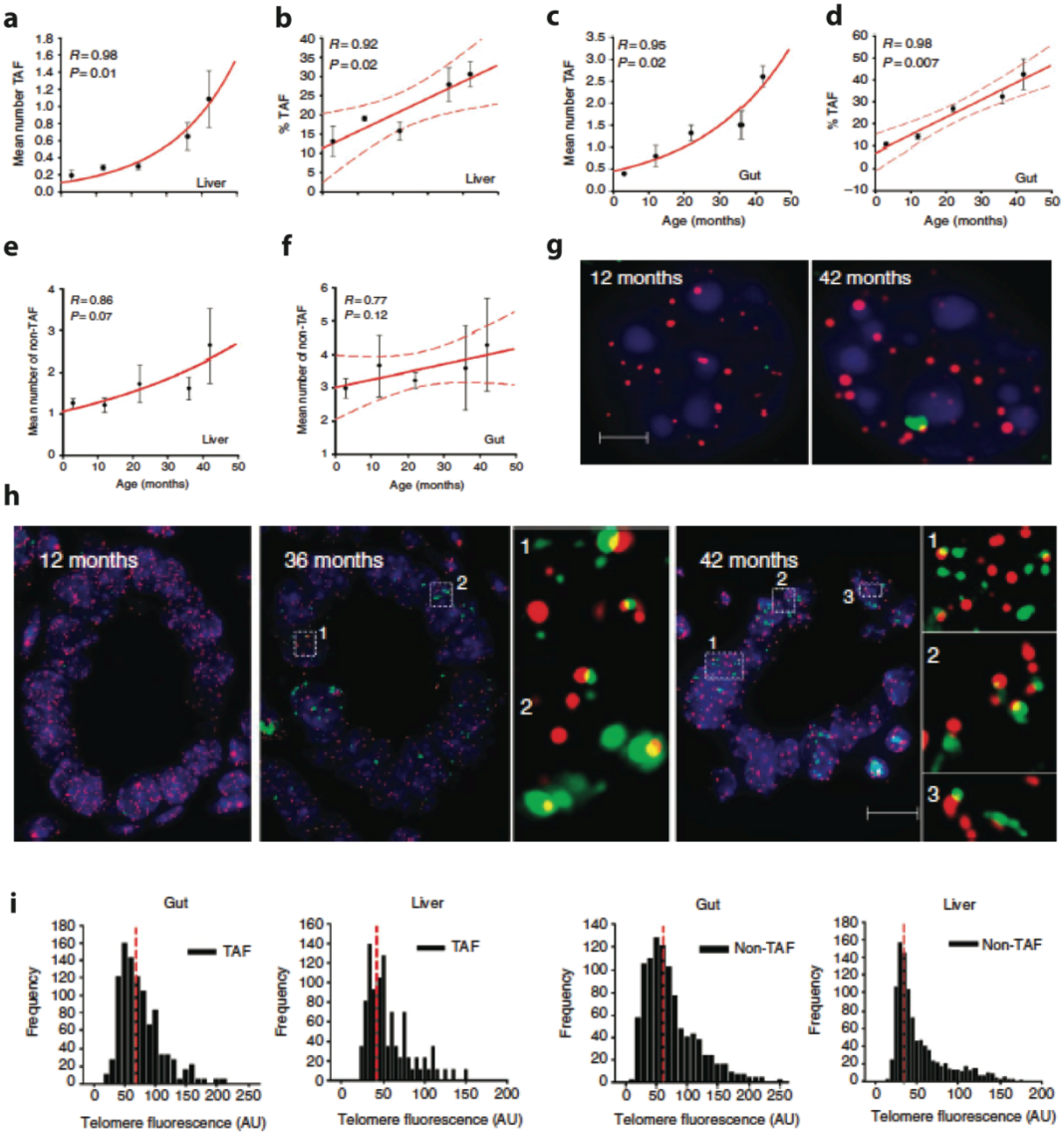
a
Mean number TAF
R=0.98
P=0.01
Liver
b
% TAF
R=0.92
P=0.02
Liver
c
Mean number TAF
R=0.95
P=0.02
Gut
Age (months)
d
% TAF
R=0.98
P=0.007
Gut
Age (months)
e
Mean number of non-TAF
R=0.86
P=0.07
Liver
Age (months)
f
Mean number of non-TAF
R=0.77
P=0.12
Gut
Age (months)
g
12 months
42 months
h
12 months
36 months
42 months
i
Gut
TAF
Liver
TAF
Gut
Non-TAF
Liver
Non-TAF
Frequency
Telomere fluorescence (AU)

**FIGURE 3.5| TAF increase with age in liver and small intestine of C57BL/6 mice**

**a)** Mean number of TAF per cell increases exponentially with age in hepatocytes from male C57BL/6 mice. Data are mean ± s.e.m. of *n*=3 per age group; **b)** Percentage of TAF increase linearly with age in hepatocytes from mice; **c)** Mean number of TAF per cells increases exponentially with age in the small intestine enterocytes from mice. Data are mean ±s.e.m. of *n*=3 per age group; **d)** Percentage of TAF increases linearly with age in enterocytes from mice; **e)** Mean number of non-TAF per cell does not increase with age in hepatocytes from mice; **f)** Mean number of non-TAF per cell does not increase with age in small intestinal enterocytes from mice; **g)** Representative immuno-FISH images of hepatocytes from 12-month- and 42-month-old mice. Green: γH2A.X; red: telomeres; blue: DAPI, Scale bar: 3μm; **h)** Representative immuno-FISH images in mice crypts at different ages (12, 36 and 42 months). Boxes indicate areas of colocalization between γH2A.X and telomeres (green: γH2A.X; red: telomeres; blue: DAPI; Scale bar: 20μm)(images are from one single Z plane); **i)** Histograms showing telomere intensity for telomeres colocalizing (or not) with DNA damage foci in both the liver and gut from 36-month-old mice; red dotted line represents median intensity. Mann–Whitney test shows no significant difference in telomere intensities distribution between TAF and non-TAF for the small gut ($p$=0.08) and a slight increase in liver telomere intensity in non-TAF ($p$=0.002). Intensity of 1,000 telomeres was analysed per condition.

## DISCUSSION

### Telomeric damage induces the DDR

Our data demonstrates that telomeres are hotspots for irreparable DSB. Here and other several reports described that telomeres are sources of senescence signals whether the damage was triggered by uncapped telomeres or genotoxic stress [14, 22]. It was previously demonstrated that telomere shortening trigger a normal DDR via p53, p21 and p16 [176][7] upon telomere uncapping. Telomere protection is regulated by the shelterin protein complex [180]. Removal of shelterin components induces acute phenotypes in which telomeres are perceived in a similar manner to genomic breaks.

Various reports have also highlighted that not only telomere shortening can induce the DNA damage response. Firstly, telomere-dependent DDR can occur not only due to telomere shortening, but also occur in long telomeres [177, 181] and in early-passage human primary cells. Additionally, replicative senescent cells harbour $DDR^{+}$ telomeres in which TRF2 and RAP1 (two shelterin proteins) are still present, therefore, evidencing presence of a DDR and a non-fusogenic state at telomeres [48]. Although TRF2 can be present at telomeric double strand breaks in senescent cells, TRF1 is about ten-fold more prevalent in its telomeric co-localisation than TRF2 [176]. Telomere uncapping triggers TRF2 displacement from telomeres [182], although its absence is not crucial for activation of a DDR [176]. This might suggest that TRF2 is a potentially limiting factor that thresholds telomere damage.

Chromosomal instability (namely anaphase bridges and metaphase fusions) arises whenever insufficient shelterin components such as TRF2 are not retained at telomere regions [182]. Uncapped telomeres spontaneously occur after telomere erosion and are characterised by the loss of the majority of shelterin proteins, and this is correlated with telomere shortening. Genetic expression of a TRF2 dominant negative form ($TRF2^{\Delta B \Delta M}$) can also drive cells into senescence [182-184] via oxidative stress [28]. Unlike genomic breaks, uncapped telomeres do not activate the G2/M checkpoint, but rather their damage is transmitted to the daughter cells which activate a p53-dependent G1 cell cycle arrest [39]. In senescent cells Chk2 is phosphorylated at

telomeres probably representing that telomeres engaged on a DDR due to uncapping [176]. Despite this observation, more insight if this process occurs at the shortest telomeres or at uncapped telomeres remains an attractive possibility.

Here we observed that human and mouse senescent cells accumulate up to 5 or 6 TAF per nucleus, which is in agreement with recent data in which the accumulation of 5 G1-phase DDR-positive telomeres are sufficient to trigger cellular senescence mediated by p53 [48]. Previous reports have observed a 20% co-localisation between γH2AX foci and telomeres [112], however our data suggests a higher percentage of TAF in senescent cells (40% in MEF and 40-60% in MRC5). Altogether these data contradict former reports in which no co-localisation was visualised between 53BP1 and TRF2 at telomeres following genotoxic stress [21].

### Why telomeres are preferentially targeted by oxidative and genotoxic damage?

Probabilistically, in order to obtain 4 or 5 TAF per cell post ionising radiation between 24000 and 30000 DSB would have to have been generated. Since this numbers hardly correspond to the reality (it is estimated that an average of 40 DSB are generated per Gy [185], this indicates that telomeres are particular susceptible to genotoxic insults and oxidative damage [42]. One reason could be the high abundance of guanine triplets present on the telomeric sequences that are highly prone to oxidative modifications [186, 187]. A second potential explanation could be the location of telomeres within the nucleus. Telomeres have been shown to be associated with the nuclear envelope during certain phases of the cell cycle (early G1) therefore, presenting themselves at the periphery of the nucleus [188]. Senescent cells are permanently arrested at G1 [1] therefore, many of their telomeres are likely to be at the nuclear periphery. Also senescent cells produce elevated levels of reactive oxidative species which cause DNA damage [28]. Another

possibility could be the proposed role of oxidative stress in reducing both TRF2 and TRF1 binding-activity to telomeres [43].

Very recent observations reinforce the idea that telomeres are hypersensitive regions to DNA damage not only during senescence. In more detail, during mitosis cells are very sensitive to ionising radiation because they inactivate DSB repair [189]. Moreover, during M-phase, DSB repair is inhibited, being therefore a conserved cellular mechanism in place to avoid telomere recombination and telomere fusions [190]. Additionally, forced activation of DNA repair during mitosis elicits telomere sister chromatid fusions leading to dicentric chromosomes and aneuploidy. This phenomenon is observed in the presence of exogenous genotoxic stress and is dependent on Aurora-B kinase [190]. This kinase has also been demonstrated to lead to telomere uncapping during prolonged mitosis arrest [191]. Finally the same study proposes that mitotic telomeres are unprotected due to Aurora B repression of shelterin [190].

Altogether, telomeres work as sentinels during cellular senescence due to a combination of vulnerability to oxidative damage, nuclear location and inhibition of DSB during mitosis.

### Telomeres and sub-telomeric regions have impaired DNA damage repair

γH2AX damage foci have the tendency to spread over adjacent areas where the DSB occurred [179]. In replicative senescent human BJ fibroblasts γH2AX have been shown to spread over 570 Kb into the sub-telomeric regions [179]. Similarly, our data also pinpoints that phosphorylation of H2AX increases when moving towards the edges of chromosomes including sub-telomeric and telomeric regions starting at approximately 250 Kb [179]. Telomeric single strand breaks and UV-induced damage are difficult to be repaired [192]. In yeast also sub-telomeric DSB repair is inhibited up to 0.6 Kb from telomeres [193]. Subtelomeres in human cancer cells have been shown to be deficient for DSB repair by unknown reasons [194]. Potentially these effects at subtelomeres are a combination of damage spread from telomeres, the telomere-position effect (TPE – reversible gene silencing due to telomere proximity) and epigenetic repression of repair mechanisms that could lead to

chromosomal instability (*e.g.* end-to-end fusions) and oncogenic transformation [195].

### Cells have more stable damage at telomeres

We observed that telomere-associated foci (TAF) are bigger than other genomic damage (data not shown and [3]), which matches previous observations in which large dimension foci are persistent in senescent cells [21]. Also our life-cell imaging corroborates that TAF are more stable than other transient damage located elsewhere in the genome. One possibility why TAF are bigger has been proposed to be due to aggregation of telomeres [48].

### Oxidative damage as instigator of TAF formation

A mixture of TAF and non-TAF is present in senescent cells (here) and [196]. Upon X-ray radiation, the percentage of TAF augments linearly with time suggesting that besides the original damage caused by radiation at telomeres, there is another motile force to induce TAF formation in cells. Prior work had shown by live-cell imaging that focus lifespan increased in both replicative senescence and irradiation-induced senescence of human fibroblasts [178, 197]. Under these conditions, half of all DDR foci were short-lived and dependent on oxidative stress [28]. Using life-cell imaging we show that TAF in MEF are long lived while the short-lived ones are transient (and likely to be ROS-dependent). Preliminary data from our group using the antioxidant N-acetyl cysteine (NAC) immediately after irradiation does not prevent the accumulation of TAF in MRC5 until day 3, pointing out that ROS scavenging for a short period of time does not prevent TAF generation. Despite the fact that TAF are not reduced *in vitro* under short antioxidant treatment, short-lived non-telomeric damage was strongly inhibited (data not shown). Overall, this negative result does not invalidate a role of ROS on TAF formation especially *in vivo* (discussed below). Besides oxidative stress, in OIS genome hyper-proliferation causes replication forks stalling and hinges full telomere DNA replication causing TAF [49]. In contrast, irreparable damage at telomeres can be irrespective of telomere length and cell proliferation (here and in [3, 4]).

### Does telomerase counteract telomere dysfunction in senescence?

In our hands, primary cells over-expressing telomerase once exposed to X-ray radiation arrested and were positivity for Sen-β Gal activity. Similarly, d'Adda di Fagagna has equally demonstrated that MRC5 overexpressing hTERT became senescent following X-ray irradiation and harboured senescent markers including Sen-β-Gal positivity [173]. Whilst we report that human MRC5 fibroblasts over-expressing telomerase have TAF, previous observations in another human primary fibroblast strain immortalised with hTERT no TIF were found [176]. A potential difference was that while we cultures our MRC5-hTERT at atmospheric oxygen conditions, Herbig *et al*. cultured their LF1 fibroblasts at hypoxic conditions (2% $O_2$)[176]. Could be this differences between TAF and TIF in hTERT over-expressing cells be due to oxidative stress? More explicitly, hTERT expression and transcription is up-regulated *in vivo* under hypoxic conditions via HIF-1a (reviewed in [198]). The presence of TAF in MRC5-hTERT cells reinforces the hypothesis that not only short telomeres can trigger a DDR. This matches the observations that hTERT expression does not stops stress-induced premature senescence (SIPS) and hence, senescence can be engaged independently of telomere attrition [199, 200]. More mechanistic insight will be required to understand why hTERT overexpressing cells have TAF but not TIF. Again telomere structural state, presence of shelterin components (such as TPP1) and a free telomere loop (t-loop) might influence hTERT activity and its recruitment to the telomere ends (reviewed in [201]).

### TAF are biomarkers of senescence

DNA damage is seen at telomeres of non-proliferating baboons' neurons, hepatocytes from mice and in baboons' skin fibroblasts [3, 4, 51]. Telomere damage bulked-up with age in mice liver and intestine and does not correlate with telomere length. Shelterin components are still present together with TAF that are not the shortest of telomeres (R. Anderson) there questions the dogma that only the shortest telomeres set a DDR. Non-telomeric damage (non-TAF) tends to increase with age, but not to significant levels, suggesting

therefore that this kind of DSB might have faster repair and turnover rates than those at telomeres.

We observe that TAF number and percentage that accumulate with age are more drastically seen in the gut (high proliferative tissue) rather than in liver (which is largely a post-mitotic tissue). Indeed, TAF are also increased in the transient-amplifying cells of the gut that have a high mitotic index (data not shown), suggesting a role for DNA replication in TAF generation, possibly due to the mitotic inhibition of telomere repair proposed *in vitro* [190].

Cellular senescence can function as a tumour suppression mechanism. Although TAF can be used as a biomarker of senescent cells and as a predictor of mean and maximum lifespan of long-lived mice cohorts [50], this marker's robustness in cancer is weak [49]. *In vivo*, TAF are observed in melanocytes of benign- and dysplastic-neavi, epithelial cells of precursor lesions to breast- and colon- cancers but, are absent in melanoma, colon- and breast carcinoma [49]. Oncogenic signals trigger hyper-proliferation, replication forks stalling and aleatory completion of telomere DNA replication [49]. Telomere damage independent of length has therefore roles in tumor suppression [49]. Furthermore, telomere length independent roles of telomerase in tumour progression can also be observed since over-expression of TERT cannot bypass TAF induction by irradiation, chemotherapy induced DNA damage (using neocarzinostatin) or hydrogen peroxide [3].

Similarly to Herbig's data [49], we observe that mouse liver treated with the carcinogenic agent diethylnitrosamine (DEN) do not have TAF in the cancer areas but, only on the adjacent non-tumorigenic tissue (observation by Diana Jurk). This perhaps supports the idea that genomic instability at telomeres might be a requisite for cellular transformation and, additionally, senescent cells that repair their telomeric damage or, that may lose their telomere integrity might be able to bypass senescence.

## Perspectives

Can telomeres trigger a DDR with shelterin components still present? Roger Reddell's and Jan Karlseder's groups have put forward a model in which telomeres can be adopt three differential protective states that regulates distinct cellular functions [202]. In more detail, telomeres adopt a closed-state that prevents the DDR activation via insulation of the chromosome end within the telomere loop (T-loop) [32]. An intermediate stage can be observed once cells reach their replicative lifespan or, in cells with insufficient insulation of telomeres by sheltering components leading to exposure of chromosome termini and elicitation of a DDR. Overall, more experiments have to be conducted to verify which shelterin components and their abundance play a role in protecting telomeres effectively from damage.

In summary, telomeres seem to be more vulnerable to DNA damage and, therefore, they may act as sentinels to oxidative- and genotoxic- stress mediated DNA damage within senescent cells.

# CHAPTER 4 – MITOCHONDRIAL BIOGENES IS CRUCIAL FOR THE INDUCTION AND DEVELOPMENT OF THE SENESCENT PHENOTYPE VIA THE mTOR PATHWAY

## INTRODUCTION

According to the endosymbiotic theory, mitochondria are derived from an ancestral α-proteobacteria that was incorporated into the eukaryotic cell [203]. With time, mitochondria have gradually transferred its genes to the nuclear genome. Nowadays, the mitochondrial genome is characterized for having only 37 genes which 13 of those encode some components of the respiratory chain, 2 ribosomal RNAs and several tRNAs. Besides ATP generation, mitochondria play important roles many cellular processes like metabolisms, development, apoptosis and ageing [204]. Mitochondria have been also implicated in cellular senescence through its capacity to produce reactive oxygen species (ROS), which impinge on random molecular damage. More precisely, mitochondrial ROS promotes genomic damage [174], accelerates telomere erosion [6] and sustain signalling pathways necessary for the maintenance of the senescent arrest active [28]. Controlling mitochondria numbers is a complex balance between biogenesis [89], fusion and fission [92] and mitophagy [91], which might have serious repercussion on disease (such as neurodegenerative diseases) [87]. Although increased mitochondrial biogenesis is benefic in settings of exercise resistance and endurance, for instance, mitochondria over-proliferation was described to promote cardiomyopathy in mice [205]. Mitochondria biogenesis is an intricate process regulated by the PPAR gamma co-activator-1 (PGC-1) family of nuclear transcriptional co-activators, which have a critical role on the control of lipid, glucose and energy metabolism. Three main PGC-1 isoforms are known: PGC-1α, PGC-1β and PPRC (PGC-1-related co-activator)[206]. Wu and colleagues demonstrated that PGC-1α co-activates nuclear respiratory factor 1 (NRF1) and -2 (NRF2)[207]. NRFs regulate expression of mitochondrial transcription factor A (mtTFA/TFAM), a nuclear-encoded transcription factor, essential for replication, maintenance and transcription of mitochondrial DNA

[208-212]. Besides PGC-1α, PGC-1β is critical for a normal mitochondrial gene program and thought to regulate basal mitochondrial biogenesis levels [213, 214] in cells and in a variety of tissues [207, 215, 216]. Despite the wide literature available on PGC-1α and mitochondrial biogenesis the role of PGC-1β-mediated mitochondria biogenesis is far less known. Overall, mitochondria content within cells have been hypothesised to be an important factor underlying cellular senescence [217].

Besides formation of new mitochondria, mitochondria content within cells is also regulated by autophagy. Autophagy is a homeostatic cellular process that eliminates old or malfunctioning proteins and organelle in the cellular cytoplasm. Furthermore, this recycling process allows the release of nutrients for cellular functions. During metabolic challenge, autophagy assumes key roles on cellular survival. The autophagic process can be categorized depending on the nature of the cargo degraded. Macroautophagy (commonly referred as autophagy) describes the mechanism by which cytoplasmic components (proteins and organelles) are engulfed in double-/multi-vesicular bodies – autophagosomes – and their posterior delivery to lysosomes for large scale degradation [218]. The molecular biology behind the autophagic process started with the discovery of the Atg (autophagy) genes in yeast in the early 1990's [219]. Atg5 protein is a major component of the canonical autophagy pathway being involved on the formation of the autophagosome membrane and it localizes preferentially on the cytoplasmic side of the outer limiting membrane. The Atg5-Atg12-Atg16 polymer has coating functions that aids the autophagosomal membrane curvature [220]. Cells without Atg5 have a compromised autophagy and have been shown to accumulate dysfunctional mitochondria [98].

Besides the role autophagy on mitochondrial dysfunction and senescence, mitochondrial morphology and numbers regulation by fission and fusion events were also shown to contribute to cellular senescence [96, 221]. In more detail, decreased mitochondrial fission by hFIS1 lead to excessive

mitochondrial elongation. This sustained mitochondrial elongation was then associated with increased ROS, decreased mitochondrial membrane potential and DNA damage. Additionally, cells in which hFIS1 was silenced are morphologically similar to senescent cells in terms of its morphology, in other words, they are large, flat, and had increased cellular granularity. Besides this, cellular proliferation was significantly reduced and cells were positive for Sen-β-Gal activity. Finally this study showed that silencing of hFIS1 or OPA1 (a protein required for mitochondrial fusion) could rescue the above-mentioned senescent markers. Altogether, this data highlight the importance of mitochondrial fusion and fission balance in cellular senescence [96].

## AIMS

Despite the fact that mitochondria is known to be contribute to cellular senescence, the molecular pathways linking mitochondrial homeostasis during cellular senescence are less understood. Based on this, we sought to investigate:

- If mitochondria biogenesis does plays a role during cellular senescence
- If impaired mitochondrial clearance (via autophagy) impacts on the senescent phenotype
- Does the mTOR pathway play a role in the induction and/or in the maintenance of stress-induced cellular senescence via mitochondria dysfunction?

## RESULTS

### I. Inhibition of the mTOR pathway reduces senescence markers

Senescent cells are phenotypically hypertrophic compared to young cycling cells [14]. Likewise, we see that primary human and mouse fibroblasts increased their size as a consequence of extensive replication or, of the activation of the DDR that would culminate in senescence (**FIGURES 4.1a-4.1c**). Cellular growth can be coordinated by the mTOR pathway [222]. We observed mTORC1 activation during early stages of senescence induction in human fibroblasts (**FIGURE 4.2a**). To address a potential role of the mTOR pathway in modulating cellular senescence we devised a series of experiments in which this pathway was targeted either chemically or genetically. Based on previous data from our group in stress-induced senescence on MRC5 cells, we chemically inhibited mTORC1 activity using 100nM of rapamycin since this concentration fully ablated mTORC1 activity (**FIGURE 4.2a**). Following this intervention, both human and mouse embryonic fibroblasts in stress-induced or replicative senescence were analysed for senescence markers including DNA damage foci, ROS, Sen-β-Gal positivity, mitochondrial mass and cell size (**FIGURES 4.2**, **4.3** and **4.6**).

Consistent with the observation that mTORC1 activity was increased following 20Gy and that rapamycin decreased fully mTORC1 activity (**FIGURE 4.2a**), human MRC5 treated with rapamycin were smaller than control irradiated cells, were more elongated and looked similar to young fibroblasts (**FIGURE 4.2b**).

The DNA damage response is one trigger and effector pathway of cellular senescence. We noticed that γH2A.X damage foci were significantly reduced on cells treated with rapamycin from day 3 post-irradiation but, not prior to that time point (**FIGURES 4.2c** and **4.2d**). Additionally, using an alkaline COMET assay (which identifies DNA double-strand breaks - DSB and single-strand

breaks - SSB) we confirmed that rapamycin treatment hinders DNA damage accumulation at those time points (data not shown). Lastly, we saw reduction of p21 protein and mRNA levels upon mTORC1 inhibition (**ANNEX 1**). Regarding proliferation, rapamycin reduced proliferation of young cells (perhaps leading to quiescence) and, did not rescue proliferation of stress-induced senescent cells (**FIGURE 4.2e**). Surprisingly, inhibition of mTORC1 for three days following irradiation with rapamycin and, subsequent removal of rapamycin lead to a 15% rescue in cellular proliferation at day ten (**ANNEX 1**). Increased mitochondrial content and reactive oxygen species are another two features of senescent cells. In X-ray irradiated cells both markers were reduced once mTORC1 was inhibited by rapamycin (**FIGURES 4.3d**, **4.8** and **4.10**).

Additionally, data from our group has demonstrated that in irradiation-induced senescent MRC5 fibroblasts pro-inflammatory IL-6 protein levels were 5-fold decreased after nine days upon rapamycin treatment (**ANNEX 1**). Besides IL-6 and while performing a cytokine mRNA array, we saw that mTORC1 inhibition stopped the majority of the SASP components expression including IL-8, GRO-α, TNF-α, IFN-γ but, had hardly any effect on IL-1α or IL-1β (**ANNEX 1**). Finally, also Sen-β-Gal positivity was reduced using rapamycin during stress-induced senescence (**ANNEX 1**).

Similarly to the aforementioned phenotype in MRC5, primary mouse embryonic fibroblasts (MEF) increased mTORC1 activity following ionising radiation and, when MEF were treated with 100nM of rapamycin mTORC1 activity was fully ablated (**FIGURE 4.3a** and data not shown). Senescence-associated markers were reduced including: cell size (**FIGURE 4.3b**), mitochondrial mass (**FIGURE 4.5a**) and ROS levels (**FIGURE 4.3d**). Additionally, 53BP1 damage foci, p21 protein levels and Sen-β-Gal positivity were diminished following rapamycin treatment (**FIGURES 4.3c, 4.3e** and **4.3f** respectively).

Overall, this data places the mTOR pathway as a central mediator of the early events that drive the senescent phenotype.

In order to strengthen the argument that mTORC1 is involved in senescence, we used human embryonic kidney (HEK293T) cells containing a doxycycline-inducible short-hairpin RNA construct against either TSC1 or TSC2 (**FIGURE 4.4a**). Knockdown (KD) efficiency and expression levels were both determined by the percentage of cells expressing the shRNA (GFP – positivity)(**FIGURE 4.4b**) or by western blot (**FIGURE 4.4c**). Doxycyclin-induced cells showed enhanced constitutively active mTORC1 activity and increased cell size (**FIGURES 4.4d** and **4.4e**). Phenotypically these hypertrophic cells had more γH2A.X damage foci and higher levels of p21 protein upon TSC2 silencing (**FIGURES 4.4h** and **4.4g**). Upon TSC2 KD, cells had enhanced ROS and higher levels of the mitochondrial biogenesis regulator PGC-1β (**FIGURES 4.4f** and **4.4i**). These preliminary results suggest that mTORC1 hyper-activation by TSC2 silencing leads to the appearance of some senescence markers.

Besides TSC2 silencing, we also constitutively activated mTORC1 using a mutated form of the GTPase Rheb - RhebN153T - in primary mouse fibroblasts (MEF)(**FIGURE 4.5**). In terms of cell size we saw an increase (**FIGURE 4.5a**), which did matched with the increased mTORC1 activity (**FIGURE 4.5b**). In proliferating conditions, MEF expressing RhebN153T show declined Ki67 levels (**FIGURE 4.5c**), increased synthesis of mitochondrial proteins (VDAC and TOMM20)(**FIGURE 4.5d**). Furthermore, more DNA damage foci were detected under concurrent activation of the DDR and RhebN153T-mediated mTORC1 activation (**FIGURE 4.5e**). Finally, RhebN153T expression lead to increase fraction of cells positive for Sen-β-Gal (**FIGURE 4.5f**).

In order to address a potential role of mTORC1 on the maintenance of cellular senescence we treated replicative senescent (RS) cells with rapamycin. Firstly we observed that senescent cells halved their cell following three days treatment and remained small during the whole experiment (**FIGURE 4.6a**). Following three days treatment we detected a reduction of mitochondrial mass but not superoxide levels (**FIGURE 4.6c**). Only at day ten of chronic rapamycin use we noticed less ROS levels (**FIGURE 4.6b**). Although no differences were seen in terms of 53BP1 foci upon rapamycin treatment, the number of Sen-β Gal positive cells significantly declined by day ten (**ANNEX 1**). Furthermore, we saw a decline of mitochondrial DNA copies (mtDNA) upon mTORC1 inhibition (**FIGURE 4.6d**). We also preliminary observed that in RS cells, rapamycin was unable to fully abrogate mTORC1 activity (personal communication from B. Carroll and V. Korolchuk). Finally, nutrient starvation (which normally halts mTORC1 activity) was also not effective in fully abolish mTORC1 activity (in collaboration with B. Carroll and V. Korolchuk - [223]. These findings indicate perhaps that the mTOR nutrient signalling pathway becomes deregulated during cellular senescence.

Altogether, mTORC1 activity is changed during cellular senescence and this pathway is required for the sustainability of certain senescent traits such as ROS, high mitochondrial mass, DNA damage, increased cell size, Sen-β-Gal positivity and the senescence secretome (SASP/SMS).

## II. The DDR is linked to mitochondrial biogenesis via the mTOR pathway

Mitochondrial mass increase has been observed in replicative and oncogene induced senescence [59, 76]. In order to investigate the link between the DNA damage response (DDR) and the mitochondrial increase we initially triggered a DDR using ionising radiation, oxidative stress (with $H_2O_2$), telomere uncapping, chemotherapeutic or DNA damaging drugs in a wide panel of mouse and human primary and cancer cells. A mitochondrial mass increase, between two- and four-fold was observed (**FIGURE 4.7a**).

Further work conducted in the lab has demonstrated that kinetically, mitochondrial proteins (e.g. NDUFB8, SDHA, UQCRC2 and TOMM20) expression and mitochondrial mass peaked between day one and three after ionising radiation. Both in human and primary mouse fibroblasts, we saw that the mitochondrial increase was linearly correlated with the dose of X-ray irradiation and consequently with the number of DDF (**FIGURES 4.7b**, **4.7c** and **4.13g**). Another positive correlation was seen between mitochondrial mass and positivity for Sen-β-Gal activity. Both in MRC5 and in MEF we observed two negative correlations between mitochondrial mass increase and proliferation, and between mitochondria mass increase and decreased p21 levels (data not shown). In order to confirm that mitochondrial numbers and volume fraction increased following X-ray irradiation, similarly to what was previously described in replicative senescence [59], we used transmission electron microscopy (TEM). Using this technique we observed increased mitochondrial number and volume fraction three days following irradiation (**FIGURE 4.7d**). Additionally, we saw that mitochondria DNA copy number was also increased following activation of a DDR in 3 different cell lines: MEF, MRC5 and HEK293T cells (**FIGURE 4.7e**).

Reactive oxygen species (ROS) and mitochondrial mass increased in parallel following activation of the DDR. Moreover, when ROS levels were normalised per mitochondrial mass unit there was no change (however one should keep in mind that there is an increased number of mitochondria in senescence). Together with this, addition of PBN or NAC quenched the ROS levels per cell but unaffected mitochondrial mass during stress-induced senescence (**FIGURE 4.7f**).

Previously, we observed that inhibition of mTORC1 with rapamycin led to decreased mitochondria mass in MRC5 and MEF. In order to verify that the effects of rapamycin were not constrained to ionising-radiation-induced

senescence in MRC5 and MEF, we took all the cell lines depicted in **FIGURE 4.4a** and we treated them with rapamycin immediately after the multiple senescence triggers. We realised that mTORC1 inhibition induced a universal response by reducing mitochondrial mass (**FIGURE 4.8a**). This was further confirmed used MitoTracker Green or immunostaining against mitochondrial protein SDHA (**FIGURES 4.8b** and **4.8e**). Additional work conducted in the lab has demonstrated by western blot that mitochondrial proteins of different complexes of the electron-respiratory chain (NDUFB8 – CI, SDHA – CII, UQCRC2 – CIII, MT-CO1 – CIV) and TOMM20 were decreased following rapamycin treatment. Using TEM we also saw that irradiated MRC5 treated with rapamycin had fewer mitochondria (**FIGURE 4.8c**). Moreover, both MRC5 cells and primary MEF under rapamycin conditions had fewer mitochondrial DNA copies (**FIGURES 4.8d** and **4.8f** respectively). Finally, addition of rapamycin does not change the ratio between ROS and mitochondrial mass (**FIGURE 4.8g**).

Next, we aimed to dissect links between the DDR towards mitochondrial mass via mTORC1. Whilst examining the literature available [224, 225], we hypothesised that the mechanism could be a phosphorylation cascade from ATM towards AKT and, from AKT towards mTORC1. Firstly, after induction of a DDR we inhibited ATM kinase and mTORC1 chemically alone or jointly. We then proceeded to analyse mitochondria mass by FACS, γH2A.X foci, p21 and SA-β-Gal positivity and we observed that both single and double inhibitions provided the same outcome, suggesting that these two signalling nodes are connected with no further cumulative effects (Rhys Anderson – **ANNEX 2**). Furthermore in MRC5, inhibition of ATM lead to decreased phosphorylated AKT (S473), less phosphorylated p70S6K1 (a direct readout for mTORC1 activity), less p21 and less NDUFB8 protein levels (data not shown). Irradiated HEK293T cells treated with ATM inhibitor Ku55933 lead likewise to a reduction of phosphorylated p70S6K1, p21 and mitochondrial VDAC protein levels (**FIGURES 4.9a-4.9c**). Of note, triple inhibition of PI3K, mTORC1 and mTORC2 by LY294002 led similarly to a reduction of mitochondrial mass in senescence (data not shown).

After establishing this link, we focused on the downstream mechanism of mTORC1 that would be interfering with mitochondrial content. We started looking into autophagy, a known process that recycles damaged organelles and proteins. The rationale behind this was that mTORC1 inhibits autophagy [226], hence inhibiting mTORC1 with rapamcyin would promote autophagy, therefore being a mechanism for the reduction of mitochondrial content observed whenever mTORC1 was inhibited.

To address this, we used ATG5 knockout (KO) MEF that have defective autophagy (for instance lacking LC-3 an essential protein for the autophagosome formation)(**FIGURE 4.10a**). Prior to induction of a DDR, Atg5-null and wild-type (WT) MEF showed no differences in terms of size, number of DDF, ROS or mitochondrial mass levels. After activation of a DDR by ionising radiation we observed that ATG5 knockout MEFs had more 53BP1 damage foci, had higher ROS and higher mitochondria mass levels compared to matched wt control MEF (**FIGURES 4.10b** and **4.10c)**. Additionally, Atg5 KO MEF had significantly larger surface areas than wild-type controls following IR (at three and six days after X-ray irradiation)(**FIGURE 4.10b).** To address if mitochondrial mass decrease observed by rapamycin treatment was dependent on autophagy, we treated both cell lines with rapamycin three-days following X-ray radiation (**FIGURE 4.10c)**. We observed that both ROS, 53BP1 foci and mitochondrial mass were significantly reduced in both cell lines upon mTORC1 inhibition (**FIGURE 4.10c**), suggesting that the effects of rapamycin observed at 3 days after X-ray irradiation are not solely dependent on activation of autophagy.

Cellular autophagic activity can be assessed by the autophagic flux analysis. This process comprises the autophagosome synthesis, the delivery of the autophagic substrates to the lysosome and the degradation of the autophagic substrates (LC3-II and p62) inside the lysosome [227]. If there is a blockage on autophagy LC3-II and p62 accumulate. Work done in the lab by Graeme Hewitt showed that the autophagic flux seems not to be altered on the first

days following activation of the DDR by X-ray radiation. This data indicates that the increased mitochondrial content on the early stages after activation of a DDR, are likely not a consequence of impaired mitochondrial degradation, but rather, activation of mitochondrial biogenesis.

## III. PGC-1β mitochondrial biogenesis is essential for cellular senescence

Based on the previous results we hypothesised that maybe the formation of new mitochondria (biogenesis) was being affected by mTORC1. Firstly we started to look into two master-regulators of mitochondrial biogenesis – PGC-1α and PGC-1β – mRNA and protein levels following a DDR.

After we induced senescence by X-ray irradiation in MRC5 human fibroblasts, and following the induction of a DDR, we observed increased protein and mRNA levels of PGC-1α and increased PGC-1β mRNA levels. That increment was halted once rapamycin was added (**FIGURES 4.11a-4.11c**). Secondly, we analysed wild-type MEF and following induction of a DDR we saw increased PGC-1α and PGC-1β (**FIGURES 4.12a** and **4.12b**). Finally, we observed increased mRNA levels for both co-transcriptional factors PGC-1α and PGC-1β once cells became senescent (**FIGURE 4.12c**).

Additionally, hyper-activation of mTORC1 by TSC2 silencing (**FIGURE 4.4e**) lead to increased p21 levels (after three days after doxycycline addition) and increased levels of PGC-1β (at ten days after doxycycline addition) and (**FIGURES 4.4g** and **4.4i**).

Since we saw that mitochondria biogenesis was being affected downstream of the mTOR pathway and, once this pathway was able to modulate the senescent phenotype, we made several working hypothesis:

1. Does mitochondria biogenesis impact on the senescent phenotype via ROS?
2. Are there cumulative effects between mitochondria biogenesis and the mTOR pathway?

To test the first question we used multiple systems that would manipulate mitochondrial biogenesis and mitochondrial content within cells. Those included decreasing mitochondrial biogenesis using PGC-1β KO MEF, increasing mitochondrial biogenesis by over-expression of PGC-1β and, increasing mitochondrial content and TCA cycle usage by pyruvate addition (this Chapter and **Chapter 5**).

Primary PGC-1β KO and wild-type matched MEF were induced to become senescent using either ionising radiation or by culturing under normoxic conditions (following the rational that MEF under atmospheric oxygen conditions became senescent) [174].

Firstly, we confirmed that MEF lacking PGC-1β had less mitochondria and, that mitochondrial biogenesis was impaired on these cells following 10Gy. This was achieved by using either Mitotracker Green staining, by flow cytometric analysis – NAO staining, by mtDNA copy assay, and by WB against VDAC (**FIGURES 4.13a-4.13d**). Furthermore, PGC-1β KO MEF were unable to increase SDHA expression back to wild-type control levels upon increased doses of ionising radiation (**FIGURE 4.13e**). Furthermore, we found no compensatory effects of PGC-1α in PGC-1β-null MEF following ionising radiation (**FIGURE 4.13f**). Finally, a very strong correlation between DNA damage (53BP1 numbers) and mitochondrial mass was observed in wild type and PGC-1β KO MEF (**FIGURE 4.13g**).

Besides mitochondrial content being altered, also senescence markers were changed among which were 53BP1 DDF, p21 and p16 levels, proliferation, Sen-β-Gal and reactive oxygen species (**FIGURE 4.14)**. Regarding the DNA damage response, we observed that in PGC-1β KO MEF 53BP1 damage foci were reduced so were p21 (a downstream target of p53) levels (**FIGURES 4.14a** and **4.14b)**. Finally, p16 mRNA levels were also dampened nine days post-irradiation (once cells became senescent)(**FIGURE 4.14c)**.

In the case of proliferation we observed that while wild-type MEF arrested, there was about 20% of PGC-1β KO MEF still cycling at day three (**FIGURE 4.14e**) and circa 5% were still proliferating at day nine after 10Gy (data not shown). Together with this, we saw that the percentage of PGC-1β KO MEF positive for Sen-β-Gal activity (at day nine and day fifteen after ionising radiation) was reduced compared to matched wild-type controls (**FIGURE 4.14h** and data not shown). Of note, we also noticed that pro-inflammatory chemokine CXCL1 (or GRO-α) was reduced in PGC-1β KO MEF nine days following irradiation, indicating perhaps that the senescence-associated secretory phenotype (SASP) might also be down-regulated in these cells (data not shown). Finally, we saw a reduction of ROS in PGC-1β KO MEF both in proliferating or following ionising radiation when compared to wild-type cells (**FIGURE 4.14f**).

Based on these results we thought that perhaps the antioxidant defence mechanisms could explain the lower ROS levels observed. To address this, we probed for superoxide dismutase 2 (enzyme responsible for the conversion of superoxide into hydrogen peroxide). The rationale for looking into SOD2 has to do with the fact that SOD2 is a know target of PGC-1α [228]. Another reason is because it was recently proposed that SOD2 can be up-regulated in certain keratinocytes cell lines upon rapamycin treatment [229]. While wild-type MEF increased mitochondrial SOD2, in PGC-1β KO cells SOD2 expression did not increased following irradiation (**FIGURE 4.14g)** suggesting perhaps, that the decreased ROS levels seen on PGC-1β KO

MEF cannot be explained by up-regulation of ROS-detoxifying enzymes such as SOD2.

Having established that PGC-1β-driven mitochondrial biogenesis impacted on cellular senescence we conducted experiments in which this biogenesis orchestrator was enhanced and we proceeded to characterise those transfected cells in terms of senescence markers. Firstly, we acquired a mouse PGC-1β plasmid (**FIGURE 4.15a**) and we checked by restriction enzyme analysis if the construct was correct (**FIGURES 4.15b** and **4.15c**). Then we proceeded to transfect MEF and we verified that PGC-1β protein was being expressed (nuclear staining)(**FIGURES 4.15d** and **4.15e**). Finally, mitochondrial SDHA protein levels were augmented upon PGC-1β transfection (**FIGURE 4.15f**), validating therefore the system. Besides SDHA, also mitochondrial mass and ROS levels were also enhanced (**FIGURES 4.16a** and **4.16c**). In terms of DNA double stranded breaks, we saw higher numbers of 53BP1 foci (**FIGURE 4.16c**). Together with this, pro-inflammatory IL-6 mRNA levels increased upon PGC-1β over-expression (**FIGURE 4.16e** – preliminary data). Lastly, we observed that enhancement of mitochondrial biogenesis lead to a premature cell cycle arrest (**FIGURE 4.16d**) and increased number of cells positive for Sen-β-Gal activity (at day six post-irradiation)(**FIGURE 4.16e**).

In order to verify if ROS was one of the signals emanating from mitochondria that would trigger DDF, we over-expressed PGC-1β and treated those cells with the antioxidant Trolox (6-hydroxy-2,5,7,8-tetramethylchroman-2-carboxylic acid)(**FIGURES 4.16g** and **4.16h**). To test the antioxidant effects of this drug, we measured ROS by DHE fluorescence after X-ray irradiation and observed a reduction in ROS levels upon Trolox administration (**FIGURES 4.16g**). Finally, Trolox reversed the 53BP1 damage accumulation derived from PGC-1β over-expression (**FIGURE 4.16h**).

Following this data, we subjected PGC-1β KO MEF to 21% oxygen (settings that lead to induction of senescence as opposed to 3% oxygen, in which MEF can grow indefinitely – [174]. Under high oxygen conditions, PGC-1β KO cells grew better than wild-type MEF (**FIGURE 4.17a**) and senesced slower – evaluated by increased p21 levels (**FIGURE 4.17b**), more 53BP1 DDF (**FIGURE 4.17c**), increased mitochondrial mass (**FIGURE 4.17d**), higher ROS levels following 4 day and 22 days at 21% $O_2$ (**FIGURE 4.17e**), increased autofluorescence levels (**FIGURE 4.17f**) and increased number of cells positive for Sen-β-Gal activity (**FIGURE 4.17g**). Finally, PGC-1β KO cells were smaller than WT controls (data not shown).

Having seen that PGC-1β KO MEF were smaller, and once cell size is regulated by the mTOR pathway, we investigated if there were additive effects of inhibition of mTORC1 and mitochondrial biogenesis (**FIGURE 4.18**). Firstly we saw that PGC-1β KO MEF had reduced mTORC1 activity after activation of the DDR by 10Gy (**FIGURE 4.18a**). Secondly, we did not see cumulative effects for 53BP1 foci nor for positivity for Sen-β-Gal activity when rapamycin was added to PGC-1β KO cells following ionising radiation (**FIGURES 4.18b-4.18d**). Regarding mitochondrial content, we saw a small reduction of mitochondrial mass between PGC-1β KO rapamycin treated MEF and control cells (**FIGURE 4.18** preliminary data). More experiments need to be made in order to confirm this result, and to verify if the effects of rapamycin reducing mitochondrial on PGC-1β KO MEF are due to reduction of PGC-1α or promotion of mitophagy. In opposition, we realised that RhebN153T over-expression in PGC-1β KO MEF was not able to promote 53BP1 foci increase that was observed on wild-type MEF (**FIGURE 4.18f**).

Overall this data indicated that PGC-1β-mediated biogenesis is a key process in the induction and stabilisation of the senescent phenotype via ROS.

# FIGURE 4.1

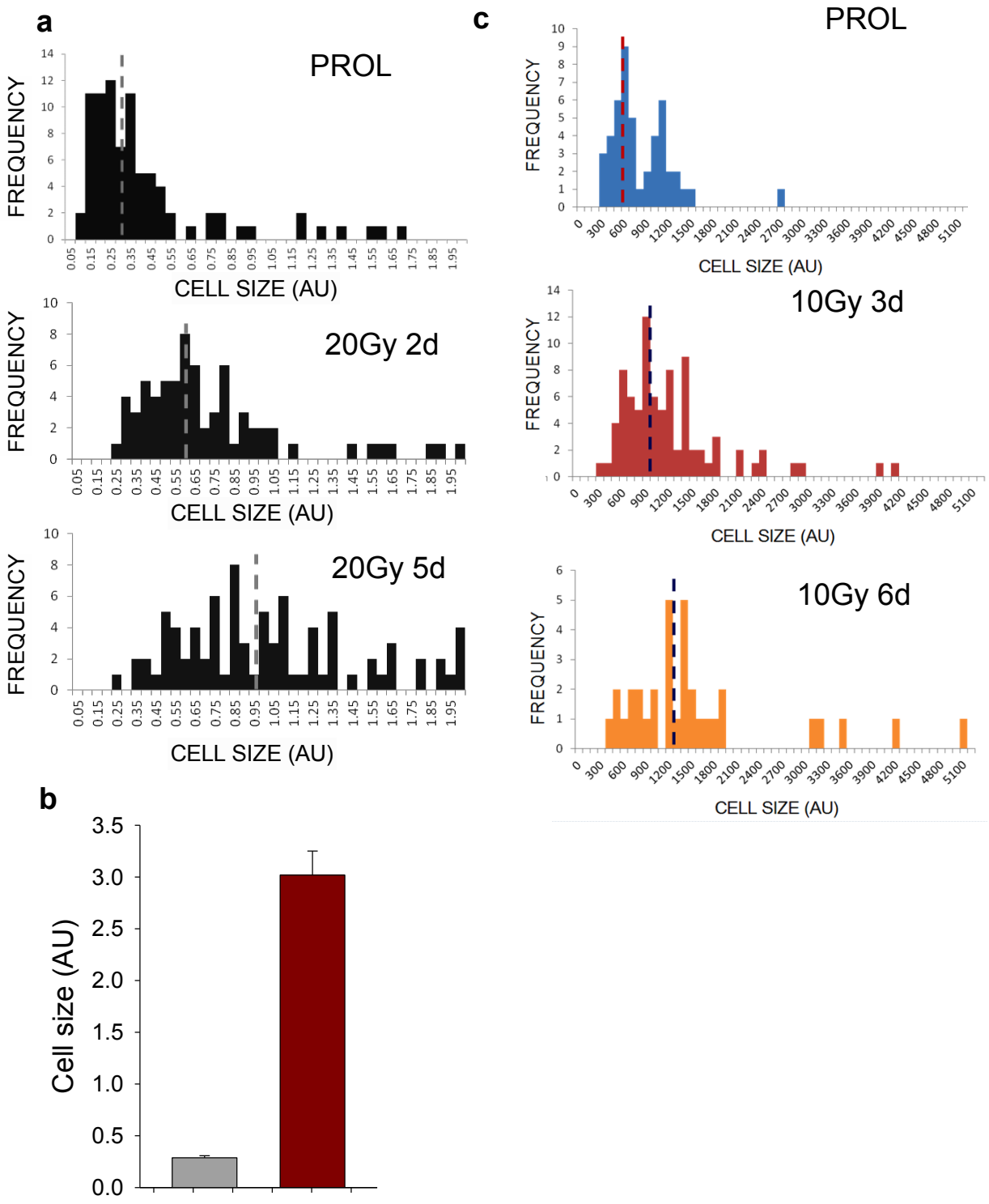
a
PROL
FREQUENCY
CELL SIZE (AU)
20Gy 2d
20Gy 5d
b
Cell size (AU)
c
PROL
10Gy 3d
10Gy 6d

**FIGURE 4.1| An activated DDR drives cell growth and increased mTORC1 activity**

**a)** MRC5 fibroblasts increase size during stress-induced senescence. Vertical dashed lines represent the median cell size - proliferating=0.30, 2 days 20Gy=0.60, 5 days 20Gy=0.95; Mann-Whitney test p-value<0.001; **b)** Cell size of young (grey) and replicative senescent MRC5 (red). One-way ANOVA p-value<0.001; **c)** Primary MEF increase their size following activation of the DDR. Vertical dashed lines denotes the median cell size – proliferating = 604 cells, 3 days 10Gy = 982 cells, 6 days 10Gy=1263 cells; Mann-Whitney test p-value<0.001 (proliferation *versus* 3d 10Gy) and p-value<0.05 (3d 10Gy *versus* 6d 10Gy).

# FIGURE 4.2

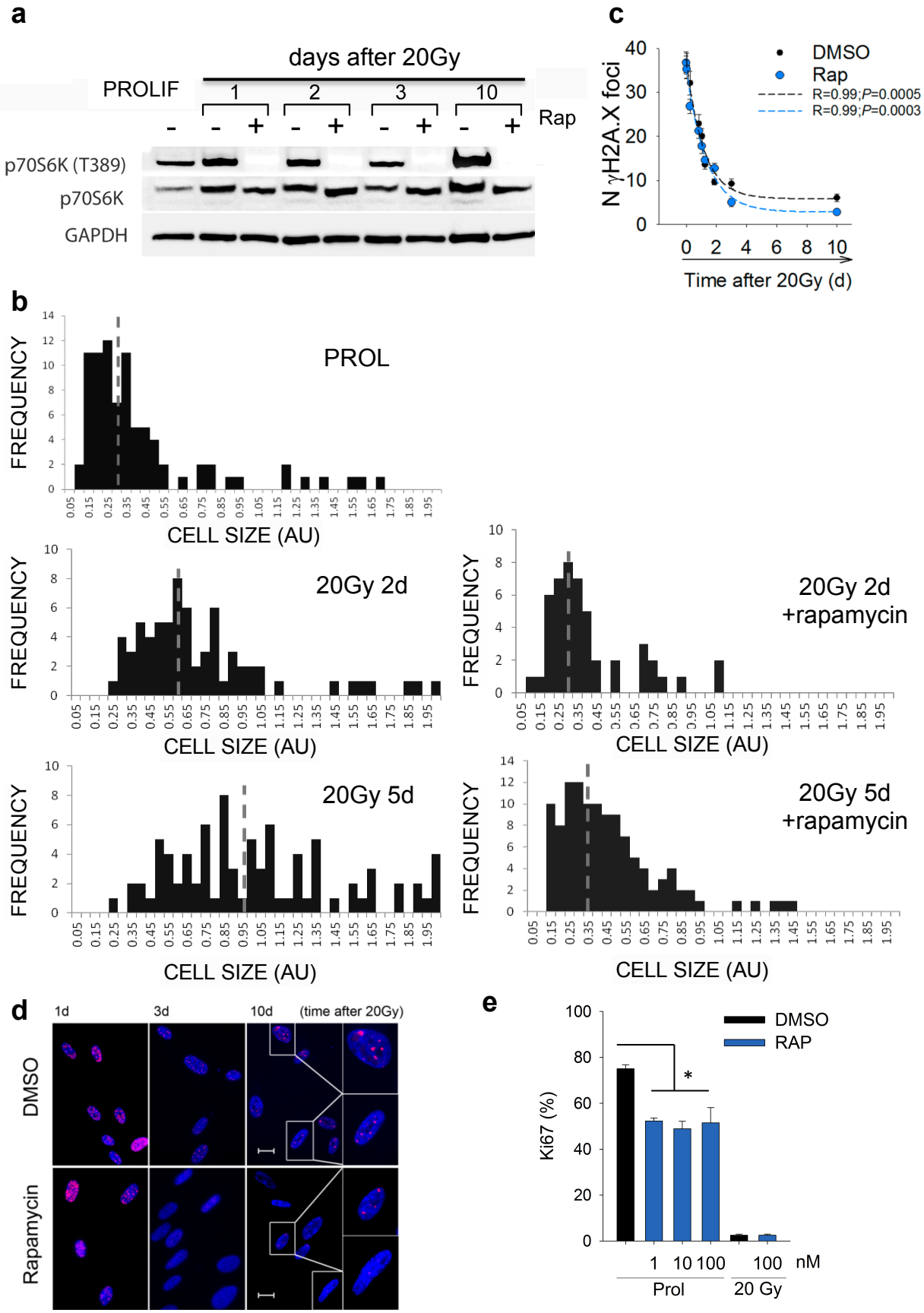
a
days after 20Gy
PROLIF
1
2
3
10
Rap
p70S6K (T389)
p70S6K
GAPDH
c
DMSO
Rap
R=0.99;P=0.0005
R=0.99;P=0.0003
N γH2A.X foci
Time after 20Gy (d)
b
PROL
20Gy 2d
20Gy 2d +rapamycin
20Gy 5d
20Gy 5d +rapamycin
FREQUENCY
CELL SIZE (AU)
d
1d
3d
10d
(time after 20Gy)
DMSO
Rapamycin
e
DMSO
RAP
Ki67 (%)
nM
Prol
20 Gy

**FIGURE 4.2| Rapamycin inhibits mTORC1 and decreases the presence of senescence markers in stress-induced senescent human fibroblasts**

**a)** Representative WB showing absence of mTORC1 activity upon 100nM rapamycin and increased mTORC1 activity following activation of the DDR; **b)** Rapamycin inhibition of mTORC1 decreases cell hypertrophy characteristic of senescence. Dotted line represent average cell size - proliferating=0.30, 2 days 20Gy=0.60, 2 days 20Gy and rapamycin treatment=0.32, 5 days 20Gy=0.95, 5 days 20Gy and rapamycin treatment=0.38. Mann-Whitney test p-value<0.001; **c)** Kinetics of γH2A.X foci repair in MRC5 after irradiation in the presence of rapamycin; **d)** Rapamycin treated MRC5 have fewer γH2A.X during stress induced senescence at day 3 and 10 post-irradiation; **e)** Rapamycin diminishes proliferation of young MRC5 and does not rescue proliferation of senescent cells (time-point analysed was three days following ionising radiation). One-Way ANOVA p-value<0.05.

# FIGURE 4.3

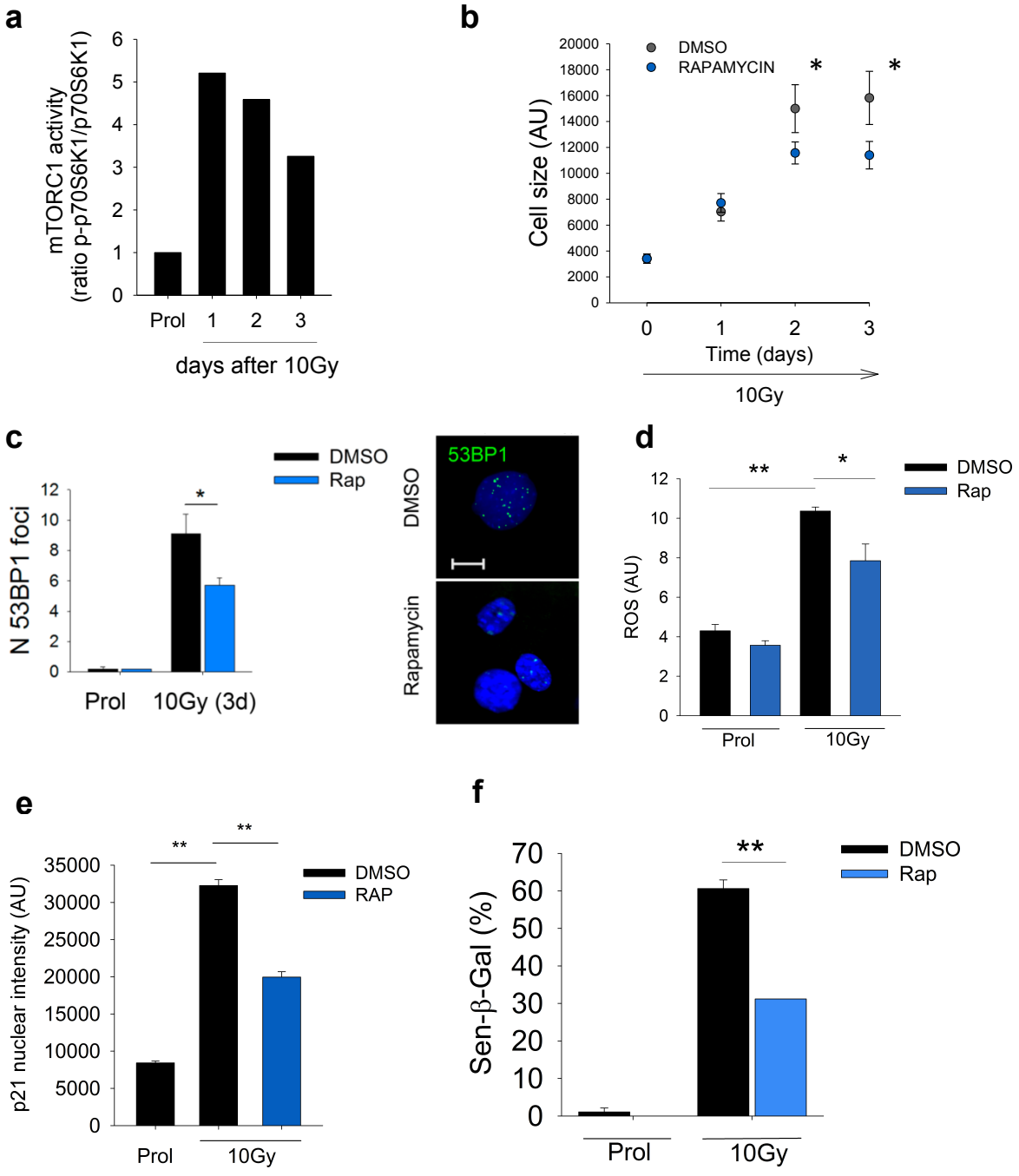
a
mTORC1 activity
(ratio p-p70S6K1/p70S6K1)
Prol
1
2
3
days after 10Gy
b
DMSO
RAPAMYCIN
Cell size (AU)
Time (days)
10Gy
c
DMSO
Rap
N 53BP1 foci
Prol
10Gy (3d)
53BP1
DMSO
Rapamycin
d
DMSO
Rap
ROS (AU)
Prol
10Gy
e
DMSO
RAP
p21 nuclear intensity (AU)
Prol
10Gy
f
DMSO
Rap
Sen-β-Gal (%)
Prol
10Gy

**FIGURE 4.3| Rapamycin inhibits mTORC1 activity and decreases the presence of senescence markers in stress-induced senescent mouse fibroblasts (MEF)**

**a)** mTORC1 activity is increased on the first 3 days following activation of a DDR in primary mouse fibroblasts (representative WB measuring p70S6K (T389)); **b)** MEF increased size in response to a DDR and, rapamycin treatment halts cellular size increase. One-Way ANOVA p-value<0.05; **c)** 53BP1 damage foci are reduced upon mTORC1 inhibition by rapamycin (n=3, at least 125 cells analysed per condition)(two-tailed T-test, p-value<0.05); **d)** ROS levels increase as response to a DDR and are decreased upon rapamycin administration during an activated DDR (n=3, two-tailed T-test, **p-value<0.001 and *p-value<0.05); **e)** Nuclear p21 intensity was measured from 200 cells following a DDR activation. Rapamycin treated cells have decreased p21 levels at 9 days post-irradiation (two-tailed T-test, **p-value<0.001 and *p-value<0.05); **f)** mTORC1 inhibition by rapamycin decreases number of cells positive for Sen-β-Gal staining at 9 days following 10Gy. One-Way ANOVA p-value<0.001.

# FIGURE 4.4

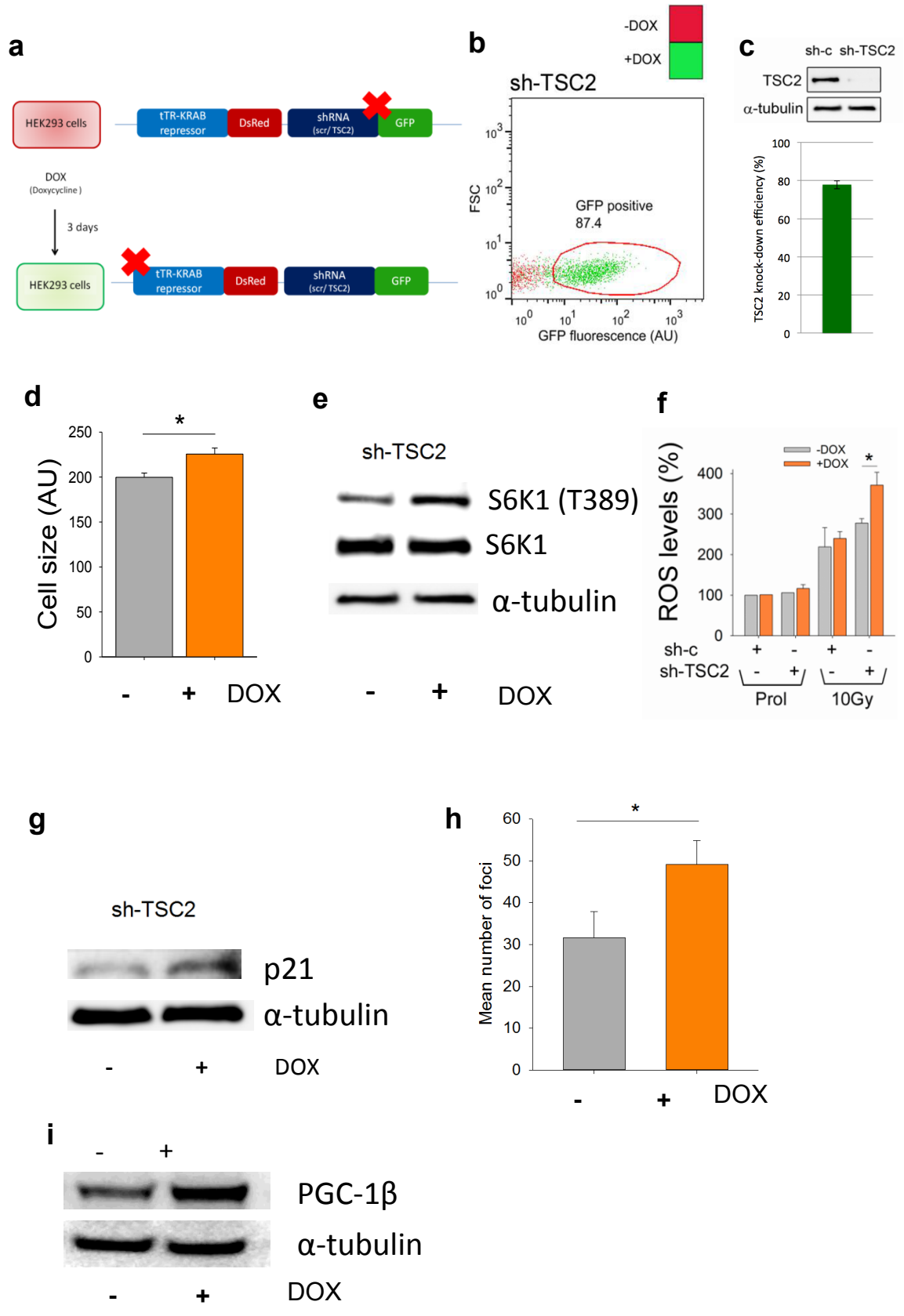
a
HEK293 cells
tTR-KRAB repressor
DsRed
shRNA (scr/TSC2)
GFP
DOX (Doxycycline)
3 days
HEK293 cells
tTR-KRAB repressor
DsRed
shRNA (scr/TSC2)
GFP
b
-DOX
+DOX
sh-TSC2
FSC
GFP positive 87.4
GFP fluorescence (AU)
c
sh-c sh-TSC2
TSC2
α-tubulin
TSC2 knock-down efficiency (%)
d
Cell size (AU)
- + DOX
e
sh-TSC2
S6K1 (T389)
S6K1
α-tubulin
- + DOX
f
ROS levels (%)
-DOX
+DOX
sh-c
sh-TSC2
Prol
10Gy
g
sh-TSC2
p21
α-tubulin
- + DOX
h
Mean number of foci
- + DOX
i
- +
PGC-1β
α-tubulin
- + DOX

**FIGURE 4.4| Silencing of TSC2 increases mTORC1 activity, drives ROS generation and triggers the DNA damage response**

**a)** HEK293T cells harbouring short-hairpins against TSC2 (sh-TSC2) or a scrambled DNA sequence (sh-c) were induced using doxycycline (DOX) for three days. Upon shRNA expression the cells express GFP; **b)** Percentage of shRNA induction – GFP positive cells by FACS; **c)** HEK293T doxycycline treated cells exhibits TSC2 KD (efficiency of 77.8% ±4.22), data are mean ± s.e.m. of n=6. Mitochondrial proteins (complex I NDUFB8, complex III UQCRC2 and TOMM20) are increased in DOX treated sh-TSC2 HEK293T cells. **d)** Cell size is increased in DOX-induced TSC2shRNA cells. Data are mean ± s.e.m. of n= 85 cells per condition. Two-tailed T-test * p-value=0.0023; **e)** mTORC1 activity is increased 1.9 fold after TSC2 knock-down (KD); **f)** DHE fluorescence intensity of HEK293T sh-TSC2 cells three days after 10Gy, data are mean ± s.e.m. of n=3; ; **g)** p21 protein levels were elevated upon mTORC1 activation via TSC2 silencing; **h)** γH2A.X foci increase upon TSC2 silencing. Data are mean ± s.e.m. of n= 20 cells per condition. Two-tailed T-test *p-value=0.0449**; i)** PGC-1β protein levels are increased upon TSC2 KD after 10 days doxycyclin induction.

## FIGURE 4.5

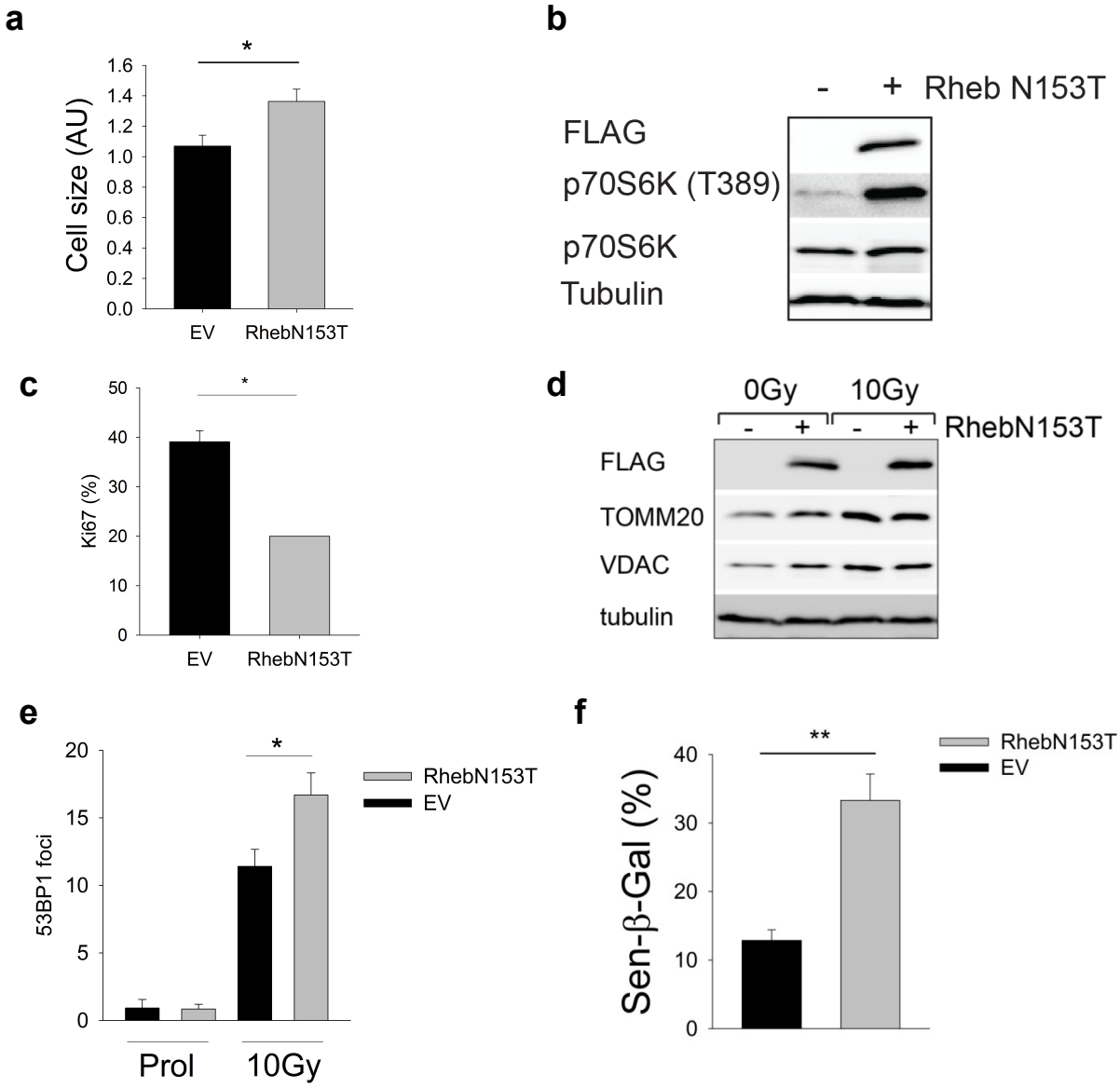


**FIGURE 4.5| RhebN153T activates constitutively mTORC1 and promotes cellular senescence in MEF**

**a)** MEF cell size is increased upon RhebN153T over-expression. Cells were analysed 3 days following transfection. n= 113/134 cells respectively. One-way ANOVA $p<0.001$; **b)** western blot showing that mTORC1 is constitutively active upon RhebN153T over-expression. p70S6K1 phosphorylation was used as mTORC1 activity readout. **c)** MEF over-expressing RhebN153T proliferate less than pcDNA (EV) transfected cells. Cells were double stained for Ki67 and FLAG and the analysis was conducted after one day. One-way ANOVA $p<0.05$. **d)** MEF over-expressing RhebN153T have more mitochondrial proteins VDAC and TOMM20. Cells were analysed 3 days following transfection, 2 days following 10Gy. e) 53BP1 DDF are increased in irradiated cells over-expressing RhebN153T. One-way ANOVA $p<0.001$; f) The fraction of Sen-β-Gal positive MEF is increased seven days following transfection with RhebN153T. One-way ANOVA $p<0.001$;

## FIGURE 4.6

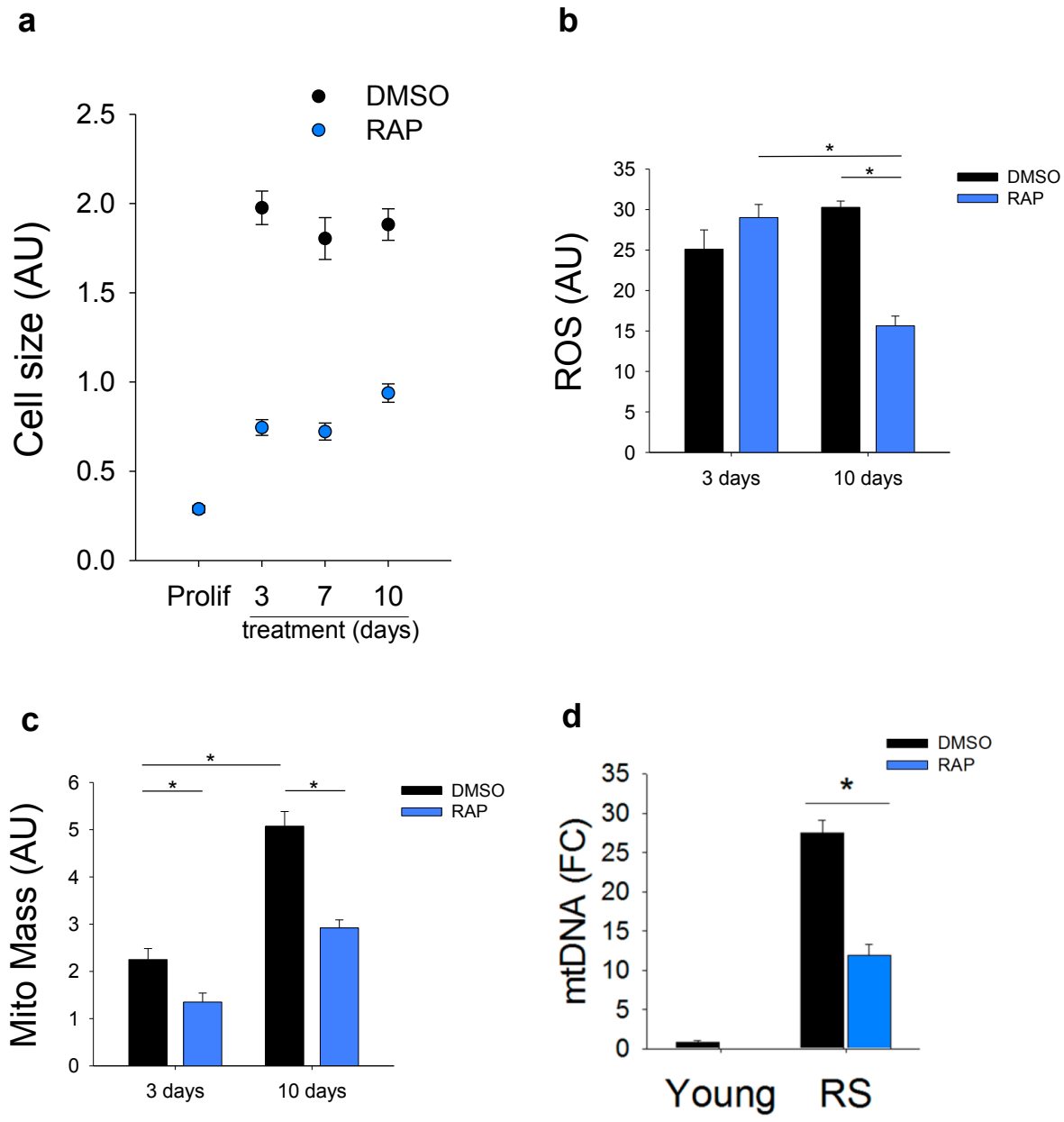


**FIGURE 4.6| Rapamycin decreases presence of senescence markers in replicative senescent (RS) human fibroblasts**

**a)** Replicative senescent cells are bigger than young proliferating cells and rapamycin treatment reduces cellular hyperthropy; **b)** ROS levels are increased in replicative senescent (RS) compared to young MRC5 fibroblasts. mTORC1 inhibition by rapamycin for 10 days decreases ROS levels (two-tailed T-test, p-value=8.53E-06); **c)** Mitochondrial mass measured by NAO staining in the FACS is reduced in RS cells upon rapamycin treatment (two-tailed T-test, p-value<0.001); **d)** Mitochondrial DNA (mtDNA) copy number is increased in replicative senescent cells and mTORC1 inhibition by rapamycin reduces its copy number (two-tailed T-test, p-value<0.001).

# FIGURE 4.7

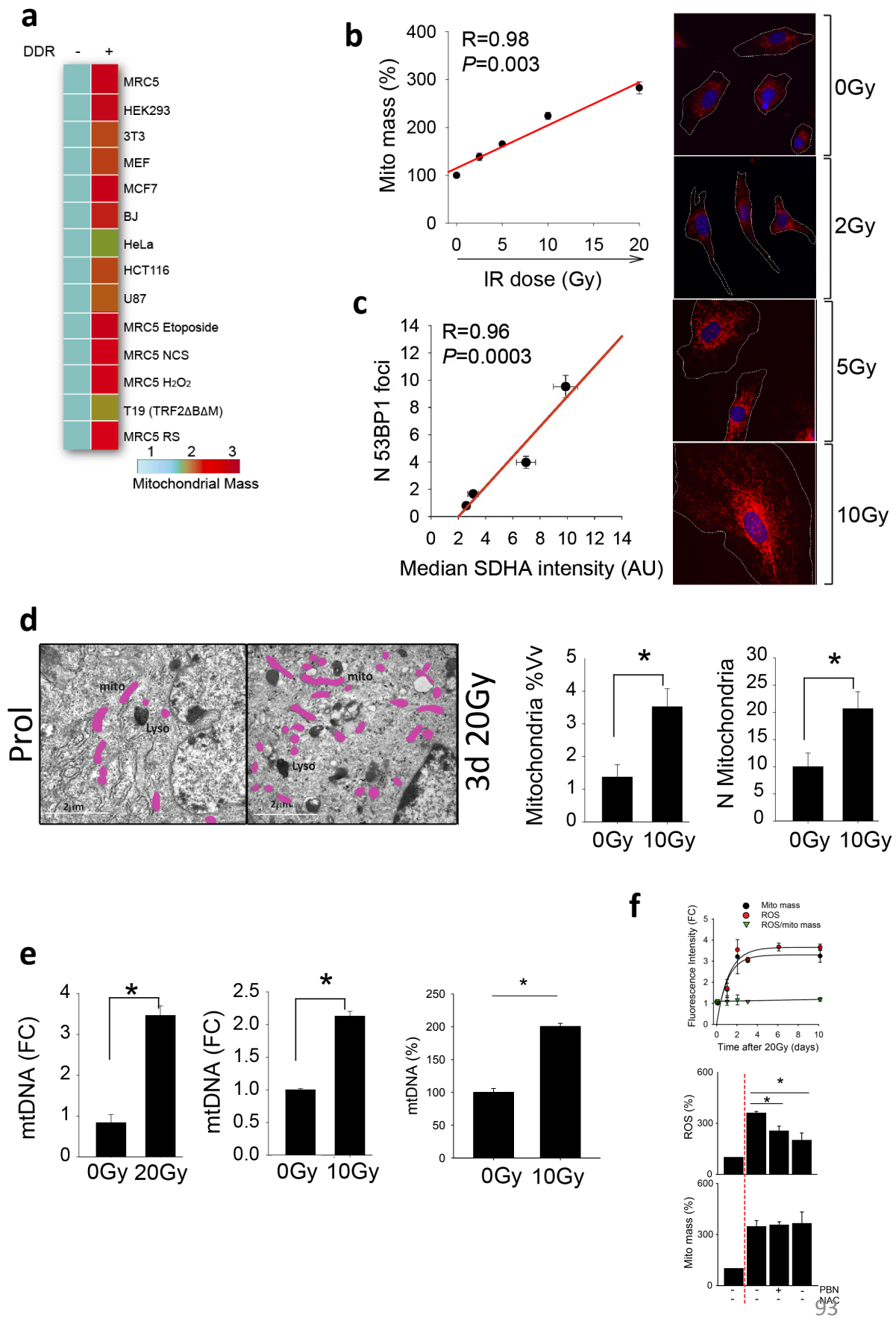
a
DDR - +
MRC5
HEK293
3T3
MEF
MCF7
BJ
HeLa
HCT116
U87
MRC5 Etoposide
MRC5 NCS
MRC5 H2O2
T19 (TRF2ΔBΔM)
MRC5 RS
1 2 3
Mitochondrial Mass
b
R=0.98
P=0.003
Mito mass (%)
IR dose (Gy)
0Gy
2Gy
5Gy
10Gy
c
R=0.96
P=0.0003
N 53BP1 foci
Median SDHA intensity (AU)
d
Prol
3d 20Gy
mito
Lyso
Mitochondria %Vv
N Mitochondria
0Gy 10Gy
e
mtDNA (FC)
0Gy 20Gy
0Gy 10Gy
mtDNA (%)
0Gy 10Gy
f
Mito mass
ROS
ROS/mito mass
Fluorescence Intensity (FC)
Time after 20Gy (days)
ROS (%)
Mito mass (%)
PBN
NAC

**FIGURE 4.7| Mitochondrial mass and proteins increase as a consequence of a DDR**

**a)** Mitochondria mass was increased between 1 and 4 days following activation of a DDR by various genotoxic stresses (X-ray irradiation, etoposide, neocarcinostatin – NCS, hydrogen peroxide $H_2O_2$ or telomere dysfunction ($TRF2^{\Delta B \Delta M}$) in multiple primary and cancer cell lines. n=3 independent experiments per cell line or treatment; **b)** Positive correlation between DNA double strand break γH2A.X foci and mitochondrial mass in MRC5 following increasing doses of X-ray radiation; **c)** Positive correlation between 53BP1 DDF and mitochondrial SDHA protein levels in MEF following different X-ray doses. Representative images of SDHA mitochondrial networks in MEF. n=3; **d)** Illustrative electron micrograph of young proliferating (Prol) and 20Gy irradiated MRC5 fibroblasts (at three days). Mitochondria were pseudo-coloured in pink. Graphs are quantification of mitochondria volume fraction (%V/v) and mitochondrial numbers N mitochondria) of at least twenty cells per condition; **e)** mitochondrial DNA copies were increased 2 to 3 days following X-ray irradiation. Data are mean±S.E.M of n=3, *$p<0.05$; **f)** (top) mitochondrial increased in parallel with ROS levels (or basal oxygen consumption rate) and when ROS was normalised per unit of mitochondrial mass it became unchanged upon induction of senescence. MRC5 were treated three days with rapamycin and mitochondrial mass and ROS was measured by NAO and DHE staining. Antioxidant treatment (PBN and NAC) reduced ROS in X-ray senescent cells but, it does not affect mitochondrial mass. ROS were measured by DHE staining and mitochondrial mass by NAO staining.

# FIGURE 4.8

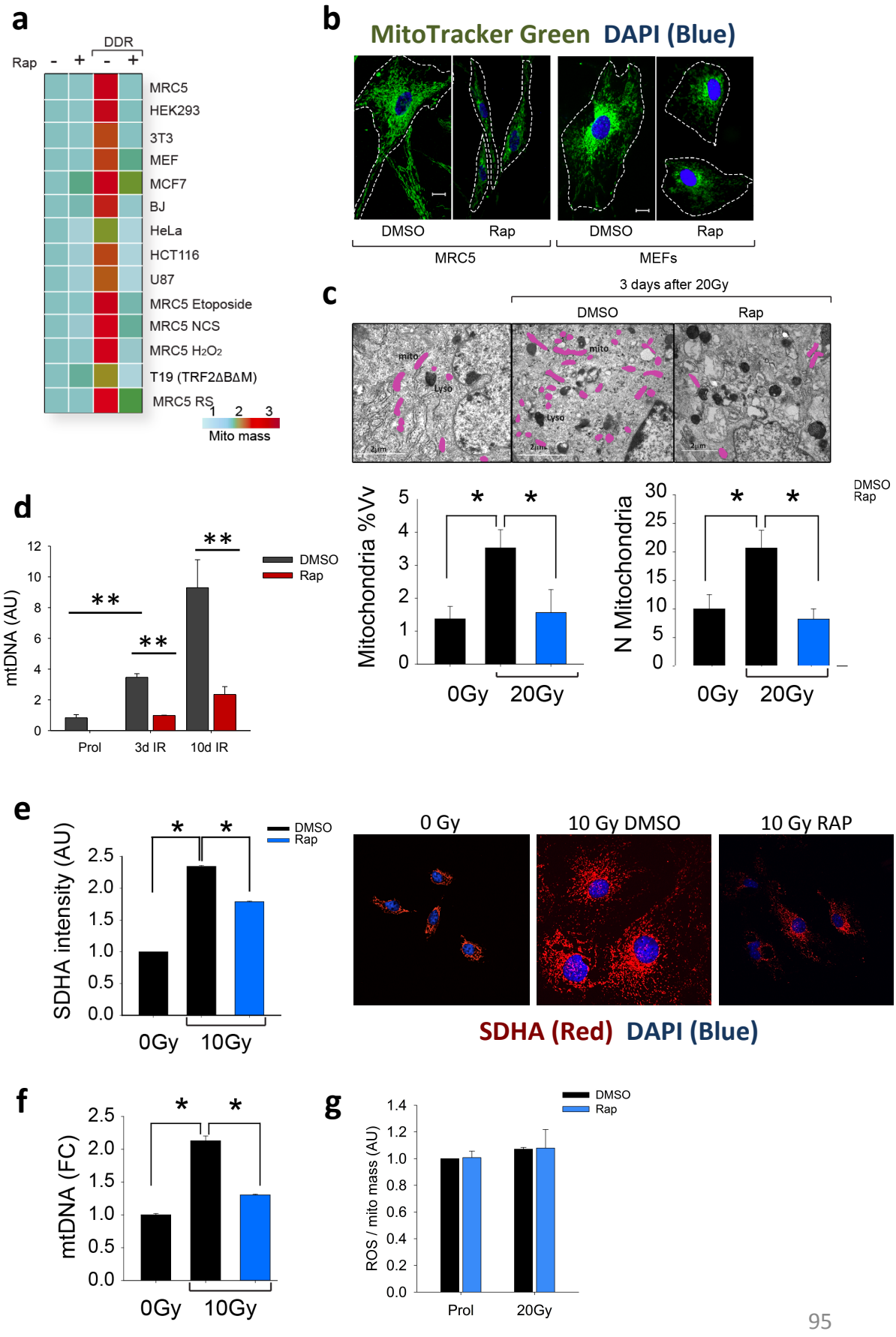
a
DDR
Rap - + - +
MRC5
HEK293
3T3
MEF
MCF7
BJ
HeLa
HCT116
U87
MRC5 Etoposide
MRC5 NCS
MRC5 H2O2
T19 (TRF2ΔBΔM)
MRC5 RS
1 2 3
Mito mass
b
MitoTracker Green DAPI (Blue)
DMSO
Rap
DMSO
Rap
MRC5
MEFs
c
3 days after 20Gy
DMSO
Rap
mito
Lyso
2µm
d
mtDNA (AU)
DMSO
Rap
Prol
3d IR
10d IR
Mitochondria %Vv
0Gy
20Gy
N Mitochondria
DMSO
Rap
0Gy
20Gy
e
SDHA intensity (AU)
DMSO
Rap
0Gy
10Gy
0 Gy
10 Gy DMSO
10 Gy RAP
SDHA (Red) DAPI (Blue)
f
mtDNA (FC)
0Gy
10Gy
g
ROS / mito mass (AU)
DMSO
Rap
Prol
20Gy

**FIGURE 4.8| mTORC1 inhibition by rapamycin descreases mitochondrial content within damaged cells**

**a)** mTORC1 inhibition by rapamycin halts the increase on mitocondrial mass. The panel of cells used here was the same one used in **FIGURE 5.1.a**; **b)** Representative MitoTracker Green images of primary human and mouse fibroblasts treated with rapamycin after activation of a DDR y ionising radiation; **c)** mTORC1 inhibition by rapamycin descreased number and volume fraction of mitochondria. Data of at least twenty T.E.M. per condition; **d)** rapamycin decreased mitochondria DNA copies number upon X-ray irradiation. n=1 q-PCR samples ran in triplicate, **p<0.001; **e)** SDHA intensity (in red) increased upon DDR activation and rapamycin decreased SDHA content within cells. Samples were analysed nine days following 10Gy. Rapamycin treatment was effectuated immediately after the DDR stimulus. Data are mean±s.e.m. of n=3-4 cells per condition. One-Way ANOVA, *p<0.05; **f)** mtDNA copies are reduced in primary MEF upon co-treatment with rapamycin and ionising radiation. Data are mean±S.E.M of n=3, *p<0.05. **g)** when ROS was normalised per unit of mitochondrial mass it became unchanged upon induction of senescence. The stoichiometric ratio between ROS and mitochondrial mass remains unchanged even when MRC5 were treated three days with rapamycin. Mitochondrial mass and ROS was measured by NAO and DHE staining.

## FIGURE 4.9

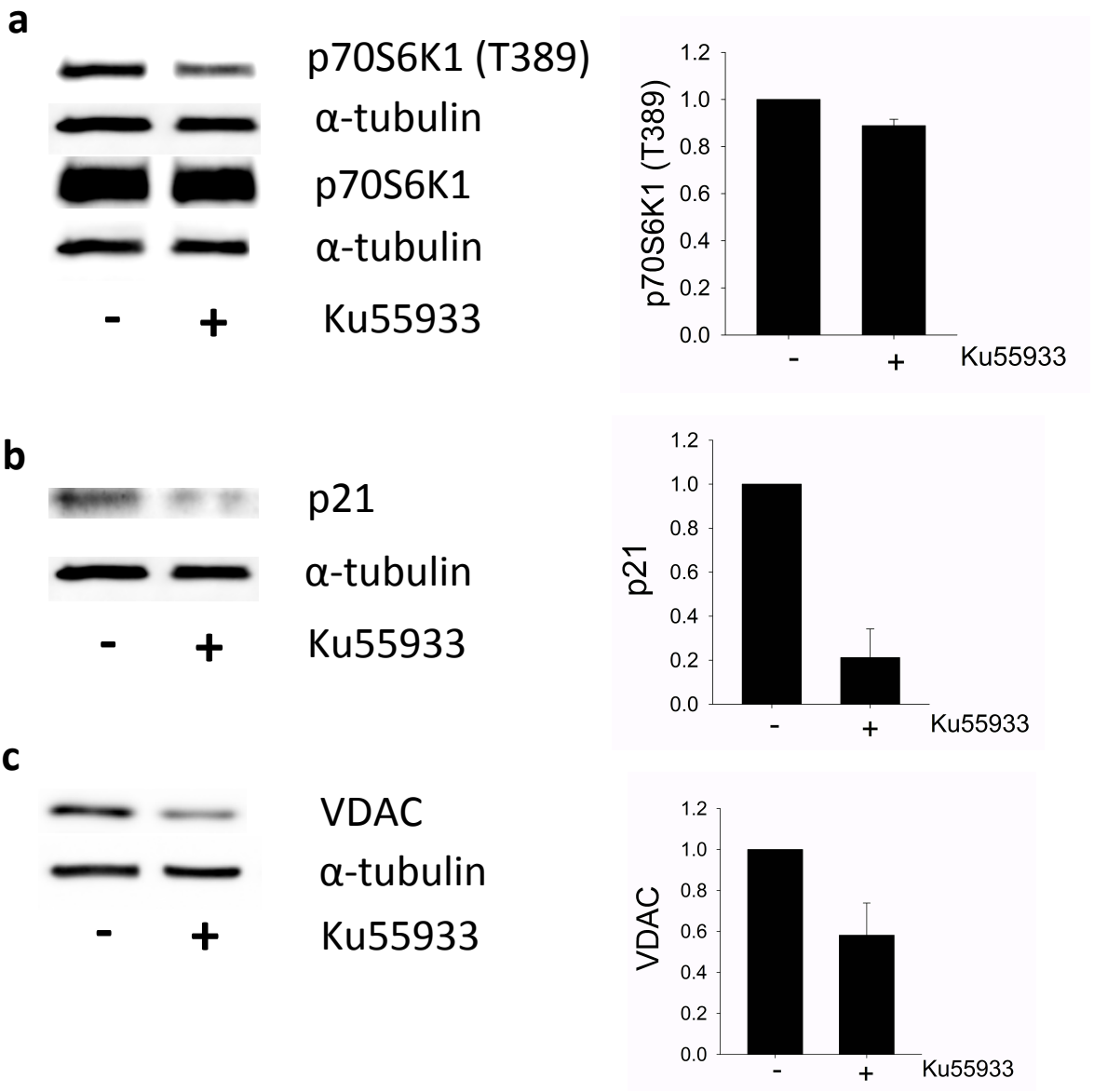


**FIGURE 4.9| ATM inhibition following a DDR leads to decreased mTORC1 activity, p21 and VDAC protein levels in HEK293T cells** (preliminary data)

**a)** mTORC1 activity (ratio phosphorylated p70S6K1/total p70S6K1/GAPDH) was reduced after one day 10Gy irradiation when ATM kinase was inhibited chemically using Ku55933; **b)** p21 protein levels were reduced following an active DDR when ATM was inhibited; **c)** mitochondrial protein VDAC levels were reduced following an active DDR when ATM was inhibited. In all conditions cells were pre-treated with 10 μM prior to X-ray irradiation. Media was refreshed with Ku55933 following irradiation and samples were collected one day following the treatment. n=2 independent WB, bars represent standard error.

# FIGURE 4.10

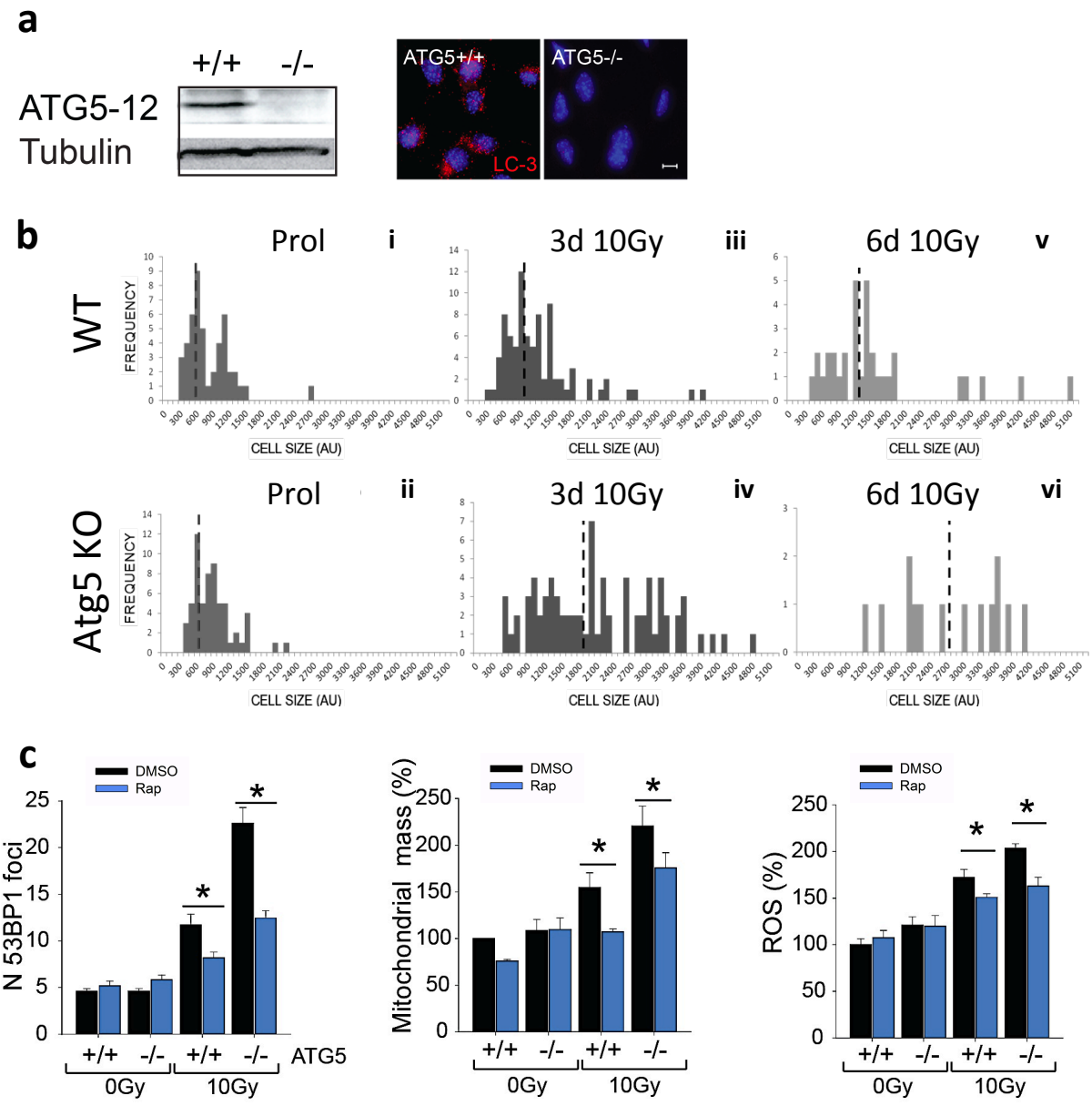


**FIGURE 4.10| Autophagy-deficient cells accumulate mitochondria, ROS and DNA damage and, rapamycin rescues this phenotype regardless of the lack of autophagy**

**a)** Positive control – representative WB depicting that Atg5 knockout (KO) MEF do not express Atg5. Representative images of LC-3 expression (red) in wild-type and Atg5 KO MEF; **b)** Atg5-null MEF are bigger than matched wild-type cells. Mann-Whitney test, (iii *vs.* iv – $p<0.001$, v *vs.* vi – $p<0.001$); **c)** effects of 10Gy irradiation and rapamycin on 53BP1 damage foci number, mitochondrial mass and ROS levels in Atg5 KO MEF. Cells were analysed three days following irradiation and treated immediately following IR with rapamycin. Data are mean±s.e.m. of n=3-4, one-Way ANOVA, *$p<0.05$. +/+ – wild-type, -/- – knockout.

# FIGURE 4.11

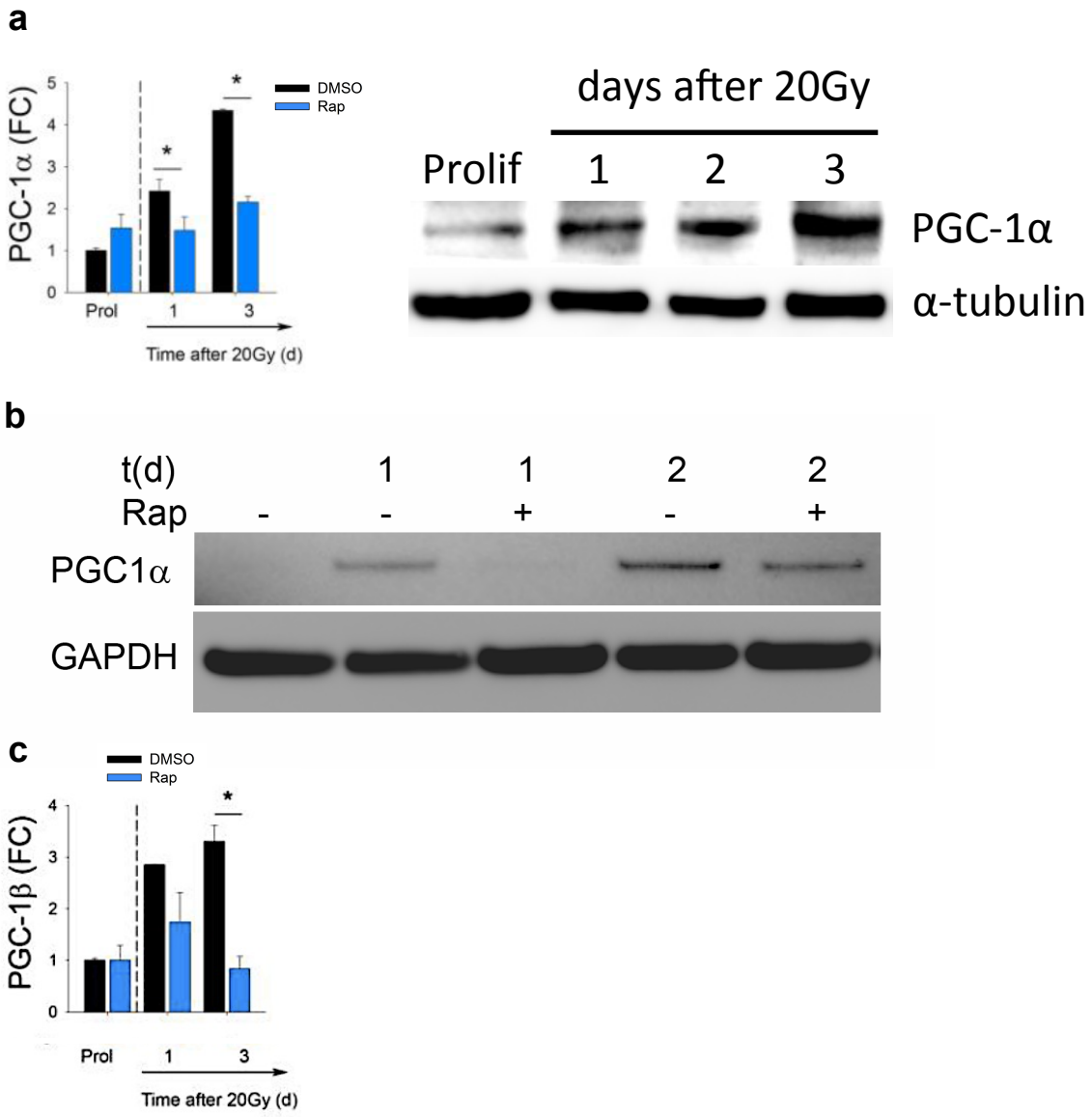


**FIGURE 4.11| Mitochondrial biogenesis is triggered following DDR activation and repressed upon mTORC1 inhibition in human MRC5**

**a)** PGC-1α mRNA increased after the DDR was activated and its expression levels were repressed once mTORC1 was inhibited using rapamycin. Data are mean± s.e.m. of n=3, one-Way ANOVA, *p<0.05. Representative WB showing an increase for PGC-1α following the DDR; **b)** PGC-1α protein levels are repressed following mTORC1 inhibition by rapamycin. n=3; **c)** PGC-1β mRNA levels increased following activation of a DDR (20Gy) and were repressed when using rapamycin. n=3, one-Way ANOVA, *p<0.05.

## FIGURE 4.12

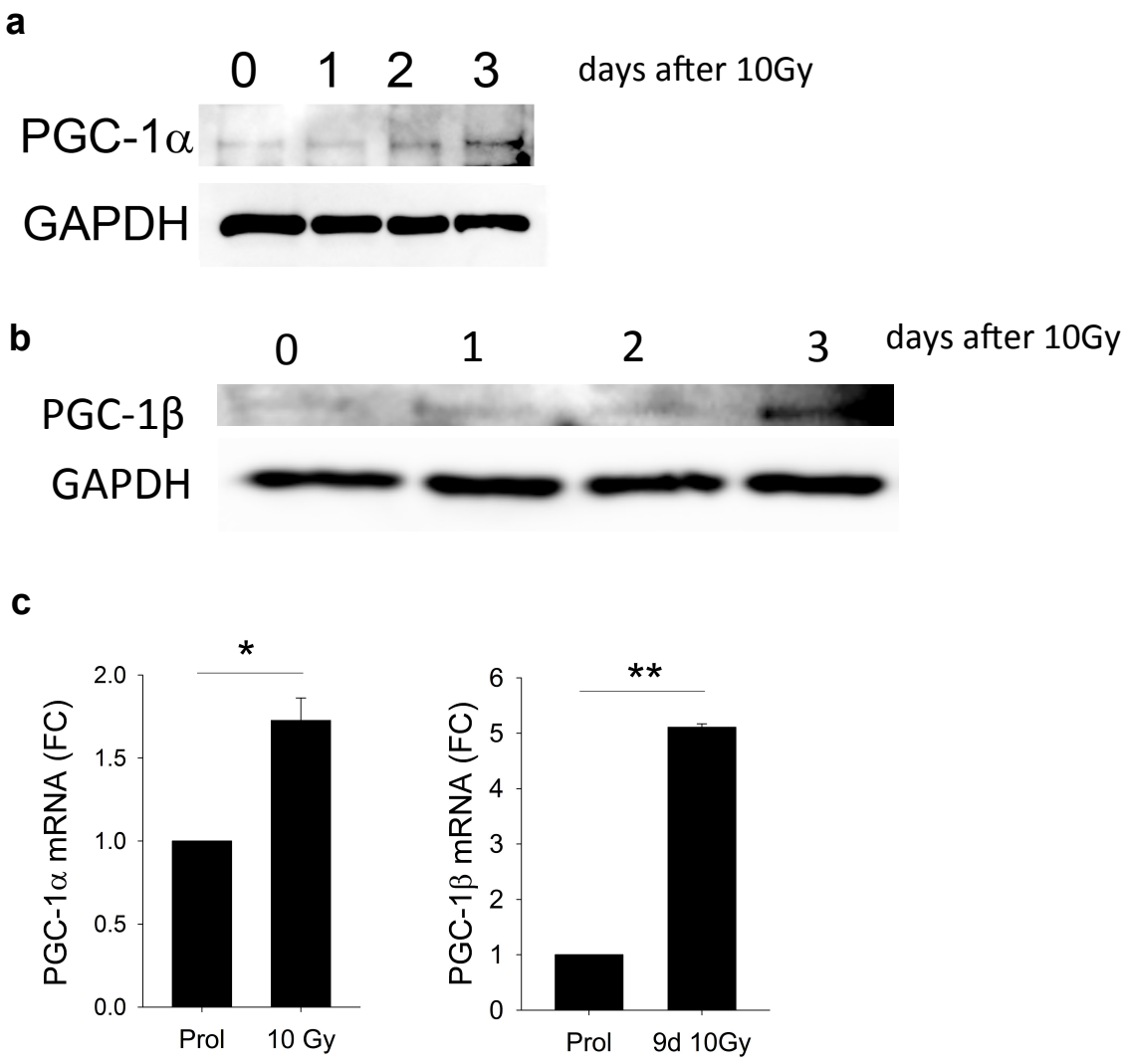


**FIGURE 4.12 | Mitochondrial biogenesis is triggered upon a DDR in MEF**

**a)** Representative WB depicting increased PGC-1α and PGC-1β following 10Gy radiation in wild-type MEF; **b)** PGC-1β protein levels are increased following activation of the DDR. n=2; **c)** PGC-1α and PGC-1β mRNA levels in senescent MEF (9 days after 10Gy). n=3, one-Way ANOVA *p<0.05 and **p<0.001, FC - fold-change.

# FIGURE 4.13

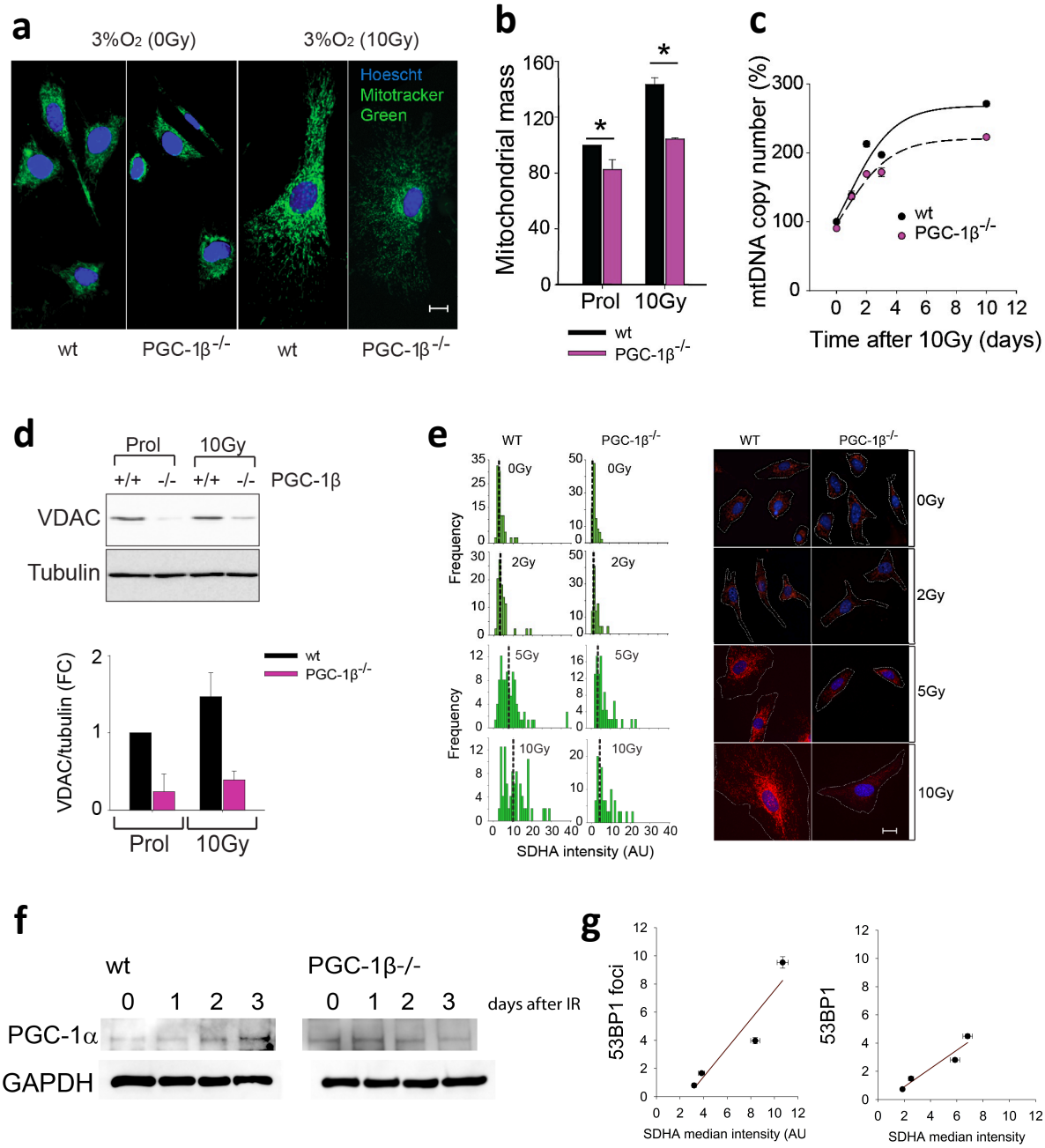
a
3%O2 (0Gy)
3%O2 (10Gy)
Hoescht
Mitotracker
Green
wt
PGC-1β-/-
wt
PGC-1β-/-
b
Mitochondrial mass
160
120
80
40
0
*
*
Prol
10Gy
wt
PGC-1β-/-
c
mtDNA copy number (%)
300
200
100
0
0 2 4 6 8 10 12
Time after 10Gy (days)
wt
PGC-1β-/-
d
Prol
10Gy
+/+ -/- +/+ -/-
PGC-1β
VDAC
Tubulin
VDAC/tubulin (FC)
2
1
0
wt
PGC-1β-/-
Prol
10Gy
e
WT
PGC-1β-/-
Frequency
0Gy
2Gy
5Gy
10Gy
0 10 20 30 40
SDHA intensity (AU)
WT
PGC-1β-/-
0Gy
2Gy
5Gy
10Gy
f
wt
PGC-1β-/-
0 1 2 3
0 1 2 3
days after IR
PGC-1α
GAPDH
g
53BP1 foci
0 2 4 6 8 10 12
SDHA median intensity (AU
53BP1
0 2 4 6 8 10 12
SDHA median intensity

**FIGURE 4.13| PGC-1β KO MEF have disrupted mitochondrial networks, less mitochondrial proteins and less mtDNA during stress induced senescence**

**a)** MitoTracker Green staining on wild-type (wt) and PGC-1β KO MEF 3 days following 10Gy irradiation; **b)** PGC-1β KO MEF have less mitochondrial mass under proliferating and irradiation conditions. Data are mean±s.e.m. of n=3, one-Way ANOVA, *p<0.05; **c)** Kinetics of mitochondrial DNA copy number in wt and PGC-1β KO MEF following 10Gy irradiation. Data are mean±s.e.m. of n=3; **d)** Mitochondrial outer membrane protein VDAC expression following activation of a DDR in wt and PGC-1β KO MEF. Data are mean±s.e.m. of n=3, +/+ − wild-type and -/- − PGC-1β KO MEF ; **e)** Histogram depicting the frequency of SDHA intensity in wt and PGC-1β KO MEF three days following different X-ray irrdation doses. n=3 and dashed line indicates median fluorescence. Representative mitochondrial SDHA networks; **f)** Representative PGC-1α WB in wt MEF and PGC-1β KO MEF kinetically after activation of the DDR with 10Gy; **g)** Positive correlation between amount of mitochondrial SDHA and 53BP1 damage foci in wt MEF (left graph) and in PGC-1β KO MEF (right graph) at three days following 10Gy.

# FIGURE 4.14

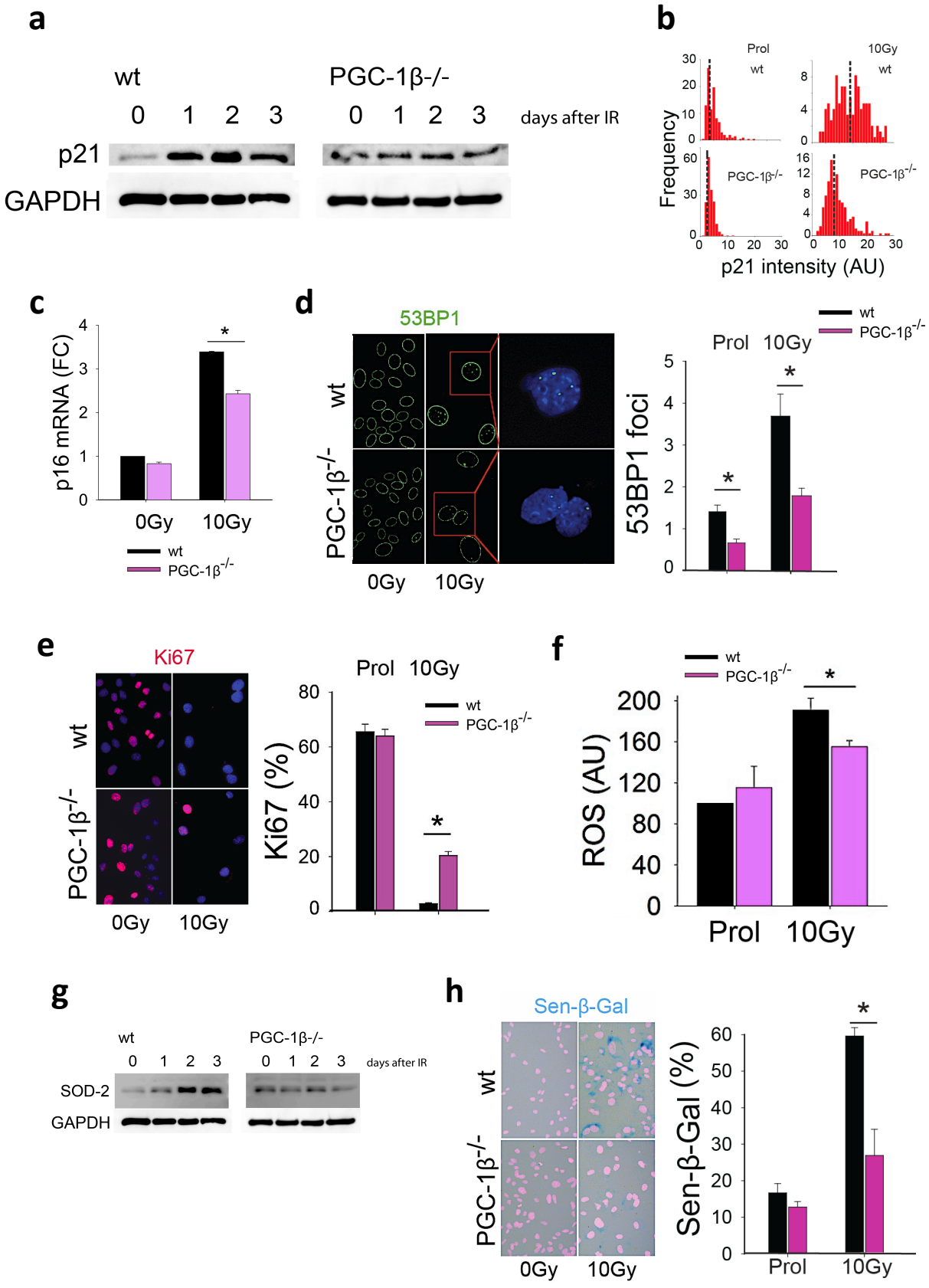
a
wt
PGC-1β-/-
0 1 2 3
0 1 2 3
days after IR
p21
GAPDH
b
Prol
10Gy
wt
wt
PGC-1β-/-
PGC-1β-/-
Frequency
p21 intensity (AU)
c
p16 mRNA (FC)
0Gy
10Gy
wt
PGC-1β-/-
d
53BP1
wt
PGC-1β-/-
0Gy
10Gy
Prol 10Gy
wt
PGC-1β-/-
53BP1 foci
e
Ki67
wt
PGC-1β-/-
0Gy
10Gy
Prol 10Gy
wt
PGC-1β-/-
Ki67 (%)
f
wt
PGC-1β-/-
ROS (AU)
Prol
10Gy
g
wt
PGC-1β-/-
0 1 2 3
0 1 2 3
days after IR
SOD-2
GAPDH
h
Sen-β-Gal
wt
PGC-1β-/-
0Gy
10Gy
Sen-β-Gal (%)
Prol
10Gy

**Figure 4.14| PGC-1β depletion slows down the senescent phenotype**

**a)** Representative WB for cyclin-depend kinase inhibitor p21 in wild-type (wt) and PGC-1β KO MEF; **b)** p21 nuclear staining intensity histograms three days following 10Gy. Dashed line indicates median fluorescence; **c)** p16 mRNA levels at day ten in wild-type (wt) and PGC-1β KO MEF. Data are mean±S.E.M. of n=3. *p<0.05. 0Gy indicate proliferating cells; **d)** Immunofluorescence staining and graphic quantification of 53BP1 DDF three days following 10Gy irradiation. Data are mean±S.E.M. of n=3, one-way ANOVA, *p<0.05; **e)** Proliferation stanining for wild-type and PGC-1β KO MEF at day nine. Ki67 proliferation marker (nuclear red staining). Data are mean±S.E.M. of n=3, one-way ANOVA, *p<0.05; **f)** ROS levels in wild-type and PGC-1β KO MEF following three days irradiation. Data are mean±S.E.M. of n=3, one-way ANOVA, *p<0.05; **g)** Superoxide dismutase protein levels followed kinetically in wild-type and PGC-1β KO MEF. n=1; **h)** Effects of 10Gy in senescence-associated β-galactosidase positivity in wild-type and PGC-1β KO MEF at day nine. Perinuclear blue precipitate indicates positivity for Sen-β-Gal activity. Data are mean±S.E.M. of n=3, one-way ANOVA, *p<0.05.

# FIGURE 4.15

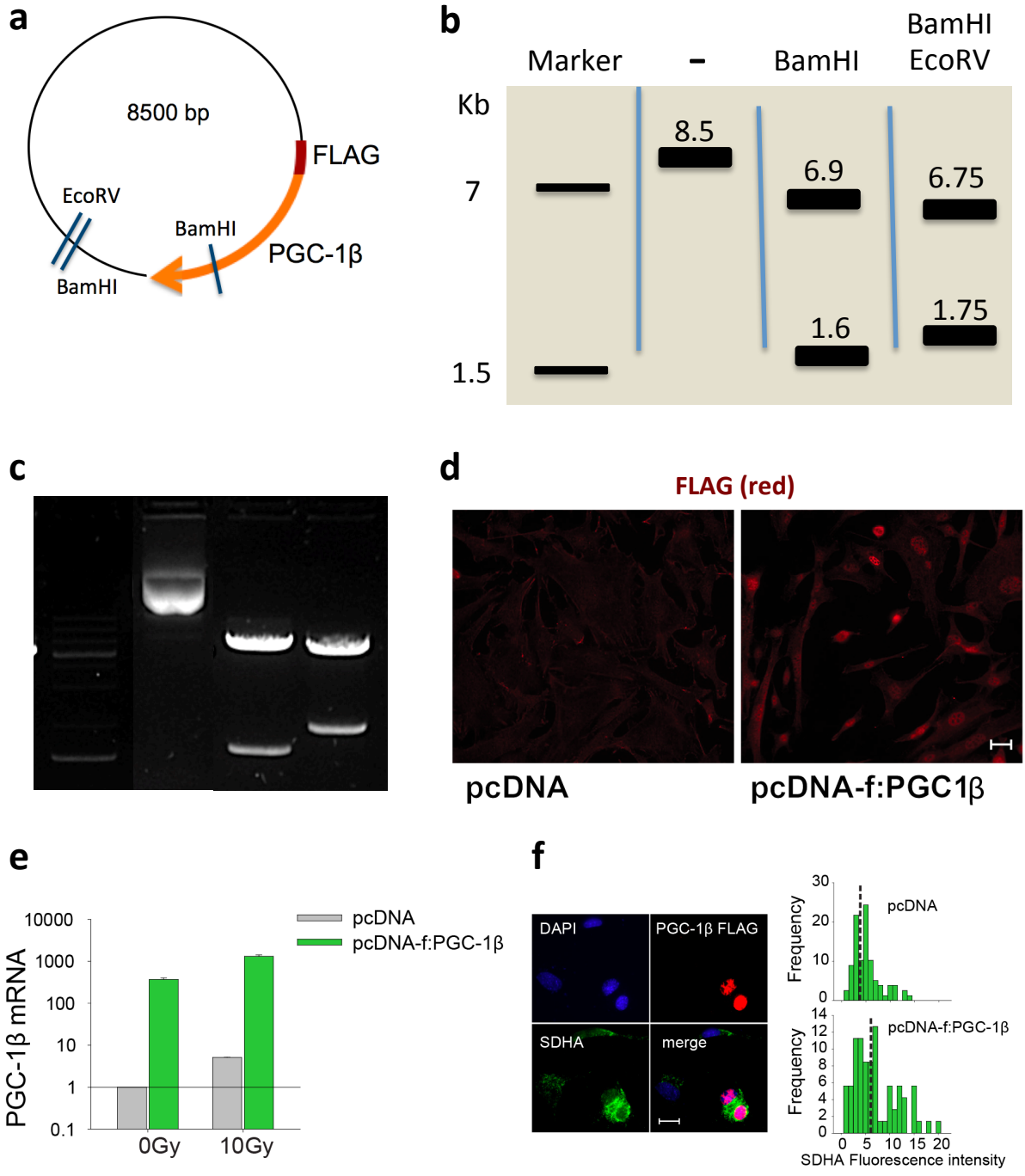


**FIGURE 4.15| PGC-1β over-expression triggers mitochondrial biogenesis**

**a)** Sheme of PGC-1β plasmid (Addgene #1031); **b)** Theoretical digestion of PGC-1β plasmid; **c)** PGC-1β plasmid single digestion with BamHI or double digestion using BamHI and EcoRV; **d)** Representative image of FLAG immunostaining following transfection of pcDNA (empty vector - EV) and pcDNAf:PGC-1β; **e)** mRNA expression of PGC-1β with or without 10Gy irradiation (ten days). Data are mean±s.e.m. of n=3; **f)** representative double staining for FLAG and mitochondrial protein SDHA two days after transfection. Dashed black line indicates median SDHA fluorescence. n=100 cells per condition.

# FIGURE 4.16

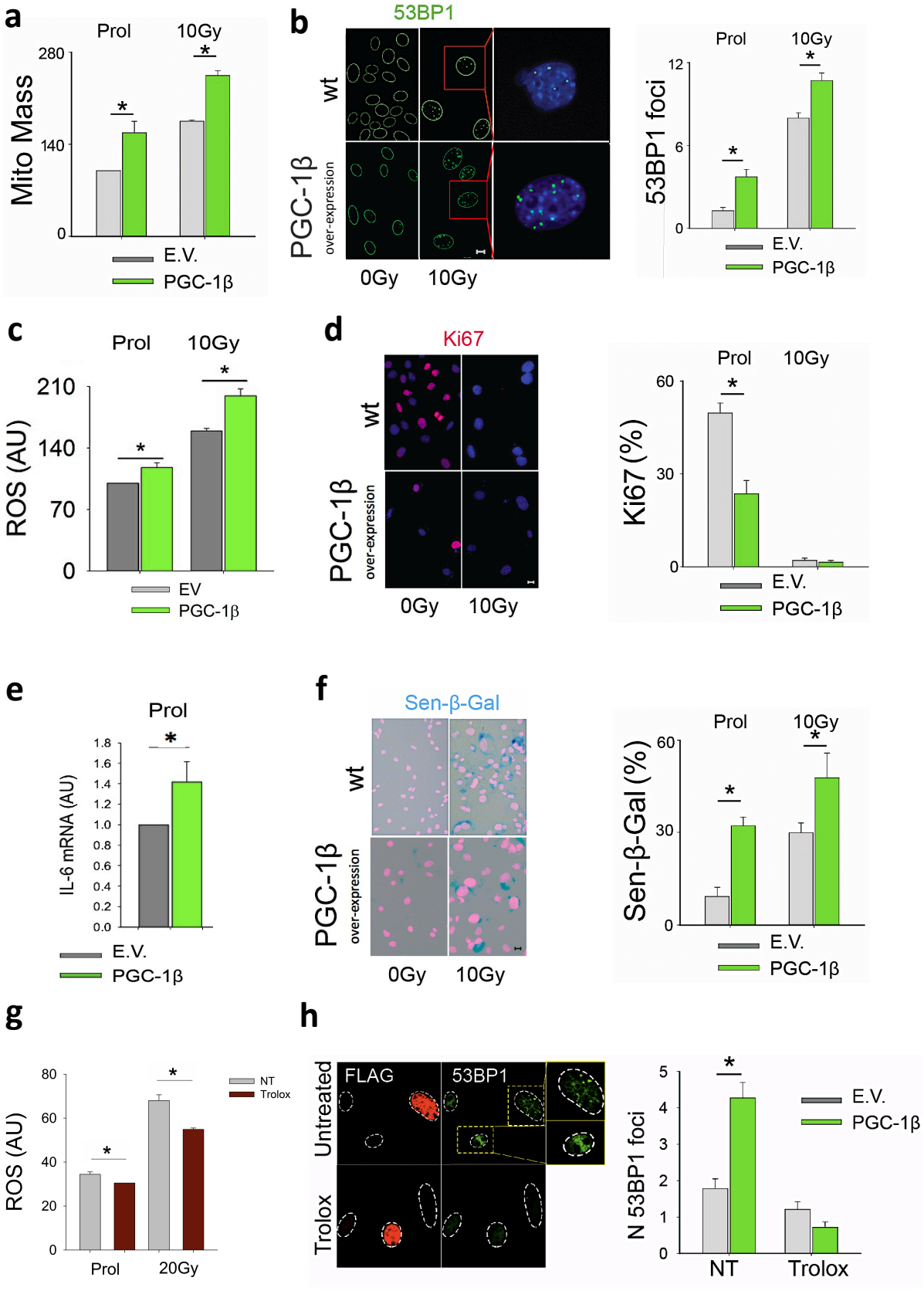
a
Prol
10Gy
Mito Mass
280
140
0
E.V.
PGC-1β
b
53BP1
wt
PGC-1β
over-expression
0Gy
10Gy
Prol
10Gy
53BP1 foci
12
6
0
E.V.
PGC-1β
c
Prol
10Gy
ROS (AU)
210
140
70
0
EV
PGC-1β
d
Ki67
wt
PGC-1β
over-expression
0Gy
10Gy
Prol
10Gy
Ki67 (%)
60
30
0
E.V.
PGC-1β
e
Prol
IL-6 mRNA (AU)
1.8
1.6
1.4
1.2
1.0
0.8
0.6
0.4
0.2
0.0
E.V.
PGC-1β
f
Sen-β-Gal
wt
PGC-1β
over-expression
0Gy
10Gy
Prol
10Gy
Sen-β-Gal (%)
60
30
0
E.V.
PGC-1β
g
ROS (AU)
80
60
40
20
0
NT
Trolox
Prol
20Gy
h
FLAG
53BP1
Untreated
Trolox
N 53BP1 foci
5
4
3
2
1
0
E.V.
PGC-1β
NT
Trolox

**Figure 4.16| PGC-1β-mediated mitochondrial biogenesis promotes cellular senescence**
**a)** Effects of PGC-1β over-expression on mitochondrial mass increase (NAO staining by flow cytometry). Data are mean±S.E.M. of n=3, one-way ANOVA, *p<0.05; **b)** PGC-1β over-expression induced increased 53PB1 damage foci in wild-type MEF. Data are mean±S.E.M. of n=3, one-way ANOVA, *p<0.05; **c)** PGC-1β over-expression induced increased ROS levels in wild-type MEF. Data are mean±S.E.M. of n=3, one-way ANOVA, *p<0.05; **d)** PGC-1β over-expression induced premature cell cycle arrest in proliferating cells. Ki67 staining (red), Data are mean±S.E.M. of n=3, 200 cells per condition, one-way ANOVA, *p<0.05; In **a)** to **d)** cells were analysed three days following transfection and two days after 10Gy irradiation; **e)** interleukin 6 (IL-6) mRNA levels increase upon PGC-1β over-expression on proliferating cells –RT-PCR n=1 samples run in triplicate; **f)** Effects of 10Gy in senescence-associated β-galactosidase positivity in wild-type and PGC-1β over-expressing MEF. Perinuclear blue precipitate indicates positivity for Sen-β-Gal activity. PGC-1β over-expressing cells were analysed seven days post tranfection, six days following irradiation. Data are mean±S.E.M. of n=3, one-way ANOVA, *p<0.05; **g)** Antioxidant trolox reduced ROS levels three days after 10Gy irradiation. n=1, samples ran in triplicate, *p<0.05; **h)** Double staining FLAG (transfected cells - red) and 53BP1 DDF (green) two days following transfection with PGC-1β plasmid and treated 1 day prior to analysis with 250 μM trolox. Data are mean±S.E.M. of n=3, one-way ANOVA, *p<0.05;

# FIGURE 4.17

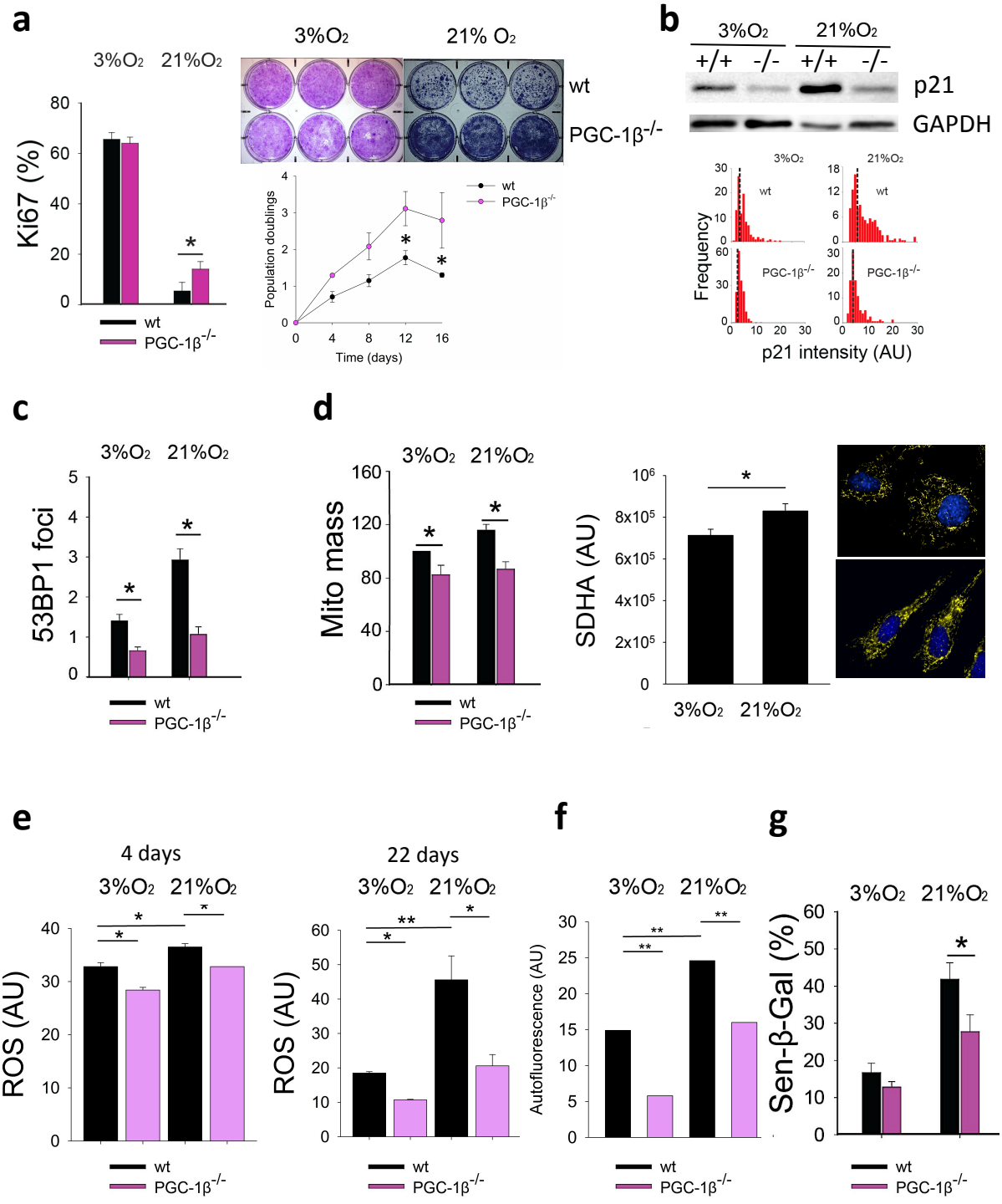
a
3%O2 21%O2
Ki67 (%)
wt
PGC-1β-/-
3%O2 21% O2
wt
PGC-1β-/-
Population doublings
Time (days)
b
3%O2 21%O2
+/+ -/- +/+ -/-
p21
GAPDH
Frequency
p21 intensity (AU)
c
53BP1 foci
d
Mito mass
SDHA (AU)
e
4 days
22 days
ROS (AU)
f
Autofluorescence (AU)
g
Sen-β-Gal (%)

**Figure 4.17| PGC-1β KO MEF senesce slower under normoxic conditions**

**a)** Quantification of cell proliferation Ki67 stanining for wild-type and PGC-1β KO MEF under 21% oxygen at day six. Clonogenic assays at 3 and 21% oxygen after three weeks. Initial cell concentration was $2x10^5$ and $5x10^3$ cells respectively. Population doubling calculation of wild-type and PGC-1β KO MEF under normoxic conditions. Data are mean ±S.E.M. of n=3, one-way ANOVA, *p<0.05; **b)** (top) representative p21 WB for wild-type and PGC-1β KO MEF following four days under 3% or 21% atmospheric oxygen levels. (bottom) p21 nuclear staining intensity histograms six days following 21% oxygen conditions. Dashed line indicates median fluorescence; **c)** Quantification of 53BP1 DDF immuno-staining ten days at 21% atmospheric oxygen conditions. Data are mean±S.E.M. of n=3, one-way ANOVA, *p<0.05; **d)** Mitochondrial mass of for wild-type and PGC-1β KO MEF under 21% oxygen at day four. SDHA fluorescence was increased in wild-type MEF under 21% oxygen at day four. One-way ANOVA, *p<0.05; **e)** ROS levels in wild-type and PGC-1β KO MEF following four and twenty-two days in normoxic conditions. Data are mean±S.E.M. of n=3, one-way ANOVA, *p<0.05, **p<0.001; **f)** Autofluorescence levels in wild-type and PGC-1β KO MEF after twenty-three days in normoxic conditions. Data are mean±S.E.M. of n=3, one-way ANOVA, *p<0.05, **p<0.001; **g)** Effects of 21% oxygen in senescence-associated β-galactosidase positivity in wild-type and PGC-1β KO MEF at day ten. Perinuclear blue precipitate indicates positivity for Sen-β-Gal activity. Data are mean±S.E.M. of n=3, one-way ANOVA, *p<0.05.

# FIGURE 4.18

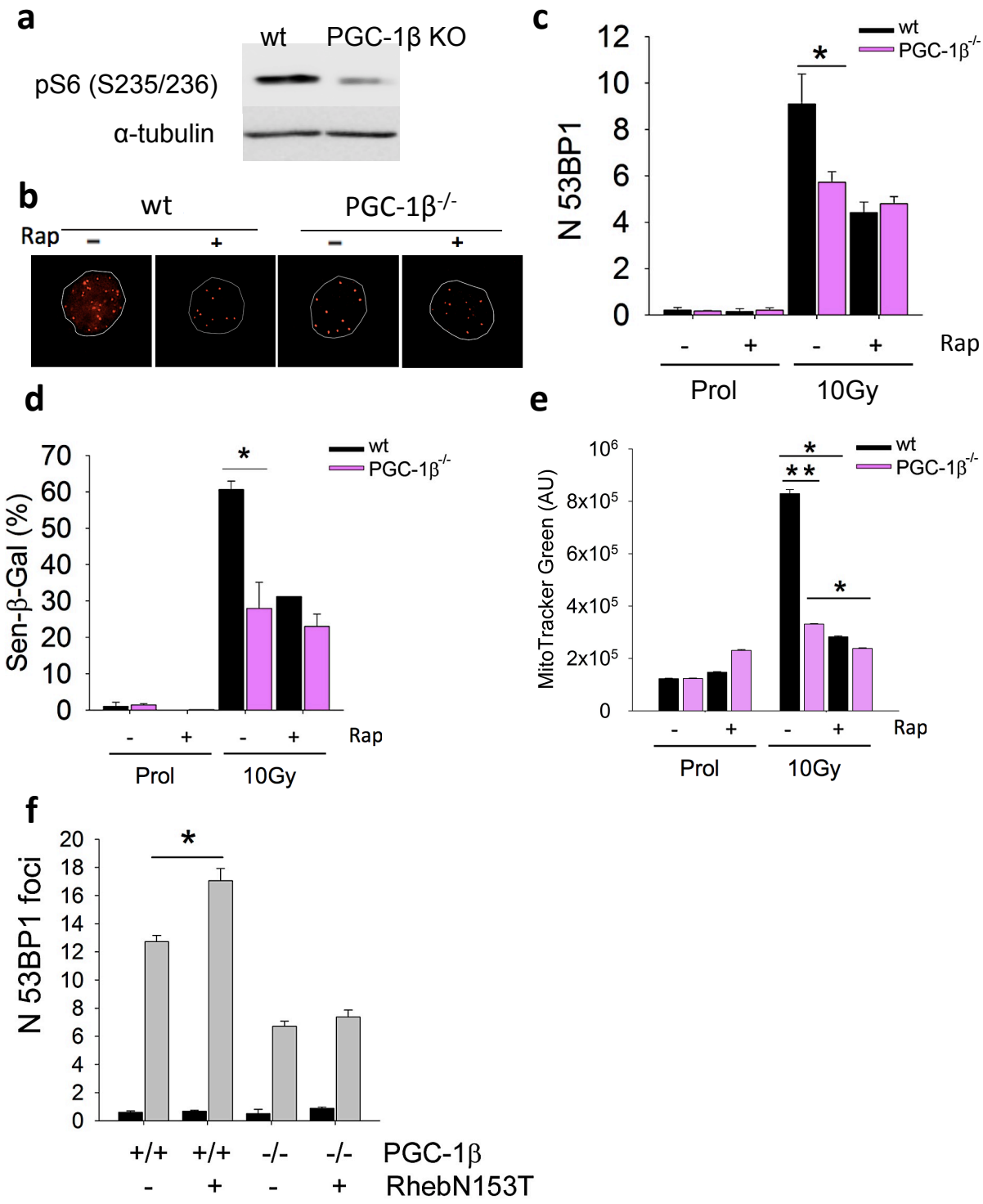
a
wt
PGC-1β KO
pS6 (S235/236)
α-tubulin
b
wt
PGC-1β-/-
Rap
c
N 53BP1
wt
PGC-1β-/-
Rap
Prol
10Gy
d
Sen-β-Gal (%)
wt
PGC-1β-/-
Rap
Prol
10Gy
e
MitoTracker Green (AU)
wt
PGC-1β-/-
Rap
Prol
10Gy
f
N 53BP1 foci
+/+ +/+ -/- -/- PGC-1β
- + - + RhebN153T

**Figure 4.18| PGC-1β and mTORC1 cooperate in the establishment of the senescent phenotype**

**a)** phophorylated ribossomal S6 protein at serine 235 and 236 (readout for mTORC1 activity) is reduced in PGC-1β KO MEF three days following 10Gy; **b)** immunofluorescence staining and **c)** graphic quantification of 53BP1 DDF three days following 10Gy irradiation. Cells were treated with rapamycin immediately after ionising radiation stimuli. Data are mean±S.E.M. of n=3, one-way ANOVA, *p<0.05; **d)** Effects of 10Gy in senescence-associated β-galactosidase positivity at day nine in wild-type and PGC-1β KO MEF treated with rapamycin. Data are mean ±S.E.M. of n=3, one-way ANOVA, *p<0.05; **e)** Effects of 10Gy on MitoTracker Green intensity in wild-type and PGC-1β KO MEF treated with rapamycin. Irradiated cells were analysed two days following 10Gy. n=33-76 cells per condition (preliminary data); **f)** Graphic quantification of 53BP1 DDF three days following 10Gy irradiation and two days following RhebN153T transfection. Data are mean±S.E.M. of n=3, one-way ANOVA, *p<0.05.

# DISCUSSION

## mTORC1 impacts on the DDR and on ROS during stress-induced senescence

The DDR is a vital component for the induction and maintenance of cellular senescence [230]. The two main nodes of the DDR shown to be crucial for senescence are the p53-p21 and the p16-Rb axis [230]. Our data shows that shortly after induction of a DDR by ionising radiation (6 hours), mTORC1 activity is up regulated. This data contrasts with the published literature, where generally is claimed that p53 activity antagonises mTORC1 and vice-versa, that mTORC1 regulates p53 stability via MDM2 phosphorylation at S163 by p70S6K1 [231, 232]. In the irradiation model, p53 serine 15 phosphorylation spikes on the first five hours and then decays, being expressed at a basal level in human fibroblasts [28]. This might allow consequently increased activation of mTORC1.

mTORC1 activity is tightly controlled by the upstream TSC and Rheb components. Here we show that silencing of TSC2 or a constitutively active Rheb GTPase promotes DDF accumulation. Additionally to our observation that p21 protein levels increase in HEK293T cells following silencing of TSC2, p21 protein increase has been also reported in TSC2-null MEF [233]. Moreover, TSC2-null MEF showed other signs of senescence such as lack of proliferation, increased fraction of cells in G1 and increased size [233]. Similarly, transient over-expression of RhebN153T in MEF leads to decreased proliferation.

Apart from the impact of TSC2 on the DDR, earlier studies in which TSC1 was deleted in hepatocytes lead to an accumulation of γH2A.X [234]. Additionally, mTORC1 activation via TSC1 loss in haematopoietic stem cells (HSC) lead not only to an up-regulation of p21, but also p16 and p19 transcription [164].

Besides these links, the DDR can also input onto mTORC1 functions via REDD1 - a known p53-transcriptional target induced following DNA damage during development [235] and during senescence [236]. This report on osteoblast senescence by γ-radiation puts forward evidence that REDD1 has protective roles in senescence since it antagonizes mTOR phosphorylation and its downstream targets, decreases Sen-β-Gal positivity in cells, as well as it dampens SASP secretion (*e.g.* IL-6 and IL-8) [236, 237]. Finally, REDD1 overexpression shortly following irradiation lead to a decline of p21 protein levels at day one, suggesting maybe a role for REDD1 in the senescence G1 arrest.

Another two possible links established between the DDR and the mTOR pathway are: the Akt direct phosphorylation by ATM [224] and the ATM activation of TSC2 via LKB1/AMPK upon high oxidative stress [238]. Any of the previously mentioned axes involving Akt, REDD1, or ATM have been shown to impact on- and to be triggered by oxidative stress [235, 239, 240]. Here we show that either TSC2 silencing promotes superoxide levels increase. Additionally, we observed that ROS levels were more drastically elevated upon TSC1 depletion than in TSC2 knockdown in HEK293T cells (data not shown). All this data is in agreement with previous observations that both hepatocytes and in haematopoietic stem cells (HSC) lacking TSC1 had higher ROS levels [164, 234]. Finally, NAC treatment reduced the ROS burden in HSC without TSC1 [164]. Overall, this puts forward the notion that the mTOR signalling is not only a sink for oxidative stress cues, but also a generator of ROS.

Besides the role of TSC2, here we showed that the small GTPase Rheb is able to induce a DDR, reduce proliferation and induce Sen-β-Gal activity in primary mouse embryonic fibroblasts. These observations are in divergence with the fact that constitutively active Rheb(N153T) mutant cells are more

clonigenic than their control cells [241]. Finally, Rheb over-expression was suggested to promote Sen-β-Gal positivity in MEF [242].

### Mitochondrial biogenesis in senescence

Mitochondrial biogenesis is a process by which cells maintain, increase and divide their pre-existing mitochondria. The core regulator of this process is the PGC-1 family, which comprises PGC-1α, PGC-1β and PPRC1 [101].

In a variety of cell types over-expression of PGC-1α and PGC-1β increases mitochondria biogenesis and enhances respiration, proposing that both co-activators are the limiting factors for mitochondrial gene expression program [101]. Increasing mitochondrial biogenesis via expression of PGC-1α speeded the rate at which senescence occurred in human diploid fibroblasts [102]. Additionally, higher PGC-1α expression increased in senescent fibroblasts concomitant with an increase in mitochondrial mass [103]. Contradictory views are defended by Ron De Pinho's group on the role of telomere dysfunction, p53 and, PGC-1α- and PGC-1β-mitochondrial biogenesis (reviewed in [243]). In mouse models of accelerated ageing due to telomere dysfunction (TERC-null mice), p53 activation downstream of telomere dysfunction binds to the promoters of PGC-1α- and PGC-1β inhibiting the expression of these biogenesis regulators [85]. As consequence, mitochondria become dysfunctional, produce less ATP and show increased ROS generation [85].

In a broader context, PGC-1α does not only impact in cellular senescence but also has multiple effects in pathological settings such as renal fibrosis [104], cardiomyopathy [105], and diabetes [106]. This later study, reports that endothelial PGC-1α overexpression induced multiple diabetic phenotypes that encompassed blunted wound healing, reduced blood flow after hindlimb ischemia and aberrant re-endothelialization following carotid injury [106].

Besides the PGC-1 family, mitochondrial biogenesis is a complex process that involve other transcription factors and proteins including the NRF1/2a (nuclear respiratory factors), PPAR (peroxisome proliferator-activated receptor) family (α, β, γ, δ), ERRα (Estrogen-related receptor) and calcium/calmodulin protein kinases II and IV (CaMKII and CaMKIV)[244-246]. Altogether, these proteins activate target genes that encode fatty-acid oxidation (FAO), oxidative phosphorylation and antioxidant defence enzymes [247].

Furthermore, during mitochondrial biogenesis there is a necessity for proliferation of mitochondrial membranes, meaning that phospholipids such as cardiolipin are essential. In heart, cardiolipin is the main structural phospholipid within mitochondrial inner membrane (representing 8 to 15% of the total phospholipidic mass). Moreover, cardiolipin is the sole phospholipid that is both produced and localized exclusively within mitochondria [246, 248].

Our data points out during stress-induced senescence mitochondrial mass increased, pinpointing therefore that mitochondrial biogenesis is occurring. Moreover we observed in MRC5 and MEF increased mRNA and protein expression of the biogenesis regulators PGC-1α and PGC-1β upon senescence induction.

### PGC-1β mitochondrial biogenesis

PGC-1β KO cells have less mitochondria. Besides mitochondrial *de novo* formation, PGC-1β endorses mitochondrial fusion and elongates mitochondrial tubules via association with mitofusin 2 (Mfn2) promoter and co-transcriptional activation of ERRα [214].

Another more plausible hypothesis for the less mitochondria present in PGC1β null cells, is that PGC-1β positively regulates mitochondrial fusion by

mitofusin 2 (Mfn2)[214], so in the absence of PGC-1β, mitochondrial fusion might be compromised thus mitochondria fail to fuse and elongate and, ultimately, fail to promote cellular senescence. Furthermore, this lack of enlarged mitochondria that can evade autophagic degradation [249], might shift the balance towards smaller mitochondria, that can potentially being more easier cleared by autophagy.

As mentioned before, senescence can be a outcome of mitochondrial elongation via Opa1 and hFIS1 silencing [96]. This makes sense, and perhaps, the accelerated senescence induction observed while over-expressing PGC-1β could be due to enhanced mitochondrial elongation.

Although PGC-1β-null MEF have impaired mitochondrial biogenesis, some degree of mitochondrial mass and mitochondrial DNA copies increase is observed during stress-induced senescence. This suggests that other mitochondrial biogenesis regulator other than PGC-1β is active (as shall be discussed later); that the existing mitochondria elongate via Mfn2 by a PGC-1β-independent process or, it could also represent that a fraction of mitochondria remain undegraded by problems in the autophagic clearance. Indeed the latter two hypotheses might be more plausible scenarios, because elongated mitochondria are known to evade autophagic degradation, in other words, the autophagic machinery is physically inability to encompass large mitochondria [249]. Secondly, because elongated mitochondria are present in senescent cells and human diploid fibroblasts from aged people [250]. Finally, long interconnected mitochondria have been reported in senescent cells due to impaired mitochondrial fission (decreased expression of Drp1 and Fis1) [54].

### PGC-1β-mitochondrial biogenesis, PGC-1α and antioxidant defence enzymes during cellular senescence

Although several reports claim redundant functions of PGC-1α and PGC-1β in regulating mitochondrial biogenesis, in the majority of PGC-1β$^{-/-}$ mice tissues (with the exception of adipose tissue) no compensatory effects have been observed, supporting a pivotal role for PGC-1β in the regulation of basal mitochondrial activity [251]. Likewise, we observed no compensatory effects of PGC-1α expression in PGC-1β$^{-/-}$ MEF following ionizing radiation were observed.

Similarly to PGC-1α, it is believed that PGC-1β induces expression of genes involved in the removal of ROS [228]. Our data contrasts with this previous report mainly in three points: firstly, because we do not see up-regulation of SOD2 protein, suggesting perhaps that other antioxidant enzymes such as catalase or glutathione peroxidase would be up-regulated thus compensating and explaining the decreased ROS levels observed on PGC-1β-null MEF; secondly, because PGC-1β-overexpressing MEF have higher levels of ROS and DNA damage, which is in divergence with the positive roles of PGC-1β and PGC-1α on transcriptional regulation of antioxidant enzymes [252]; thirdly, our PGC-1β KO MEF are less senescent despite the reduced SOD2 expression thus, contrasting with the phenotype seen in skin ageing where partial loss of SOD2 sponsors mitochondrial oxidative stress and cellular senescence [86]. Additional experimental validation of SOD2 expression levels upon PGC-1β overexpression and SOD2 enzymatic activity assays would strengthen this data.

Here we show that PGC-1β and PGC-1α increased their expression both at the protein and mRNA level as a consequence of X-ray induced senescence. PGC-1β mRNA expression was also been demonstrated to build-up following γ-irradiation [253]. Although hypothesized, this study does not causally link that the mitochondrial mass increase observed following γ-ray treatment is PGC-1β driven. Interestingly, they show by complementation experiments in human cancer cells with mutated p53 or without p53, that PGC-1β expression is not affected and it still increases following irradiation [253]. This data

questions with the canonical view that in mouse with telomere dysfunction, p53 sits on PGC-1β and PGC-1α promoters acting as a transcriptional repressor [85].

## Interactions between the mTOR pathway and, mitochondrial biogenesis and function

Besides being an energy and oxygen sensing system, the mTOR pathway also coordinates metabolic features including glycolysis, the oxidative branch of the pentose phosphate pathway and *de novo* lipid synthesis [254]. When analysing the signalling upstream of mTORC1 we came across many potential nodes for interaction with mitochondrial function (**FIGURE 4.19**).

- **the AKT – PTEN axis**

Regulation of mitochondrial biogenesis and function by PTEN-Akt has led to contrasting results. Firstly upon PTEN loss, Akt becomes hyper-activated and respiratory complexes I, III and IV activity was enhanced [255]. Moreover, this seems not to be regulated by PGC-1α nor by its downstream targets NRF1 and TFAM. This study proposes that Akt regulates mitochondrial respiration through the eukaryotic translation initiation factor 4E (eIF4E)-binding proteins (4E-BP)-protein translation pathway [255]. Indeed, mTORC1 favours translation of nuclear-encoded mitochondria related mRNA (such as TFAM and components of complex V) by inhibiting 4E-BP [256]. In more detail, mTORC1 inhibition using PP242 or Ink1341 in MCF7 breast cancers lead to decreased ATP turnover, total mitochondrial respiration as well as decreases mtDNA and mitochondrial mass (measured by MitoTracker). Additionally, Rictor (specific mTORC2 subunit) and Raptor (specific mTORC1 subunit) silencing, dampened TFAM protein levels, but only Raptor knockdown (KD) reduced mtDNA levels. Thus pointing out again that mTORC1 is the main complex that impacts onto mitochondrial function. This is in accordance with our data in which decreased mtDNA copy number, decreased mitochondrial mass and fewer mitochondrial proteins were observed with rapamycin

treatment (which quenches mTORC1 activity and only mTORC2 upon extended administration)[257].

Goo's findings [255] contrast with following studies in which PTEN loss lead to increase mitochondrial mass by up-regulation of ERRα-PGC-1α biogenesis in hepatocytes [258] and that in heart, Akt overexpression inhibited PGC-1α gene expression [259].

- **the TSC1/TSC2 complex**

MEF without TSC2 catalytic subunit showed signs of premature senescence [233]. Loss of TSC2 resulted in increased mitochondrial DNA replication – higher levels of TFAM and mtDNA copy number – higher ATP levels and total mitochondria respiration [256, 260]. We also observed that upon TSC2 silencing in HEK293T cells higher ROS levels. Similarly, this data is in accordance with other studies namely those on hematopoietic stem cells and hepatocytes lacking TSC1 with consequent increased ROS and mitochondrial biogenesis levels [261] [234]. Despite this, and although Morita and colleagues [256] proposed a link from TSC2 towards 4E-BP-translation of TFAM and Complex V proteins, we have preliminary data suggesting that PGC-1β protein levels are enhanced upon TSC2 abrogation.

- **AMPK**

Other potential link between mTORC1 and mitochondrial function is the energy-sensing AMPK node. AMP kinase becomes phosphorylated upon energy stress and it is often seen in this state during oncogene-induced senescence (OIS)[76]. Muscle-specific AMPK deletion decreased PGC-1α-mediated mitochondrial biogenesis [262].

- **VHL-HIF1α**

Von Hippel-Lindau (VHL) deficient renal carcinoma cells have higher mtDNA copies together with increased ETC proteins and activity [263]. VHL is also a

negative-regulator of hypoxia factor-1α (HIF-1α), a key protein responsive to oxygen changes and whose loss accelerates cellular senescence onset [264]. HIF-1α hinders mitochondrial mass and mtDNA increase, and increased oxygen consumption [265]. Mechanistically, HIF-1α phenotype can be explained by its ability to block c-Myc protein activity, which directly promotes PGC-1β-mediated mitochondrial biogenesis [265]. Not only PGC-1β is a transcriptional target of c-Myc, so is TFAM [266]. Although not tested, our MEF senescence data under normoxia could be explained by HIF-1α degradation [267], which would up-regulate PGC-1β-mitochondrial biogenesis and promote cellular senescence.

- **mTORC1 - Raptor and mTOR kinase**

Mice models with organ specific mTOR or Raptor deletion have shown to impact on mitochondrial function. More detailed, Raptor deletion in muscle lead to decreased PPARα**,** PPARδ and mitochondrial proteins (MCAD, LCAD, COXI and COXIV)[268]. Likewise, those same targets were dampened in mTOR muscle knockout mice [268] and these mice have mitochondria with altered morphology and oxidative capacity [269]. In adipose tissue, Raptor deletion up-regulates UCP1 expression [270] which very recently has been shown to promote mitochondrial biogenesis through fission [271].

In proliferating cells, rapamycin-mediated mTORC1 inhibition reduced PGC-1α expression and transcripts together with reduced mtDNA copies and oxygen consumption [272]. Besides these effects on muscle cells, also in Jurkat cells positive correlations between mTORC1 activity and mitochondrial function (e.g. mitochondrial membrane potential, oxidative capacity and ATP levels) was observed [260]. In our hands, rapamycin treated primary human and mouse fibroblasts had higher mitochondrial membrane potential during stress-induced senescence (data not shown).

- **p70S6K1**

p70S6K1 KO mice have higher mitochondrial content in skeletal muscle and adipose tissue probably driven by enhanced PGC-1α and UCP1 expression [273]. In muscle AMPK is activated on these mice, indicating energy stress and potentially explain the elevation of PGC-1α levels [274]. At the cellular level, p70S6K1 phosphorylates PGC-1α weakening its co-activation interaction with HNF4α in liver, leading consequently to a block gluconeogenic target genes expression [275]. Of note, HNF4α was also highly enriched as transcription factor/ binding element in promoters of mTORC1-induced genes [276].

Notably, mTOR kinase knock-in mice (where exon 12 was replaced by with BALB/c sequences) – [277] [278], rapamycin treated mice or whole body p70S6K1 KO mice have extended lifespans [140, 278, 279].

### Non-canonical nuclear mTOR complex

Besides the described nodes of interaction from the mTOR pathway towards mitochondrial orchestrators PGC-1α and PGC-1β, these proteins also impact on mTORC1 activity. Firstly, it was observed that PGC-1α over-expression in skeletal muscle lead to increased phosphorylated mTOR and S6 phosphorylation [280, 281] and decreased p65 phosphorylation (therefore less NF-κB transcriptional activity)[280]. Additionally, PGC-1α over-expression in raptor-muscle KO mice ameliorated mitochondrial function but was unable to prevent muscle myopathy [268]. Finally, PGC-1β silencing in human breast cancer cells lead to reduced phosphorylated AMPK, reduced Rictor (Thr1135) and reduced Raptor and S6 protein levels, but enhanced Akt (Ser473-mediated apoptosis [282]. Moreover, according to the authors “PGC-1β and mTOR levels were correlated with overall mitochondrial activity”. In combination to our data on PGC-1β KO MEF having less phosphorylated S6 levels and the ability of PGC-1β to prevent DNA damage accumulation upon constitutively active mTORC1, overall this data on PGC-1α and PGC-1β might

indicate that mitochondrial biogenesis acts as a positive forward loop onto mTORC1 activity.

### mTORC1 regulation of ROS and antioxidant defence enzymes

We have seen that activation of the DDR was accompanied by increased mRNA expression of antioxidant enzymes SOD1, catalase, SOD2 (data not shown), which is in accordance with higher expression and activity of antioxidant enzymes in replicative senescence [68]. This evokes an adaptive, albeit deficient, response to elevated ROS and it is consistent with our observation that rapamycin despite suppressing the increased expression of antioxidant enzymes (e.g. SOD2) and the increased PGC-1α and PGC-1β levels, it also decreased ROS levels significantly during senescence in MEF and replicatively senescent MRC5.

The decreased ROS observed upon rapamycin treatment has also reported in HSC [261] and in senescent normal oral keratinocytes [283]. This last report tries to explain that the decreased ROS was derived from a rapamycin-positive effect on SOD2 protein expression. Interestingly, rapamycin treatment does not interfere with SOD1 and even decreases catalase expression [283].

In summary we show that mitochondria biogenesis is an early event and, it contributes to cellular senescence onset. Additionally, high content of mitochondria is necessary for the maintenance of a stable cell cycle arrest. Finally, we described mechanistic links between the DDR pathway and mitochondria biogenesis by induction of the mTOR pathway (**FIGURE 4.20**).

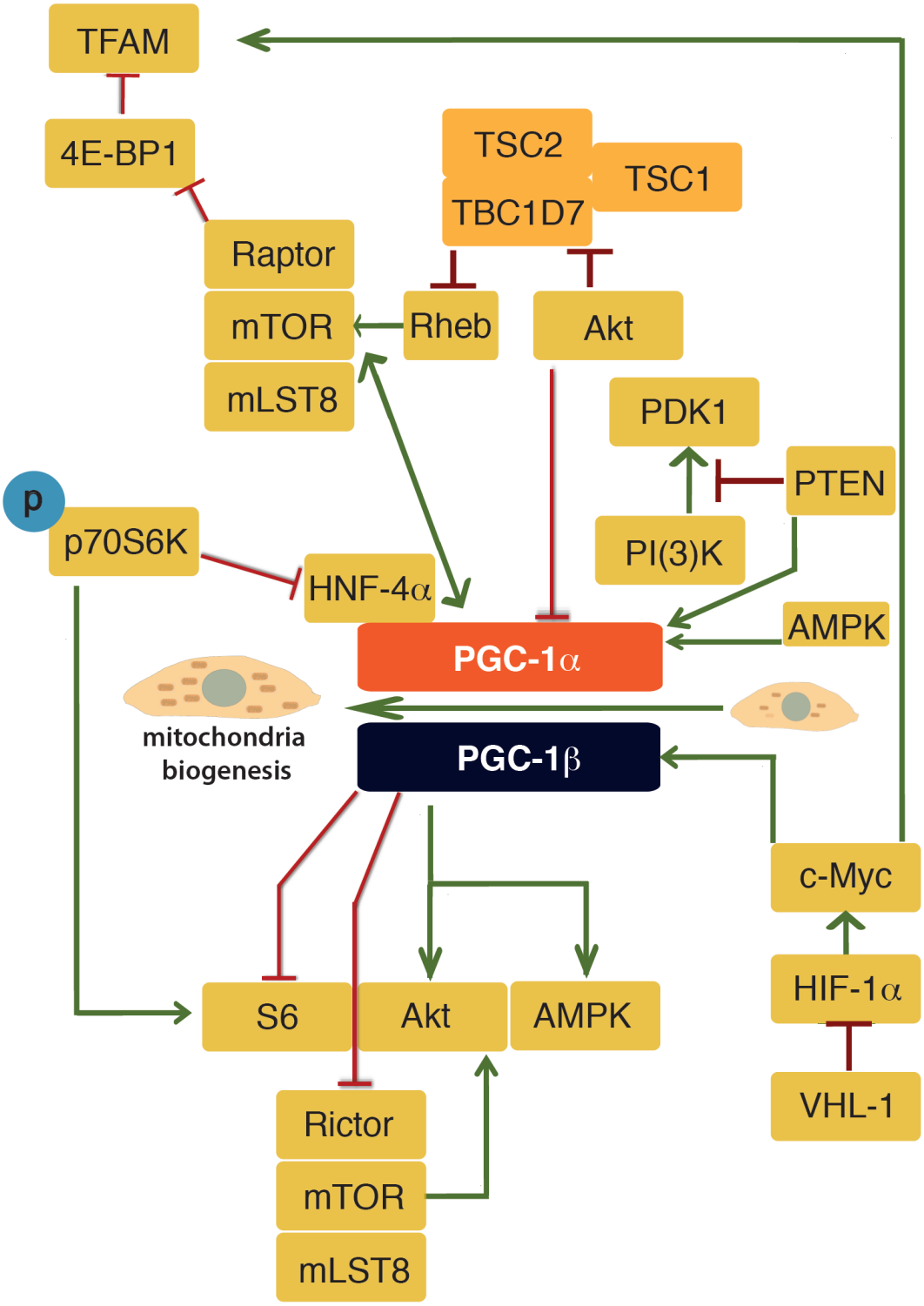


**FIGURE 4.19| Mechanistic links between mitochondrial biogenesis (PGC-1α and PGC-1β) and the mTOR pathway.**

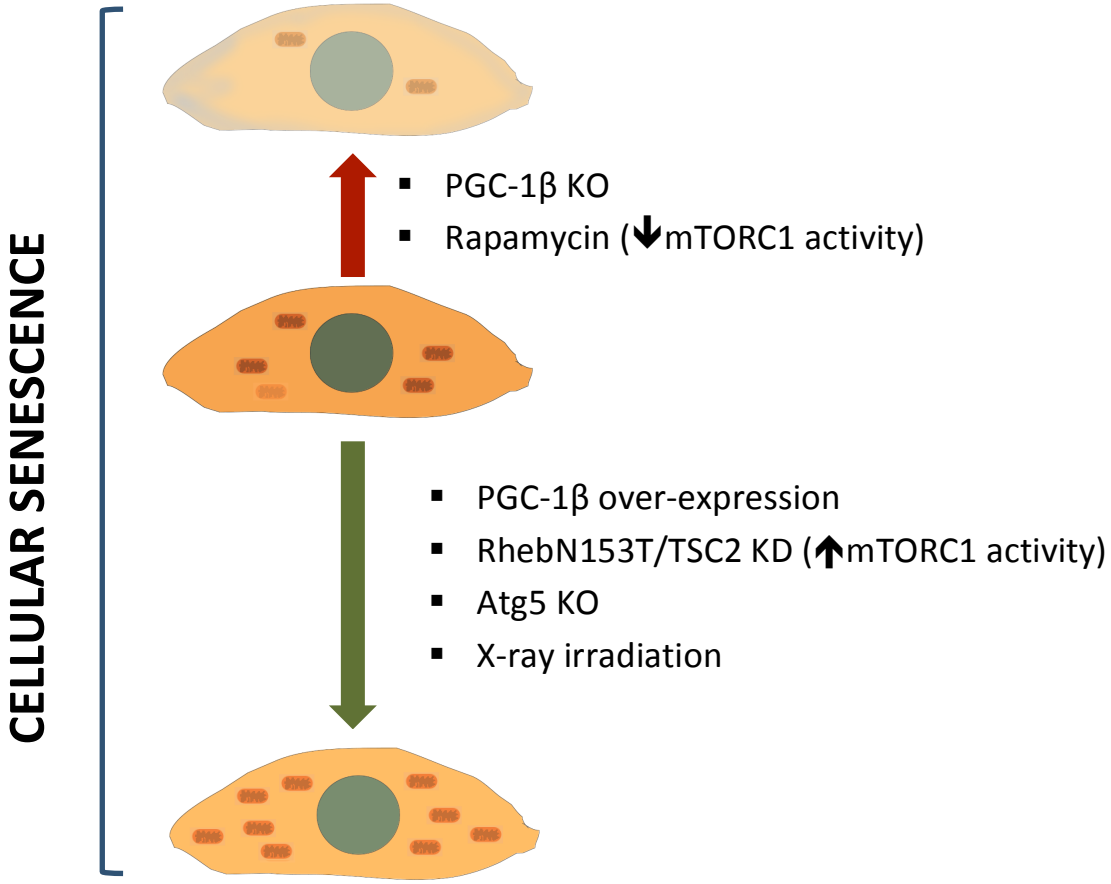


**FIGURE 4.20| Modulation of mitochondrial biogenesis, mTORC1 and autophagy alters mitochondrial numbers within cells and it impacts on the development of the senescent phenotype.**

# CHAPTER 5 – PYRUVATE-INDUCED SENESCENCE (PIS)

## INTRODUCTION

Pyruvate is an organic acid that is the final product of glycolysis and it is a major substrate for the tricarboxylic acid (TCA) cycle within mitochondria. Besides this, pyruvate can be metabolised back to glucose (via gluconeogenesis), can be converted to fatty acids by acetyl-CoA, or it can be synthesised into alanine.

Addition of sodium pyruvate (10mM) to diploid fibroblasts leads to cell proliferation arrest within 5 days, increased the fraction of cells positive for Sen-β-Gal activity and, cells treated with pyruvate had increased p53, p21 and p16 protein levels [102]. More recently, pyruvate metabolism has been implicated in oncogene-induced senescence (OIS) [284].

Besides roles in senescence, pyruvate has also been shown to stimulate mitochondrial biogenesis in PGC-1α-independent manner in C2C12 myoblasts [285, 286].

Based on this data, we thought that pyruvate might be a suitable tool to study the impact of mitochondrial biogenesis during senescence.

## AIMS

- Does pyruvate induce DNA damage foci?
- Does pyruvate induces cellular senescence by enhancing mitochondrial mass independently of PGC-1α-mitochondrial biogenesis?
- Do antioxidants and rapamycin alleviate pyruvate-induced senescence?

## RESULTS

### Pyruvate addition induces cellular senescence

Firstly, we tested several concentration of sodium pyruvate (10, 50 and 100 nM) based on the observations that 50mM increases mitochondrial proteins levels and increases respiration in myoblasts [285, 286]. We observed that 100nM was toxic for MRC5 fibroblasts, leading to cell death in three days. As standard, we treated cells with 10mM sodium pyruvate since this concentration was sufficient to trigger cellular senescence as previously reported [102](**FIGURE 5.1**).

In more detail, MRC5 fibroblasts growing in pyruvate supplemented media increased expression of several OXPHOS proteins including SDHA, UQCRC2, VDAC and MT-CO2 (**FIGURE 5.1g**), increased the cell-cycle inhibitor kinase p21 levels (**FIGURE 5.1c**) and, ultimately lead to premature senescence (measured by Sen-β-Gal activity after 20 days of this pyruvate regime)(**FIGURE 5.1h**). We found that pyruvate supplementation for three days was sufficient to induce a significant increase in the number of γH2A.X foci (**FIGURE 5.1d**), reactive oxygen species (**FIGURE 5.1e**), cell size (**FIGURE 5.1f**) and inhibition of cellular proliferation (measured by colony assays and by expression of the proliferation marker Ki67)(**FIGURES 5.1a** and **5.1b**).

Following the observations that pyruvate prompted an increase on mitochondrial content and promoted ROS generation, we hypothesised that combinatory use of pyruvate and the antioxidant N-acetylcysteine (NAC) would rescue appearance and maintenance of senescence markers by decreasing ROS levels. Firstly, we have seen that addition of NAC and pyruvate rescued the number of MRC5 colonies and there were higher frequencies of cells proliferating (**FIGURES 5.2a** and **5.2b**). Secondly, we

observed that synchronous addition of these two compounds lead to a reduction of the number of γH2A.X damage foci (**FIGURES 5.2c** and **5.2d**). Finally, we also report that combination of pyruvate with NAC quenches the cellular levels of ROS (**FIGURE 5.2e**).

Earlier in this thesis we have shown that rapamycin was able to reduce senescence markers during stress-induced senescence. Thus, we hypothesised that combined addition of rapamycin and pyruvate would delay/rescue senescence markers. Moreover, pyruvate supplementation to proliferating cells lead to higher mTORC1 activity (increased p70S6K1 phosphorylation)(B. Carrol and V. Korolchuck personal communication).

As predicted, we observed that combined addition of pyruvate and rapamycin reduced the mitochondrial content (**FIGURE 5.3a**), decreased the number of γH2A.X damage foci (**FIGURES 5.3b** and **5.3d**) and, moderately rescued cellular proliferation (**FIGURES 5.3c** and **5.3e**).

Overall, this set of data highlights the importance of cellular metabolism on the induction of cellular senescence. Finally, we show that the use of antioxidants and rapamycin might alleviate or prevent the appearance of senescence markers during pyruvate-induced senescence (PIS).

# FIGURE 5.1

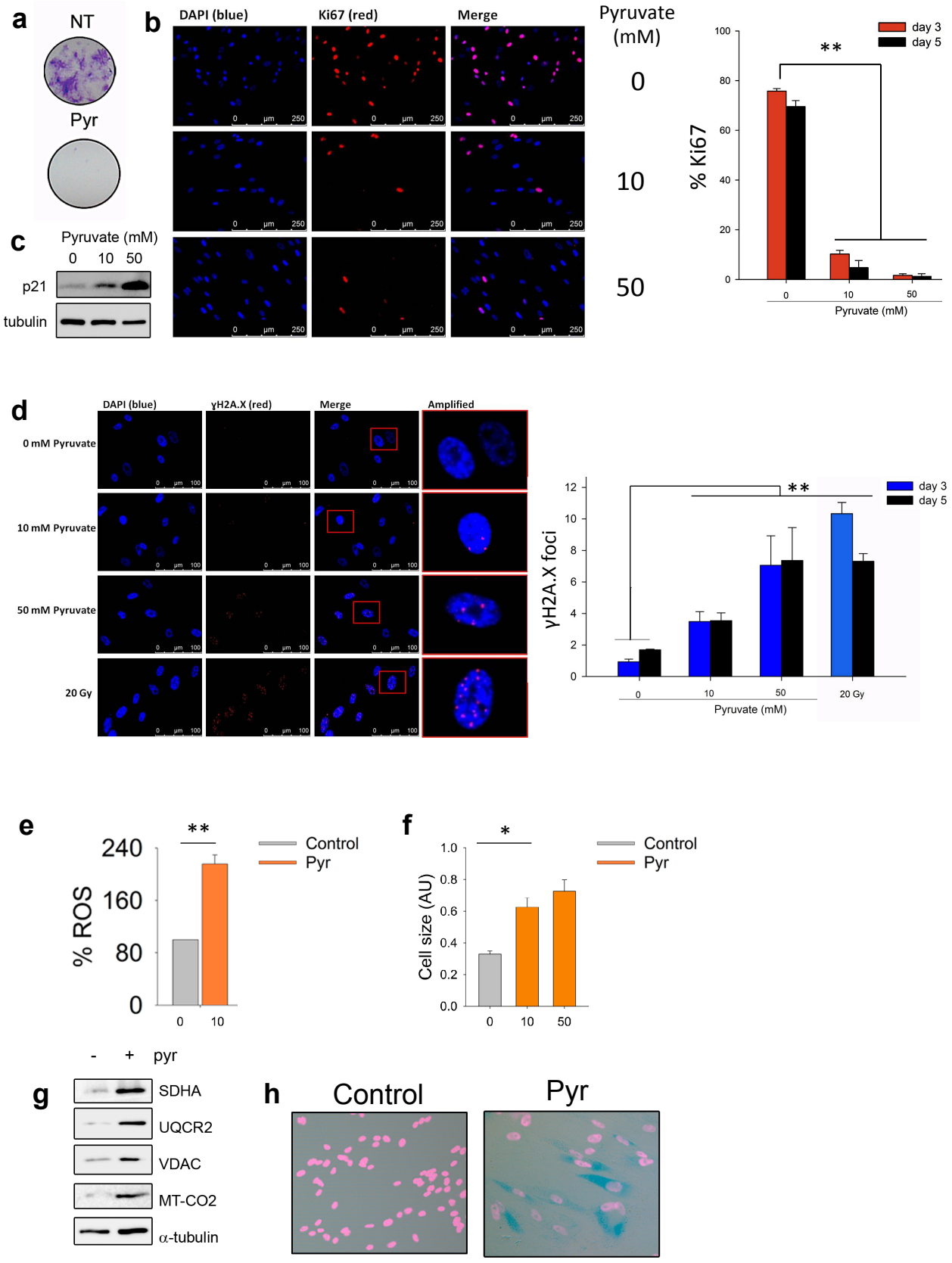
a
NT
Pyr
b
DAPI (blue)
Ki67 (red)
Merge
Pyruvate (mM)
0
10
50
day 3
day 5
**
% Ki67
Pyruvate (mM)
c
Pyruvate (mM)
0 10 50
p21
tubulin
d
DAPI (blue)
γH2A.X (red)
Merge
Amplified
0 mM Pyruvate
10 mM Pyruvate
50 mM Pyruvate
20 Gy
γH2A.X foci
e
% ROS
Control
Pyr
f
Cell size (AU)
g
- + pyr
SDHA
UQCR2
VDAC
MT-CO2
α-tubulin
h
Control
Pyr

**Figure 5.1| Chronic pyruvate supplemmentation leads to cellular senescence**

Clonogenic assay showing that sodium pyruvate (Pyr) inhibited proliferation on MRC5 cells. 10mM was used for two weeks, n=3; **b)** Pyruvate halts cellular proliferation in a dose dependent manner. Cells were cultured three or five days with 10 or 50 mM pyruvate. Data are mean± s.e.m., n=4, one-way ANOVA **p<0.001; **c)** Representative WB depicting a linear p21 increase with increased levels of pyruvate (at day three post-treatment); **d)** γH2A.X damage foci increased with pyruvate addition. Data are mean±S.E.M. of n=4, one-way ANOVA, p<0.001; **e)** ROS are increased upon 10mM pyruvate addition (3 days). Data are mean±S.E.M. of n=3, one-way ANOVA, p<0.001; **f)** cell size increased upon addition of 10mM and 50mM pyruvate after 3 days. Fresh media was added every 48 hours. Data are mean± standard deviation of n=2 experiments, 100 cells analysed per condition. Two-tailed t-test, p<0.05; **g)** Mitochondrial proteins from complexes II, III and IV and VDAC increase upon pyruvate treatment (3 days); **g)** Chronic use of pyruvate leads to Sen-β-Gal positivity at day twenty. NT-non-treated 3.41%±0.191/ Pyr-sodium pyruvate (10mM) 69.35%±13.82. Data are mean± standard deviation of n=2.

# FIGURE 5.2

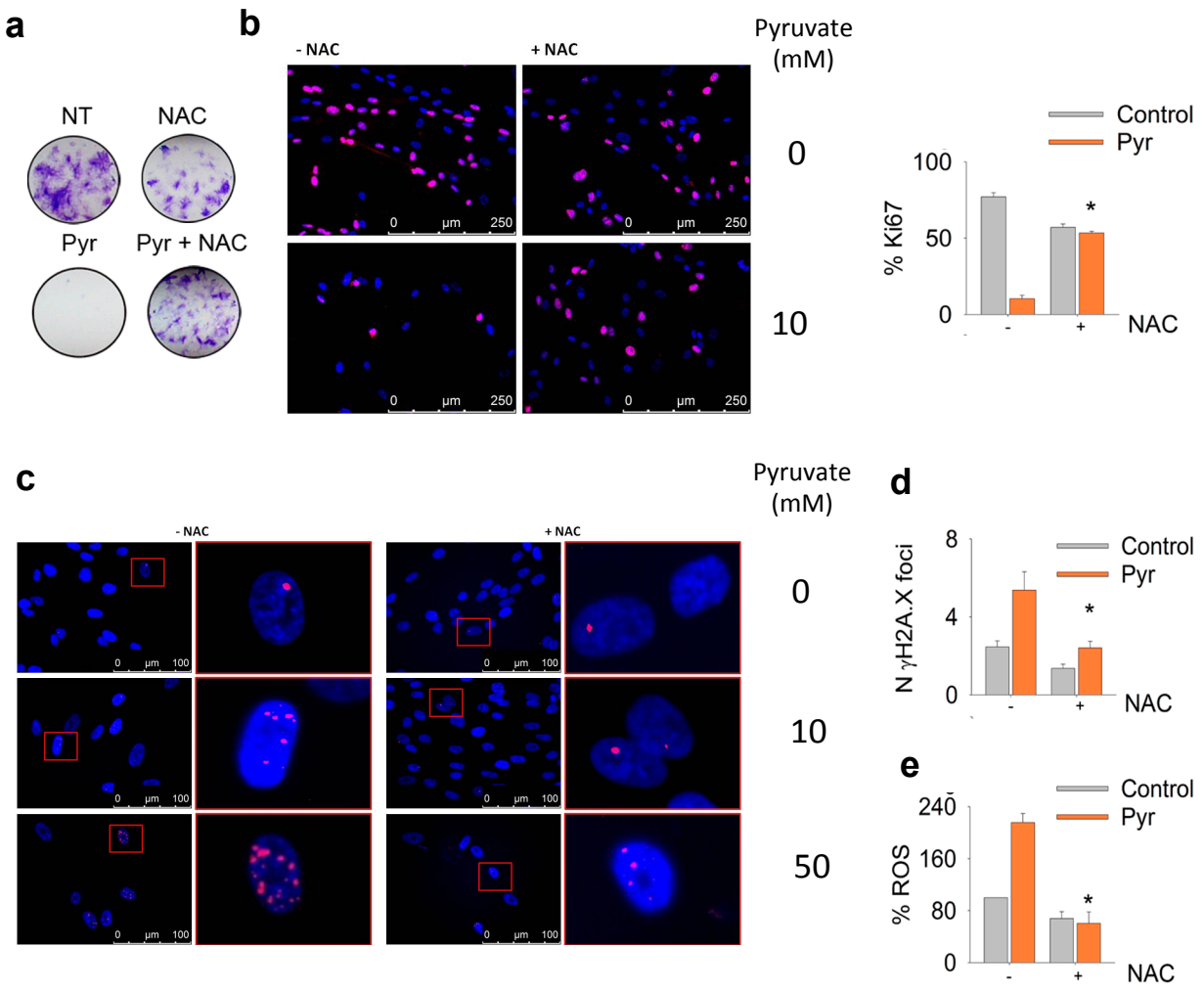


**Figure 5.2| N-acetylcysteine (NAC) rescues pyruvate-induced senescence (PIS) markers**

**a)** Synchronous treatment of young MRC5 cells with sodium pyruvate (10 mM) and NAC rescues proliferation in MRC5 fibroblasts. Colony assay (n=3) and **b)** representative images Ki67 staining. Data are mean±s.e.m. of n=3, one-way ANOVA, $p<0.001$; **c)** representative images of γH2A.X (red) of cells jointly treated with pyruvate and NAC (n=3); **d)** number of DNA damage foci after 3 days of combined pyruvate and NAC treatments. Data are mean±s.e.m. of n=3, one-way ANOVA, $p<0.05$; **e)** ROS levels measured by DHE staining. For ROS analysis NAC was only administered one day prior to analysis. Data are mean±s.e.m. of n=3, one-way ANOVA, $p<0.05$

# FIGURE 5.3

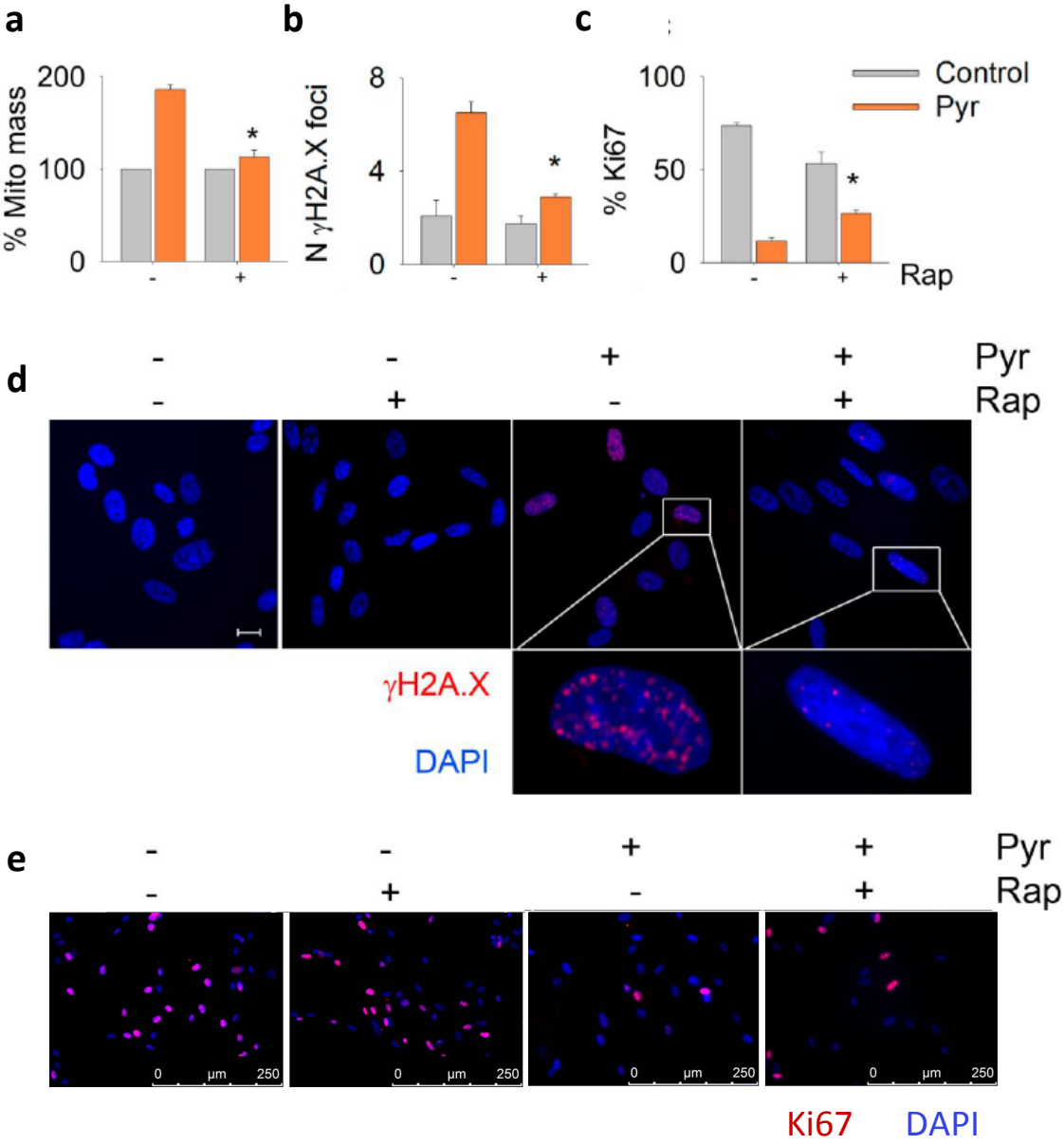


**Figure 5.3| Rapamycin rescues pyruvate-induced senescence (PIS) markers**

**a)** MRC5 increase their mitochondrial mass after pyruvate administration and combined treatment with rapamycin rescues mitochondrial mass increase. Data are mean±S.E.M. of n=3, one-way ANOVA, $p<0.05$; **b)** γH2A.X damage foci increase is halted by rapamycin co-treatment. Data are mean±S.E.M. of n=3, one-way ANOVA, $p<0.05$; **c)** increased fraction of Ki67 positive cells upon concurrent pyruvate-rapamycin treatment. Data are mean±S.E.M. of n=3, one-way ANOVA, $p<0.05$; **d)** representative images of γH2A.X (nuclei-blue, γH2A.X-red); **e)** representative images of Ki67(nuclei-blue, cell proliferation marker Ki67-red).

## DISCUSSION

### Pyruvate-induced senescence and the role of metabolism in senescence

Pharmacological targeting of pyruvate network has been suggested for treatment some age-related diseases such as of diabetes and ischemic heart disease [287], however very few is actually known regarding effects of pyruvate in cellular senescence.

Pyruvate acts as a pivot metabolite between many catabolic and anabolic pathways by being involved in redox signalling, ATP generation, oxygen consumption, fuel selection and biomass production [288]. Here we showed that pyruvate addition functions as trigger metabolite inducing cellular senescence. Despite our findings on senescence markers induction post-pyruvate addition are similar to an earlier report [102], the novelty lies on the fact that pyruvate supplementation triggers γH2A.X damage foci formation. This observation is contradictory with the present view that senescence triggered by $BRAF^{V600E}$ due to metabolic up-regulation of pyruvate dehydrogenase is DDR-independent [10]. However, our data in pyruvate-induced senescence is compatible with the evidence that early events that lead to pyruvate metabolization promote cellular senescence [10]. The Kaplon study states that pyruvate oxidation can hinder tumour growth in BRAF-mediated melanoma via induction of oncogene-induced senescence [10]. This same study demonstrated that $BRAF^{V600E}$-induced senescent fibroblasts had enhanced mitochondrial tricarboxylic acid (TCA) cycle usage and, that the effects of pyruvate seem to precede the onset of oncogene induced senescence (OIS) rather than being a result of it. Mechanistically, pyruvate dehydrogenase (PDH) acts as the gatekeeper protein that bonds glycolysis to the TCA cycle. Senescent cells exhibited higher PDH activity, which was linked with decreased PDH2 inhibitory-phosphorylation due to less expression of PDH kinase 1 (PDK1) [10]. Activation of PDH is mandatory for oncogene-induced senescence (OIS) under mutant BRAF mutation settings. *In vivo*, knockdown of PDK1 thwarts tumours formation by human melanoma cell lines and moreover, nude-mice tumours retrogress. In another model of OIS –

$KRAS^{G12V}$, PDH activity remains elevated in senescence, despite the fact that altered PDH flux was not due to changes in PDP2 nor PDK1 [10]. In summary, while PDP2 is required for OIS induction and keeps TCA on, PDK1 switches of the TCA cycle and make cells bypass OIS.

The rescue of senescence markers upon mTORC1 inhibition by rapamycin on cells undergoing pyruvate-induced senescence is different from the data in which activation of phosphatidylinositol 3-kinase (PI3K) (and consequent activation of mTORC1) reverses $BRAF^{V600E}$ oncogene-induced senescence [289]. The differences may lie in the fact that, PI3K activation does not only promote mTORC1 activation, but also can impinge on mTORC2 activity (via Akt) and induce a different cellular response.

Besides pyruvate involvement in $BRAF^{V600E}$ OIS, IMR90-HRAS cells show distinct metabolic and bioenergetics signatures from replicative senescent cells [15]. IMR90-HRAS cells had preeminent levels of fatty acid oxidation (FAO), which lead to an unforeseen increment of basal oxygen consumption. Afterwards, the authors determined the effect of decreasing the activity of carnitine palmitoyl transferase (CPT1A) – the rate-limiting step in mitochondria fatty acid oxidation (FAO) – and found that it restored the pre-senescent metabolic rate and, it resets SASP components secretion (including GM-CSF, GRO-α, IL-8, MIP1-α, but not IL1β)[15].

Altogether my data supports a role for pyruvate as a metabolite that can promote cellular senescence and, these results highlight the importance of metabolism, mitochondria and reactive oxygen species in the induction and maintenance of the senescence arrest. Additionally, it establishes a new connection between pyruvate and the mTOR pathway during cellular senescence not previously described.

## GRAPHICAL SUMMARY

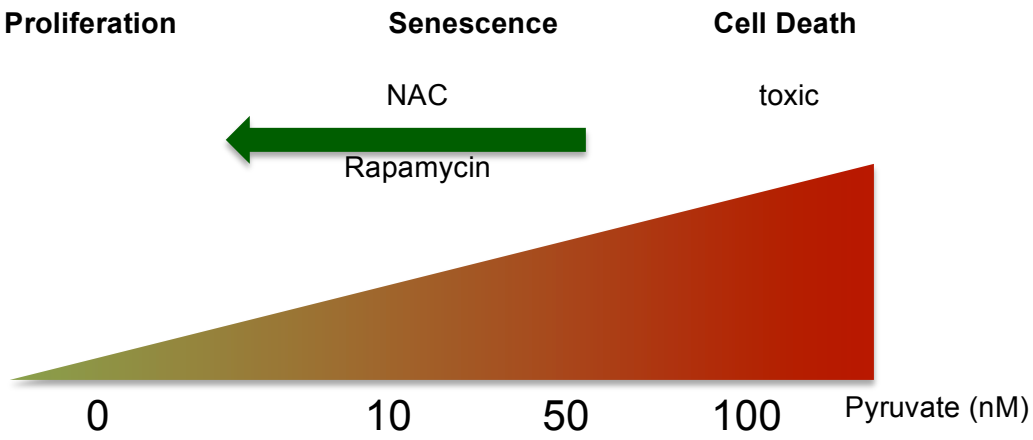


**FIGURE 5.4| Pyruvate addition induces cellular senescence. Jointly addition of pyruvate and NAC or, pyruvate and rapamycin delays senescence onset.**

# CHAPTER 6 – EFFECTS OF RAPAMYCIN DIET AND PGC-1β DELETION ON MICE CELLULAR SENESCENCE *IN VIVO*

## INTRODUCTION

Ageing is a process that leads to overlay decay of organ physiologic homeostasis and increases the vulnerability of death with time [290]. This decline constitutes a primordial risk for development of many diseases namely cancer, diabetes and neuropathologies. Lately, many efforts have been made to pin down key genetic and biochemical processes that control the rate of aging including the role of the nutrient-sensing pathway IGF-1/mTOR [291]. Numerous studies from different laboratories have uncovered the positive impacts of dietary restriction and IGF-1/mTOR pathway mutants on lifespan extension [149, 153, 292, 293]. The IGF-1/mTOR pathways control cellular growth by mediating cell proliferation, survival, and energy metabolism. In mammals, lifespan extension was also observed in $IGF1^{-/-}$ mice or mice treated with rapamycin (an mTORC1 inhibitor) [140, 294, 295]. Rapamycin has been advertises as the next “longevity pill” [296], not only due to the promotion of lifespan increase [140, 152], but also due to its positive effects on halting tumour growth, increasing survival of mouse models of cancer and modulating age-related diseases [154-159].

It is tentative to argue that ageing can be explained by a mTOR centric model - in which organismal ageing may result from an un-resolved developmental and growth “programme” that contributes ultimately to disease and death [18]. Behind this concept are the notions that while inhibiting the mTOR pathway, many known aspects of ageing, including protein aggregation (likely by potentiating autophagy), cellular senescence or stem cell exhaustion can be attenuated [163, 164, 297]. Therefore the use of rapamycin or other mTOR inhibitors constitutes a good set of drugs to combat ageing and age-related diseases [145, 298].

Other aspects of mammalian ageing are telomere and mitochondria dysfunction [85]. In fact, mice models of telomere dysfunction show accelerated ageing phenotypes [53], impaired mitochondria function,

decreased mRNA levels of the biogenesis regulators PGC-1α and PGC-1β, increased ROS generation and increased oxidative lesions (measured by 8oxodG) [28] [85]. One of the aforementioned studies claims that the effects on mitochondrial biogenesis are due to the repressive functions of p53 on promoters of mitochondrial biogenesis genes [85]. Although this seems valid for PGC-1α, p53 binding to PGC-1β has been recently questioned [299].

Regarding the regulation of mitochondrial function by the mTOR pathway there are disparate reports. Inhibition of mTORC1 axis either via rapamycin or Raptor knockout results in decreased mitochondria content in muscle [268, 300].

Based on the evidence that rapamycin has beneficial effects on lifespan and it modulates mitochondrial function, we sought to understand the impact of mTORC1 inhibition in liver as mice age.

## AIMS

- Analyse the impact of mTORC1 inhibition by rapamycin on mitochondrial dysfunction in liver of wild-type mice during ageing.
- Analyse the impact of PGC-1β absence in telomere-associated foci *in vivo*.

## RESULTS

### Rapamycin fed mice have fewer senescent markers in liver

In order to study the impact of mTORC1 inhibition by rapamycin on organismal ageing, we began to feed rapamycin to two mice cohorts (**FIGURE 6.1a**). In the first study mice were continuously fed a rapamycin-diet starting at 3.5 months of age, and mice were culled at 6.5, at 12.5 and at 15.5 months of age. In these settings, we observed that rapamycin promoted increased body weight and liver weight increase after nine months of chronic exposure to rapamycin (**FIGURES 6.1b** and **6.1c**). Combined with increased mTORC1 activity, we also saw increased p21 protein levels in liver with age (**FIGURE 6.1h** – top western blot and **FIGURE 6.1e**, respectively).

On the second study (4 months rapamycin diet starting at 12 months of age - **FIGURE 6.1a** – blue arrow), we noticed an increment of Sen-β-Gal activity in old livers that could be attenuated upon rapamycin administration (**FIGURE 6.1e**). Additionally, in the subcutaneous adipose tissue we also observed a reduction of Sen-β-Gal activity in animal fed with rapamycin (**FIGURE 6.3b**). As proof of concept, rapamycin dampened mTORC1 activity (measured by the phosphorylation status of ribosomal S6 protein (**FIGURE 6.1d**). On this short-term rapamycin study, we observed a reduction of p21 levels (**FIGURE 6.1e** top-right western blot). Furthermore, on mice under rapamycin treatment we saw reduction of SASP components at the mRNA level such as CXCL1 and CXCL5 (data not shown).

Previously, we described that telomeric associated foci build-up with age and that they are good markers of senescence *in vivo* [3]. Here, we saw that 12 months-old mice fed for 4 months with a rapamycin supplemented diet had less damage at telomeres (**FIGURE 6.1f**) and, furthermore, no differences were spotted regarding telomere length between damage at telomeres and other genomic located damage (**FIGURE 6.1h** right). Besides liver, we also observed that TAF were reduced on small intestinal crypts (data not shown).

On the same mice cohort, we observed that mTORC1 inhibition lead to decreased mitochondrial number and volume fraction (by electron microscopy

analysis) and, also reduced levels of NDUFB8 and mitochondrial DNA copies in liver (**FIGURE 6.1g**). Further analysis of the transmission electron micrographs showed increased percentage of lipids within hepatocytes (**FIGURE 6.3a**). In order to test whether rapamycin was affecting cellular respiration or only the overall mitochondrial contentment within the cell, we measured cellular respiration using the Seahorse machine. As result, no mitochondrial respiratory differences were present in livers from rapamycin-diet and control-diet fed mice (**FIGURE 6.1g**). Furthermore in the liver, we saw that PGC-1β biogenesis orchestrator levels were increased as mice aged and, that mTORC1 inhibition reduced PGC-1β protein levels (**FIGURE 6.1h**). Finally, in livers from rapamycin treated mice we did not observed increased expression of SOD2 - mitochondrial antioxidant enzyme that catalyses the conversion of hydrogen peroxide into diatomic oxygen and is a marker of oxidative stress (**FIGURE 6.1h**). This data can therefore indicate that rapamycin does not affect mitochondrial respiration *per se*, but rather, decreases the amount of ROS-generator sites present in the cells.

Having identified PGC-1β as core regulator of biogenesis in cellular senescence *in vitro*, we established collaboration with Dr. Antonio Vidal-Puig group in University of Cambridge (United Kingdom) to study senescent markers on PGC-1β-null mice in liver (**FIGURE 6.2**).

### PGC-1β knockout mice have fewer mitochondria and less telomere-associated foci (TAF) in liver

PGC-1β KO mice are leaner than wild-type littermates, metabolically healthier (better age-dependent glucose and insulin resistance) and, had lower energy expenditure levels compared to wild-type mice (data not shown and [7]). Furthermore, in liver there is no compensatory effects of PGC-1α on mitochondrial biogenesis were reported [301, 302].

From the material accessible from PGC-1β knockout animals at 7 and 18 months of age, we observed that liver weighed less in 18 months-old PGC-1β-null mice (**FIGURE 6.2b**) and, that there was a reduction of mitochondrial

components (SDHA and mtDNA copy numbers) on PGC-1β KO mice at 7 months (**FIGURES 6.2c** and **6.2d**). Next, we analysed the impact of PGC-1β deficiency on telomere associated DNA damage in hepatocytes (**FIGURE 6.2e**). Despite PGC-1β KO animal have fewer TAF, we measured significant differences in telomere length (**FIGURE 6.2e**). More precisely, TAF were shorter than non-TAF in both genotypes (**FIGURE 6.2e**). Lastly, since many ROS detoxifying enzymes are under the control of the PGC-1 family we investigate if SOD2 protein levels were changed in the livers from old PGC-1β KO mice. We report no significant changes in SOD2 expression on these animals (**FIGURE 6.2f**).

### Den-induced hepatocellular carcinoma is associated with fewer DNA damage, lower mitochondrial and PGC-1β protein levels

In order to examine the hypothesis that mitochondrial hypertrophy stabilizes the senescent arrest and maintains tumour suppression, we prompted liver cancer by continuous intraperitoneal injections of N-Nitrosodiethylamine (Den) in wild-type mice. After dissection of tumour and adjacent non-tumour tissue, we realised that tumour regions had decreased mtDNA copy number, reduced expression of PGC-1β and mitochondrial protein SDHA **(FIGURES 6.2h** and **6.2g)**, and lastly, tumour areas had less γH2A.X foci **(FIGURE 6.2i**).

# FIGURE 6.1

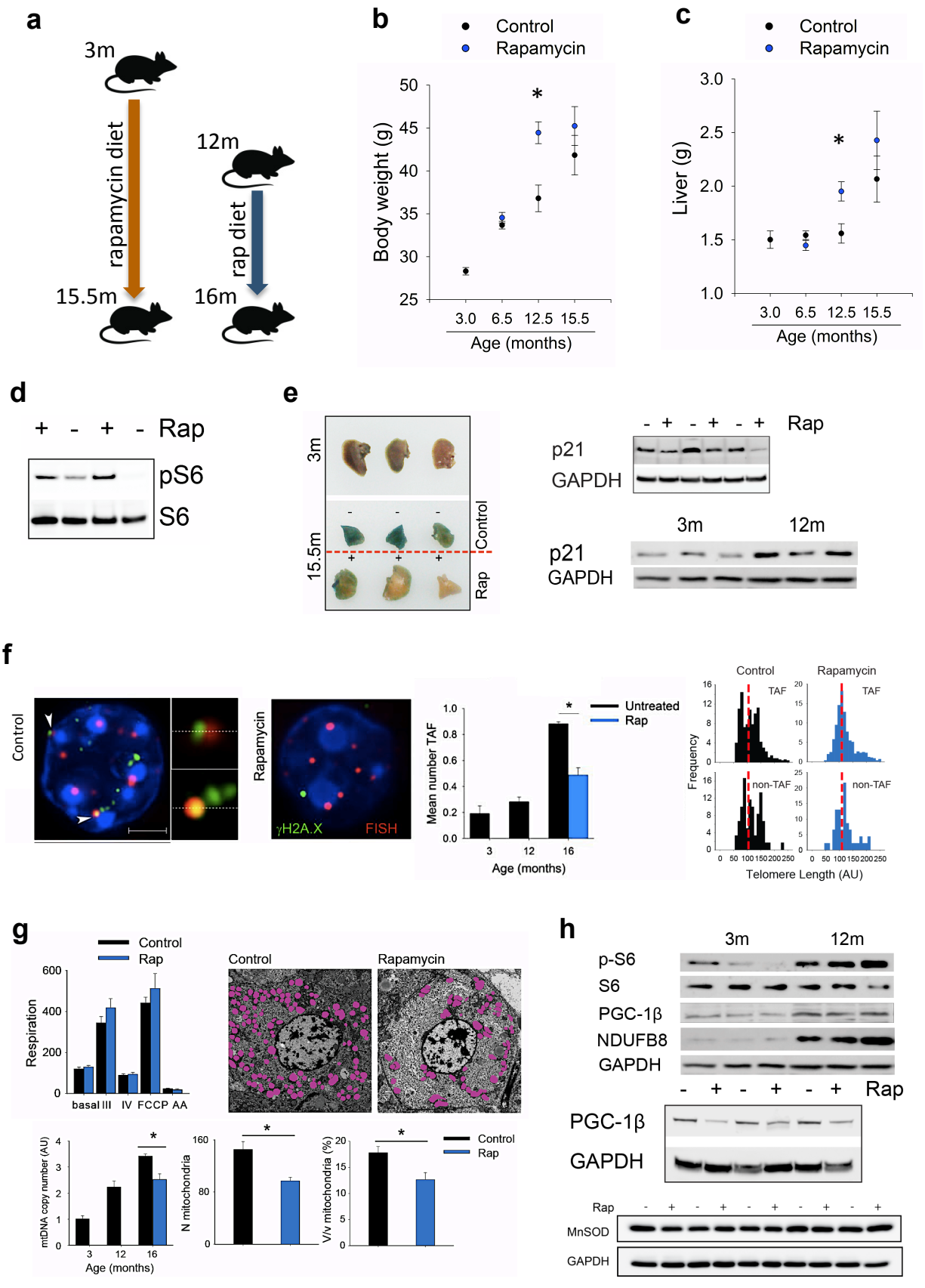
a
3m
rapamycin diet
15.5m
12m
rap diet
16m
b
Control
Rapamycin
Body weight (g)
Age (months)
c
Control
Rapamycin
Liver (g)
Age (months)
d
Rap
pS6
S6
e
3m
15.5m
Control
Rap
p21
GAPDH
f
Control
Rapamycin
γH2A.X
FISH
Mean number TAF
Untreated
Rap
Age (months)
Frequency
TAF
non-TAF
Telomere Length (AU)
g
Control
Rap
Respiration
basal III IV FCCP AA
mtDNA copy number (AU)
N mitochondria
V/v mitochondria (%)
Age (months)
h
3m
12m
p-S6
S6
PGC-1β
NDUFB8
GAPDH
Rap
MnSOD

**FIGURE 6.1| mTORC1-PGC-1β dependent increased mitochondrial content contributes to senescence *in vivo***

**a)** summary scheme of C57BL6 mice experiments involving rapamycin supplemented diets; **b)** body weight evolution on the longitudinal mice cohort treated with rapamycin since three months of age. 6.5, 12.5 and 15.5 represent the age (in months) of sacrifice and those mice were under rapamycin diet for 3, 9 and 12 months respectively (n=5-12 mice per group and bars represent standard error); **c)** liver weight at the above mentioned conditions (n=5-12 mice per treatment and bars represent standard error); **d)** representative western blot of the expression of pS6 and S6 in sixteen months old mice liver with four months rapamycin-supplementation; **e)** Three months old and fifteen months old mice livers [control (-) or rapamycin (+)] stained for Sen-β-Gal activity (n=3 mice per group); representative western blot showing effect of four months rapamycin feeding on p21 expression in sixteen months old mice; representative western blot for p21 in mouse livers at three and twelve months of age (n=3 mice per group); **f)** representative ImmunoFISH images of hepatocytes from sixteen months old mice treated for four months with or without rapamycin (control). Co-localising foci are amplified in the right panel; (middle) telomere-associated foci (TAF) increase with age and four months rapamycin treatment reduces its number, n=3 mice per group. Histograms depicting mean telomere intensity for both telomeres co-localizing (TAF) or not co-localising (non-TAF) with γH2A.X DNA damage foci in liver from sixteen months old mice treated for four months with rapamycin (n=4 mice per condition) - red dotted line denotes median intensity. No statistical significance was observed using the Mann-Whitney test between telomere intensities distribution of TAF and non-TAF. Circa a thousand telomeres were analysed per condition; **g)** (top left) oxygen consumption rates (OCR) in liver mitochondria in the presence of pyruvate/malate. Data are mean ± S.E.M of n = 5 mice per group; (top right) representative electron micrographs of hepatocytes from sixteen months old mice under four months rapamycin-diet - mitochondria are labeled in pink; (bottom left) mtDNA copy number qPCR assay at three, twelve, sixteen months and at sixteen months after four months rapamycin treatment. Data are mean±S.E.M of n=3-4 mice per group; (bottom right) T.E.M. quantification of mitochondrial number (N mitochondria) per cross section and mitochondrial volume fraction (%$V_v$); **h)** (top) western blots for pS6, total S6, PGC-1β and NDUFB8 in mouse livers at three and twelve months of age (n=3 mice per group), (middle) four months of rapamycin-supplemented diet reduces PGC-1β expression in mice at sixteen months of age (n=3 mice per group), (bottom) western blots showing expression of SOD2 in 15.5 months old mice fed with rapamycin for twelve months.

# FIGURE 6.2

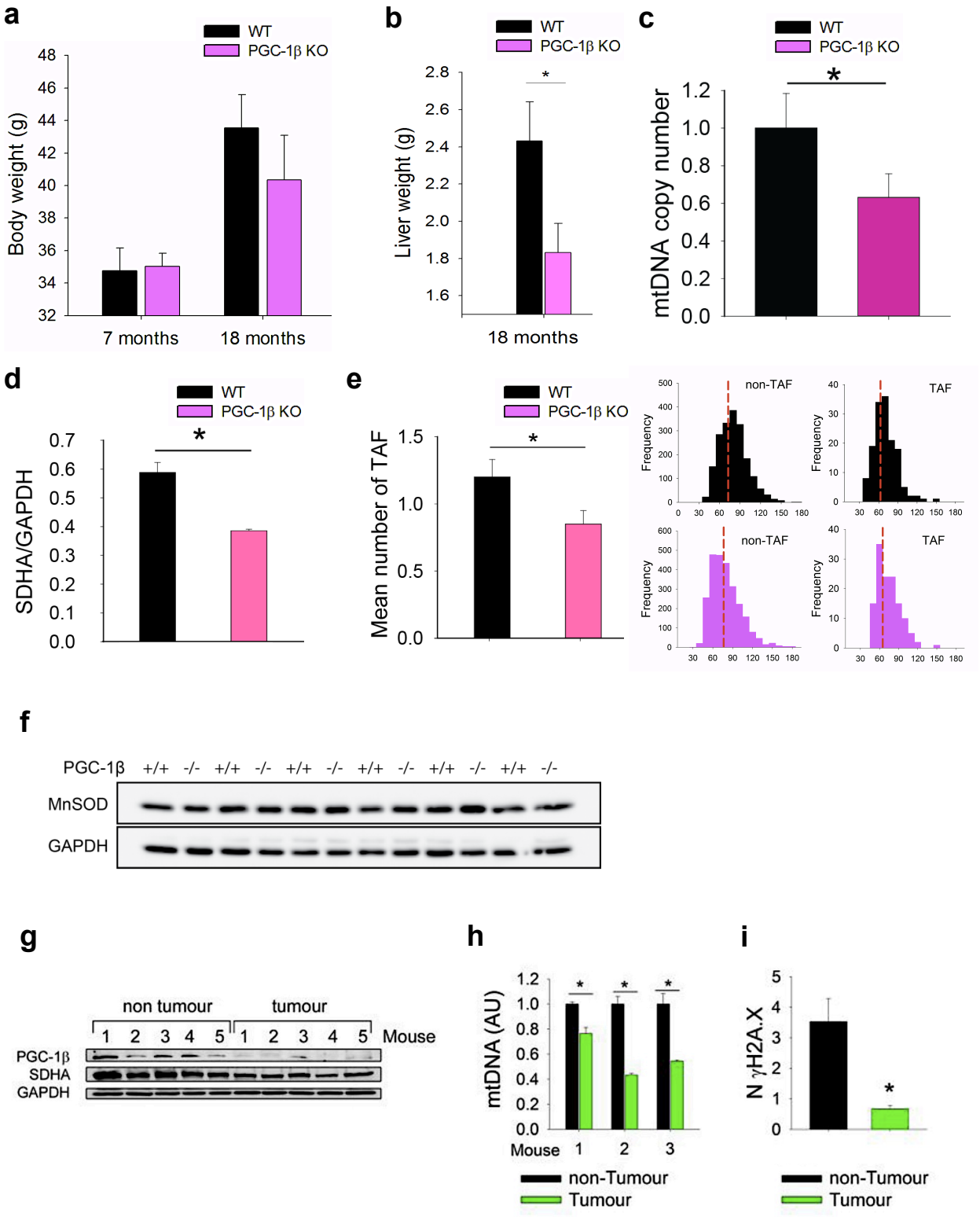
a
WT
PGC-1β KO
Body weight (g)
48
46
44
42
40
38
36
34
32
7 months
18 months
b
WT
PGC-1β KO
Liver weight (g)
2.8
2.6
2.4
2.2
2.0
1.8
1.6
*
18 months
c
WT
PGC-1β KO
mtDNA copy number
1.2
1.0
0.8
0.6
0.4
0.2
0.0
*
d
WT
PGC-1β KO
SDHA/GAPDH
0.7
0.6
0.5
0.4
0.3
0.2
0.1
0.0
*
e
WT
PGC-1β KO
Mean number of TAF
1.5
1.0
0.5
0.0
*
non-TAF
TAF
non-TAF
TAF
Frequency
f
PGC-1β +/+ -/- +/+ -/- +/+ -/- +/+ -/- +/+ -/- +/+ -/-
MnSOD
GAPDH
g
non tumour
tumour
1 2 3 4 5 1 2 3 4 5 Mouse
PGC-1β
SDHA
GAPDH
h
mtDNA (AU)
1.2
1.0
0.8
0.6
0.4
0.2
0.0
*
*
*
Mouse 1 2 3
non-Tumour
Tumour
i
N γH2A.X
5
4
3
2
1
0
*
non-Tumour
Tumour

**FIGURE 6.2| PGC-1β-mediated mitochondrial biogenesis impacts on telomere-associated damage and cancer in liver**

**a)** body weight of PGC-1β KO mice at seven and eighteen months of age. n=4-10 mice per genotype per age - bars represent standard error; **b)** liver weight of PGC-1β KO mice at seven and eighteen months of age. n=4-10 mice per genotype per age - bars represent standard error. Two-tailed T-test, * denotes $p<0.05$; **c)** mtDNA copy number qPCR assay on liver from PGC-1β KO mice at seven months of age. Data are mean±s.e.m. of n=4 mice per genotype; **d)** SDHA western blot on eighteen months old livers from PGC-1β KO mice. Data are mean±s.e.m. of n=5 mice per genotype; **e)** (left) mean telomere-associated foci (TAF) at eighteen months of age in PGC-1β KO mice. Data are mean±s.e.m. of n=4 mice per genotype. (right) histograms depicting mean telomere intensity for both telomeres co-localizing (TAF) or not co-localising (non-TAF) with 53BP1 DNA damage foci in liver from eighteen months old PGC-1β KO mice treated (n=4 mice per condition) - red dotted line denotes median intensity. No statistical significance was observed using the Mann-Whitney test between telomere intensities distribution of TAF and non-TAF from wild-type or PGC-1β KO. Statically differences were observed in both PGC-1β KO and wild-type controls, regarding mean telomere lenght between non-TAF and TAF. p=0.001 and 0.018 respectively. In total, between 130 and 150 TAF were analysed and 1900-2550 non-TAF were analysed per condition; **f)** western blot showing expression of SOD2 in PGC-1β KO and wild-type at 18 months of age; **g)** Diethylnitrosamine (Den)-induced liver tumours exhibit lower protein expression of PGC-1β-biogenesis regulator and mitochondrial SDHA in tumour areas than in adjacent non-tumour tissue. n=5 mice per condition; **h)** mitochondrial DNA copy number is reduced in DEN-tumours compared to non-tumour areas. Data are mean±s.e.m. of n=3 mice per condition. Two-tailed T-test, * denotes $p<0.05$; **i)** γH2A.X DNA foci numbers are reduced in hepatocytes of tumour areas compared to non-tumour areas. Data are mean±s.e.m. of n=3 mice. Two-tailed T-test, * denotes $p<0.05$;

# FIGURE 6.3

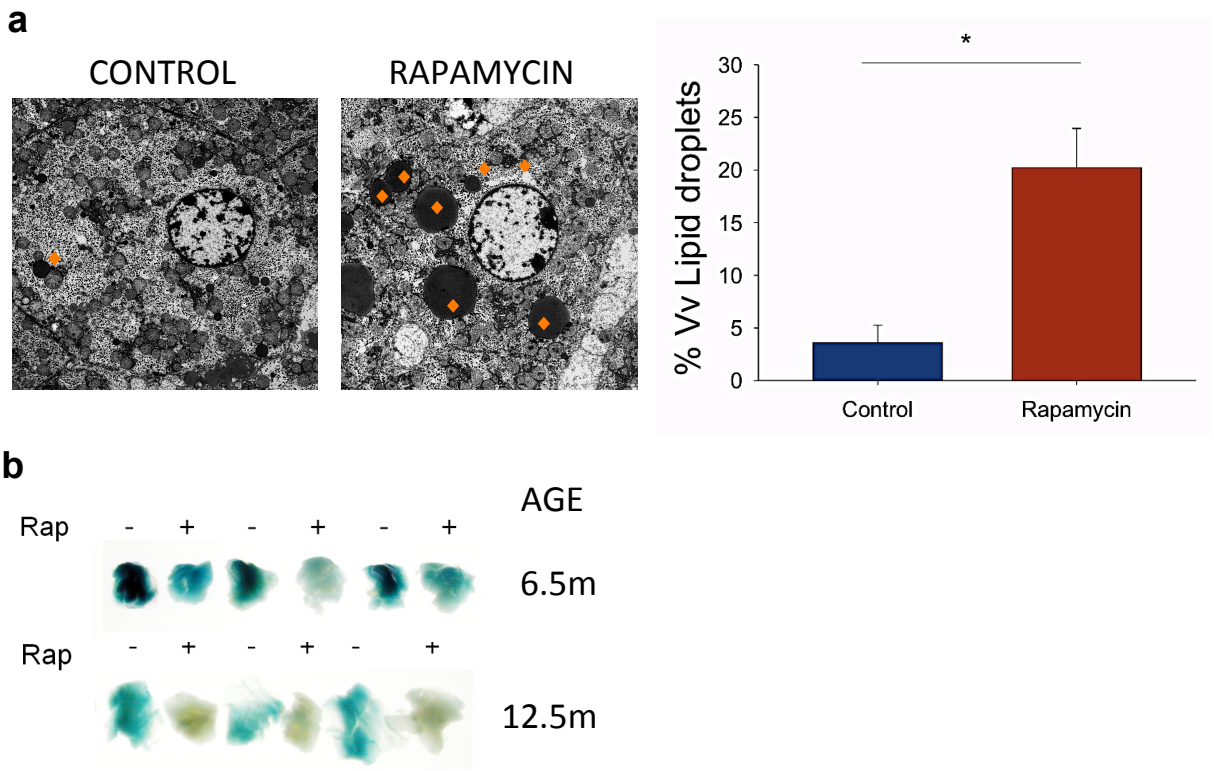


**FIGURE 6.3| Mice under rapamycin diet show increased lipid content in hepatocytes and more senescence-associated β-Galactosidase activity in the sub-cutaneous adipose tissue**

**a)** Mice treated with rapamycin for 4 months starting at 12 months of age show increased lipidic vesicles within hepatocytes**.** Data are mean± s.e.m., n=3 animals per treatment, n=10 hepatocytes per animal, at least 300 lipid droplets quantified per condition, Two-tailed T-test, *p=0.01526; **b)** Sen-β-Gal assay on sub-cutaneous fat from mice subjected to 3 and 6 months rapamycin diet starting at 3 months of age. Rapamycin-fed mice have less senescent adipocytes than control animals.

## DISCUSSION

### Hepatocytes from rapamycin treated mice and from PGC-1β KO mice have reduced telomeric associated damage

Our data on mTORC1 inhibition by rapamycin provides new insights into telomere biology. Previously we have identified that telomere-associated damage is persistent and irreparable in liver [3]. To our understanding, the prevention of TAF formation upon rapamycin treatment may represent one of the first evidences for the impact of the mTOR pathway on telomeres in mammals. In mammalian cells, mTORC1 inhibition by rapamycin increased telomerase expression [165] suggesting perhaps that mTORC1 promotes telomere erosion. In the literature, the data linking mTOR to telomeres comes primordially from disparate yeast data. For instance, while in *Saccharomyces cerevisiae* rapamycin induced telomere shortening [303], in *Schizosaccharomyces pombe* rapamycin does not alter telomere length [304].

Despite the fact that we cannot discard some contribution of telomere shortening into TAF formation, telomeres shorted similarly in both wild type and PGC-1β KO mice however, PGC-1β KO animals' telomeres were less damaged. This piece of evidence reinforces our previous reports and hypothesis that telomere shortening might not be the sole reason for telomere damage [3]. Perhaps, the reduction of TAF observed in PGC-1β$^{-/-}$ hepatocytes could be due to decreased number of mitochondria and, hence, less number of ROS-generating sites that would impinge on nuclear damage (rather than changes in the the antioxidant defense mechanims via SOD2). Another possibility could be that PGC-1β KO animals would have less oxidative stress (similar to our observations in cells), that would keep more TRF1 and TRF2 bound and protecting telomeres from damage [43].

Telomeric associated damage has been proposed to function as qualitative readout for mean and maximum lifespan of short- and long-lived mice cohorts [50]. It is possible therefore, that some of the benefic effects of rapamycin on lifespan extension [140] may be due to decreased telomeric dysfunction. mTORC1 has been shown to be activated during ageing in X-ray irradiated mice [283]. In this settings, rapamycin treatment suppressed mTORC1 activity.

### A role of rapamycin and PGC-1β deletion on mitochondria

Notwithstanding with the fact that short-term rapamycin treatment in mice reduced mitochondrial mass, it did not alter mitochondrial respiration. Our data is also in accordance with the study from Johnson and collaborators, in which rapamycin treatment did not change respiratory rates of COX IV null mice's brain (a model of Leigh syndrome) [161]. Opposingly, *in vitro*, Jurkat cells treated with rapamycin or after Raptor silencing results in decreased oxygen consumption rates [260, 305].

The impact of mTORC1 inhibition on reduction of mitochondrial content (mitochondrial complexes proteins and mitochodnrial biogenesis regulators) has been previously observed in muscle [268, 300].

In brain of *Ndufs4*$^{-/-}$ mice (a model of Leigh syndrome) daily rapamycin injections promote lifespan and health-span extension. Despite no changes are observed in complex I assembly or mitochondrial respiration, in wild-type mice rapamycin treatments effects mitochondrial protein levels differently. In more detail, it decreases cytochrome c and COX IV, it increases NDUFB3 (complex I) and, it did not altered NDUFS9 (complex I) and HSP60 protein levels [161]. Similar increment of HSP60 was observed on isolated primary hepatocytes [306]. Additionally, this study show increased ATP5 (complex V) and SDHB (complex II) protein increase, however decreased UQCR2 (complex III) and decreased MT-CO1 (complex IV) was present. Overall, this data seems indicate differential effects of rapamycin on mitochondrial proteins. Nevertheless, in a transcriptomic study in mice under rapamycin diet, mitochondrial function was the category on which the more than 80% of the genes expression was altered [307].

Also in isolated stem cells with increased mTORC1 activity (caused by TSC1 deletion) higher mitochondria density and more ROS levels were observed. Moreover, the use of the antioxidant NAC halts the loss of stemness and haematopoiesis on these settings [164].

PGC-1β loss is not deleterious but, it hinges the ordinary mitochondrial metabolic genes and the ability to cope with physiological stresses [302]. PGC-1β absence drives a general reduction in OXPHOS and ETC genes and this induces tissue-specific mitochondrial changes [302]. PGC-1β$^{-/-}$ animals are leaner that wild-type littermate controls due to diminished WAT content [302].

In liver, lipid homeostasis is extremely relevant and, PGC-1β-deficient animals under short-term saturated fat diet have hepatic lipid accumulation and increased liver/body weight ratio caused by lipid infiltration. [301, 302]. Lastly, in liver there is no PGC-1α compensation in the absence of PGC-1β (similar to what we observed on PGC-1β KO MEF) but, on mice under a high-fed diet, PGC-1α compensation occurs in liver [301, 302].

### mTOR impacts on liver hepatosteatosis

The mTOR pathway is also involved in lipid metabolism including lipogenesis, lipolysis, ketogenesis and adipogenesis (reviewed in [308]). When analysing transmission electron micrographs from mice treated with rapamycin we observed a large fraction of lipids within hepatocytes. Those lipid vesicles can perhaps either be due to enhanced lipogenesis or due to a lack of lipolysis. Mechanistically, this lipid accumulation phenotype under rapamycin diet could be a consequence of mTORC2 activation of lipogenesis (reviewed in [308]), rather than the axis rapamycin-mTORC1-Lipin1-SREBP1, once rapamycin suppresses the expression of the lipogenesis inducer SREBP1 [309].

Although mice under high fat diet (HFD) and treated with rapamycin have fewer lipid droplets and lower ROS levels in liver, the impact of rapamycin on mice under normal chow diet (LFD) was not examined [310]. Moreover, liver deletion of Raptor (which decreases mTORC1 activity) induces increased DNA damage levels (measured by γH2A.X), increased immune infiltrations and increased apoptosis, which could be actually due to a survival effect mediated by the activation of mTORC2 branch (via phosphorylation of Akt, GSK3 and STAT3)[310]. Similarly to our observations that rapamycin reduced p21 levels in liver, also Raptor KO liver after partial hepatectomy show reduced p21 levels (plus reduced p27 levels)[310]. Altogether these observations reinforce the idea

that p21 levels changes are most likely a mTORC1-downstream event, rather than a mTORC2 dependent effect.

This same study puts forward that mice lacking Raptor, have more liver fibrosis and have increased DEN-induced hepatocellular carcinoma [310].

### Is mitochondria biogenesis a tumour suppressor mechanism?

In DEN-hepatic carcinogenesis, we observed that γH2A.X lesions are suppressed in tumour areas when compared to adjacent healthy zones. This is in accordance with very recent study, in which a persistent DDR at telomeres has been connected to tumour suppressor properties of cellular senescence in naevi melanocytes but, not in malignant melanoma [311].

Our data showing decline of PGC-1β and mitochondrial proteins on the DEN-induced liver cancer, opens the exciting possibility that high mitochondrial content by PGC-1β acts as tumour suppression mechanism. In fact, PGC-1β homolog - PGC-1α was recently suggested to be key in tumour progression [312]. In more detail, tumour volume was reduced in nude mice that were subcutaneously injected with A375P melanoma cells with silenced PGC-1α. The authors suggest that the reduction of tumour growth was due to the activation of apoptosis by increased ROS levels once PGC-1α was silenced [312]. In another earlier report, PGC-1α was found to promote tumour growth by fuelling lipogenesis. Additionally, DEN-induced liver carcinogenesis was reduced in PGC-1α KO mice compared to wild-type mice [313].

Finally, mitochondrial biogenesis is a common downstream consequence of activated oncogenes (*e.g.* c-Myc [266]). Therefore, mitochondria biogenesis and mitochondrial metabolism are perhaps suitable druggable targets, in combination with ROS or SASP (senescence associated secretory phenotype) suppressing compounds in order to combat senescence and cancer, and promote healthy ageing.

## CONCLUSION

In this dissertation, I have shown that the nutrient-sensing mTOR pathway is deeply intertwined and, is required for multiple aspects of cellular senescence both in cells and in mice tissues. In more detail, mTORC1 inhibition by rapamycin alleviates the DDR, reduces the mitochondrial content within cells and tissues, and it modulates the senescence-associated secretome.

This work describes telomere-associated damage (TAF) as a senescence marker in cells. Moreover, irreparable TAF are a robust senescence biomarker present in both proliferative and in post-mitotic mice tissues and, it accumulates with age. Here, we observe and describe new effects of the mTOR pathway into telomere biology and, into telomere damage prevention *in vivo*. To my knowledge it is one (if not the first) description that links mammalian telomere biology to this signaling pathway.

In this thesis, I have also shown that mitochondrial biogenesis is an early event that results from an active DNA damage response. Moreover, inhibition of mitochondrial proliferation impacts on how the senescent phenotype develops and is maintained. The reduction of the number of ROS-generator sites seems to alleviate the presence of senescence markers, pinpointing that this organelle is essential for the early events of senescence.

I have also shown that addition of sodium pyruvate drive cells into senescence, via increased mitochondrial content, increased ROS, and presence of DNA damage foci. Once more these effects are linked to the mTOR pathway.

Finally, mitochondria biogenesis can function and represent a common tumour suppression mechanism or, a novel “checkpoint”, required for senescence establishment and durability. This seems particularly important since tissues without PGC-1β have less TAF, cells without PGC-1β can escape a permanent cell cycle arrest and, furthermore, cancer lesions have less mitochondrial components and expression of this mitochondrial biogenesis orchestrator.

## REFERENCES


1. Sherwood, S.W., et al., *Defining cellular senescence in IMR-90 cells: a flow cytometric analysis.* Proc Natl Acad Sci U S A, 1988. **85**(23): p. 9086-90.
2. Gorgoulis, V.G. and T.D. Halazonetis, *Oncogene-induced senescence: the bright and dark side of the response.* Curr Opin Cell Biol, 2010. **22**(6): p. 816-27.
3. Hewitt, G., et al., *Telomeres are favoured targets of a persistent DNA damage response in ageing and stress-induced senescence.* Nat Commun, 2012. **3**: p. 708.
4. Fumagalli, M., et al., *Telomeric DNA damage is irreparable and causes persistent DNA-damage-response activation.* Nat Cell Biol, 2012. **14**(4): p. 355-65.
5. Moiseeva, O., et al., *DNA damage signaling and p53-dependent senescence after prolonged beta-interferon stimulation.* Mol Biol Cell, 2006. **17**(4): p. 1583-92.
6. von Zglinicki, T., *Oxidative stress shortens telomeres.* Trends Biochem Sci, 2002. **27**(7): p. 339-44.
7. Jacobs, J.J.L. and T. de Lange, *Significant Role for p16INK4a in p53-Independent Telomere-Directed Senescence.* Current Biology, 2004. **14**(24): p. 2302-2308.
8. Nadine Hein, E.S., Jaclyn Quin, Katherine M. Hannan, Austen Ganley and Ross D. Hannan, *The Nucleolus and Ribosomal Genes in Aging and Senescence, Senescence*, ed. D.T. Nagata. 2012.
9. Baker, D.J., et al., *Opposing roles for p16Ink4a and p19Arf in senescence and ageing caused by BubR1 insufficiency.* Nat Cell Biol, 2008. **10**(7): p. 825-836.
10. Kaplon, J., et al., *A key role for mitochondrial gatekeeper pyruvate dehydrogenase in oncogene-induced senescence.* Nature, 2013. **498**(7452): p. 109-+.
11. Schmidt, S., et al., *The centrosome and mitotic spindle apparatus in cancer and senescence.* Cell Cycle, 2010. **9**(22): p. 4469-73.
12. Hayflick, L. and P.S. Moorhead, *The serial cultivation of human diploid cell strains.* Exp Cell Res, 1961. **25**: p. 585-621.
13. Kim, Y.-M., et al., *Implications of time-series gene expression profiles of replicative senescence.* Aging Cell, 2013. **12**(4): p. 622-634.
14. Bayreuther, K., et al., *Differentiation of fibroblast stem cells.* J Cell Sci Suppl, 1988. **10**: p. 115-30.
15. Quijano, C., et al., *Oncogene-induced senescence results in marked metabolic and bioenergetic alterations.* Cell Cycle, 2012. **11**(7): p. 1383-92.
16. Hampel, B., et al., *Differential regulation of apoptotic cell death in senescent human cells.* Exp Gerontol, 2004. **39**(11-12): p. 1713-21.
17. Cristofalo, V.J. and R.J. Pignolo, *Replicative senescence of human fibroblast-like cells in culture.* Physiol Rev, 1993. **73**(3): p. 617-38.
18. Shelton, D.N., et al., *Microarray analysis of replicative senescence.* Curr Biol, 1999. **9**(17): p. 939-45.
19. Mehta, I.S., et al., *Alterations to nuclear architecture and genome behavior in senescent cells.* Ann N Y Acad Sci, 2007. **1100**: p. 250-63.
20. Narita, M., et al., *Rb-mediated heterochromatin formation and silencing of E2F target genes during cellular senescence.* Cell, 2003. **113**(6): p. 703-16.
21. Rodier, F., et al., *DNA-SCARS: distinct nuclear structures that sustain damage-induced senescence growth arrest and inflammatory cytokine secretion.* Journal of Cell Science, 2011. **124**(1): p. 68-81.
22. Kuilman, T., et al., *Oncogene-Induced Senescence Relayed by an Interleukin-Dependent Inflammatory Network.* Cell, 2008. **133**(6): p. 1019-1031.

23. Coppé, J.-P., et al., *Senescence-Associated Secretory Phenotypes Reveal Cell-Nonautonomous Functions of Oncogenic RAS and the p53 Tumor Suppressor.* PLoS Biol, 2008. **6**(12): p. e301.
24. Nelson, G., et al., *A senescent cell bystander effect: senescence-induced senescence.* Aging Cell, 2012. **11**(2): p. 345-9.
25. Acosta, J.C., et al., *A complex secretory program orchestrated by the inflammasome controls paracrine senescence.* Nat Cell Biol, 2013. **15**(8): p. 978-90.
26. Liu, D. and P.J. Hornsby, *Senescent Human Fibroblasts Increase the Early Growth of Xenograft Tumors via Matrix Metalloproteinase Secretion.* Cancer Res, 2007. **67**(7): p. 3117-3126.
27. Krtolica, A., et al., *Senescent fibroblasts promote epithelial cell growth and tumorigenesis: A link between cancer and aging.* Proceedings of the National Academy of Sciences of the United States of America, 2001. **98**(21): p. 12072-12077.
28. Passos, J.F., et al., *Feedback between p21 and reactive oxygen production is necessary for cell senescence.* Mol Syst Biol, 2010. **6**: p. 347.
29. Olovnikov, A.M., *[Principle of marginotomy in template synthesis of polynucleotides].* Dokl Akad Nauk SSSR, 1971. **201**(6): p. 1496-9.
30. Watson, J.D., *Origin of concatemeric T7 DNA.* Nat New Biol, 1972. **239**(94): p. 197-201.
31. Greider, C.W. and E.H. Blackburn, *A telomeric sequence in the RNA of Tetrahymena telomerase required for telomere repeat synthesis.* Nature, 1989. **337**(6205): p. 331-7.
32. Griffith, J.D., et al., *Mammalian telomeres end in a large duplex loop.* Cell, 1999. **97**(4): p. 503-14.
33. de Lange, T., *Shelterin: the protein complex that shapes and safeguards human telomeres.* Genes Dev., 2005. **19**(18): p. 2100-2110.
34. Harley, C.B., A.B. Futcher, and C.W. Greider, *Telomeres shorten during ageing of human fibroblasts.* Nature, 1990. **345**(6274): p. 458-60.
35. Bodnar, A.G., et al., *Extension of life-span by introduction of telomerase into normal human cells.* Science, 1998. **279**(5349): p. 349-52.
36. Griffith, J.D., et al., *Mammalian Telomeres End in a Large Duplex Loop.* Cell, 1999. **97**(4): p. 503-514.
37. d'Adda di Fagagna, F., et al., *A DNA damage checkpoint response in telomere-initiated senescence.* Nature, 2003. **426**(6963): p. 194-198.
38. Takai, H., A. Smogorzewska, and T. de Lange, *DNA Damage Foci at Dysfunctional Telomeres.* Current Biology, 2003. **13**(17): p. 1549-1556.
39. Cesare, A.J., et al., *The telomere deprotection response is functionally distinct from the genomic DNA damage response.* Mol Cell, 2013. **51**(2): p. 141-55.
40. Shiloh, Y., *The ATM-mediated DNA-damage response: taking shape.* Trends in Biochemical Sciences, 2006. **31**(7): p. 402-410.
41. Sfeir, A. and T. de Lange, *Removal of shelterin reveals the telomere end-protection problem.* Science, 2012. **336**(6081): p. 593-7.
42. Petersen, S., G. Saretzki, and T. von Zglinicki, *Preferential Accumulation of Single-Stranded Regions in Telomeres of Human Fibroblasts.* Exp Cell Res, 1998. **239**(1): p. 152-160.
43. Opresko, P.L., et al., *Oxidative damage in telomeric DNA disrupts recognition by TRF1 and TRF2.* Nucl. Acids Res., 2005. **33**(4): p. 1230-1239.
44. van Steensel, B., A. Smogorzewska, and T. de Lange, *TRF2 protects human telomeres from end-to-end fusions.* Cell, 1998. **92**(3): p. 401-13.
45. Karlseder, J., et al., *p53- and ATM-dependent apoptosis induced by telomeres lacking TRF2.* Science, 1999. **283**(5406): p. 1321-5.
46. Goytisolo, F.A. and M.A. Blasco, *Many ways to telomere dysfunction: in vivo studies using mouse models.* Oncogene, 2002. **21**(4): p. 584-91.

47. Hockemeyer, D., et al., *POT1 protects telomeres from a transient DNA damage response and determines how human chromosomes end.* Embo j, 2005. **24**(14): p. 2667-78.
48. Kaul, Z., et al., *Five dysfunctional telomeres predict onset of senescence in human cells.* EMBO Rep, 2012. **13**(1): p. 52-9.
49. Suram, A., et al., *Oncogene-induced telomere dysfunction enforces cellular senescence in human cancer precursor lesions.* EMBO J, 2012. **31**(13): p. 2839-51.
50. Jurk, D., et al., *Chronic inflammation induces telomere dysfunction and accelerates ageing in mice.* Nat Commun, 2014. **2**: p. 4172.
51. Herbig, U., et al., *Cellular senescence in aging primates.* Science, 2006. **311**(5765): p. 1257.
52. Lee, H.-W., et al., *Essential role of mouse telomerase in highly proliferative organs.* Nature, 1998. **392**(6676): p. 569-574.
53. Rudolph, K.L., et al., *Longevity, stress response, and cancer in aging telomerase-deficient mice.* Cell, 1999. **96**(5): p. 701-12.
54. Choudhury, A.R., et al., *Cdkn1a deletion improves stem cell function and lifespan of mice with dysfunctional telomeres without accelerating cancer formation.* Nat Genet, 2007. **39**(1): p. 99-105.
55. von Zglinicki, T., R. Pilger, and N. Sitte, *Accumulation of single-strand breaks is the major cause of telomere shortening in human fibroblasts.* Free Rad Biol Med, 2000. **28**(1): p. 64-74.
56. Serra, V., et al., *Extracellular superoxide dismutase is a major antioxidant in human fibroblasts and slows telomere shortening.* J Biol Chem, 2003. **278**(9): p. 6824-30.
57. Forsyth, N.R., et al., *Developmental differences in the immortalization of lung fibroblasts by telomerase.* Aging Cell, 2003. **2**(5): p. 235-43.
58. Richter, T. and T. von Zglinicki *A continuous correlation between oxidative stress and telomere shortening in fibroblasts.* Exp Gerontol, 2007. **42**(11): p. 1039-42.
59. Passos, J.F., et al., *Mitochondrial Dysfunction Accounts for the Stochastic Heterogeneity In Telomere-Dependent Senescence.* PLoS Biology, 2007. **5**(5): p. e110.
60. von Zglinicki, T., et al., *Mild Hyperoxia Shortens Telomeres and Inhibits Proliferation of Fibroblasts: A Model for Senescence?* Exp Cell Res, 1995. **220**(1): p. 186-193.
61. Lee, A.C., et al., *Ras Proteins Induce Senescence by Altering the Intracellular Levels of Reactive Oxygen Species.* J. Biol. Chem., 1999. **274**(12): p. 7936-7940.
62. Macip, S., et al., *Influence of Induced Reactive Oxygen Species in p53-Mediated Cell Fate Decisions.* Mol. Cell. Biol., 2003. **23**(23): p. 8576-8585.
63. Macip, S., et al., *Inhibition of p21-mediated ROS accumulation can rescue p21-induced senescence.* EMBO J., 2002. **21**(9): p. 2180-2188.
64. Takahashi, A., et al., *Mitogenic signalling and the p16INK4a-Rb pathway cooperate to enforce irreversible cellular senescence.* Nat Cell Biol, 2006. **8**(11): p. 1291-7.
65. Ogrunc, M., et al., *Oncogene-induced reactive oxygen species fuel hyperproliferation and DNA damage response activation.* Cell Death Differ, 2014. **21**(6): p. 998-1012.
66. Talior, I., et al., *PKC-delta-dependent activation of oxidative stress in adipocytes of obese and insulin-resistant mice: role for NADPH oxidase.* Am J Physiol Endocrinol Metab, 2005. **288**(2): p. E405-11.
67. Imai, Y., et al., *Crosstalk between the Rb Pathway and AKT Signaling Forms a Quiescence-Senescence Switch.* Cell Rep, 2014. **7**(1): p. 194-207.
68. Allen, R.G., et al., *Differences in electron transport potential, antioxidant defenses, and oxidant generation in young and senescent fetal lung fibroblasts (WI-38).* J Cell Physiol, 1999. **180**(1): p. 114-22.

69. Guo, Z., et al., *ATM activation by oxidative stress.* Science, 2010. **330**(6003): p. 517-21.
70. Koli, K., et al., *Transforming growth factor-beta activation in the lung: focus on fibrosis and reactive oxygen species.* Antioxid Redox Signal, 2008. **10**(2): p. 333-42.
71. Torres, M. and H.J. Forman, *Redox signaling and the MAP kinase pathways.* Biofactors, 2003. **17**(1-4): p. 287-96.
72. Hecker, L., et al., *Reversal of persistent fibrosis in aging by targeting Nox4-Nrf2 redox imbalance.* Sci Transl Med, 2014. **6**(231): p. 231ra47.
73. Hubackova, S., et al., *IL1- and TGFbeta-Nox4 signaling, oxidative stress and DNA damage response are shared features of replicative, oncogene-induced, and drug-induced paracrine 'bystander senescence'.* Aging (Albany NY), 2012. **4**(12): p. 932-51.
74. Wallace, D.C. and W. Fan, *Energetics, epigenetics, mitochondrial genetics.* Mitochondrion, 2010. **10**(1): p. 12-31.
75. Turrens, J.F., *Mitochondrial formation of reactive oxygen species.* J Physiol, 2003. **552**(Pt 2): p. 335-44.
76. Moiseeva, O., et al., *Mitochondrial Dysfunction Contributes to Oncogene-Induced Senescence.* Mol. Cell. Biol., 2009. **29**(16): p. 4495-4507.
77. Hutter, E., et al., *Replicative senescence of human fibroblasts: the role of Ras-dependent signaling and oxidative stress.* Exp Gerontol, 2002. **37**(10-11): p. 1165-74.
78. Zwerschke, W., et al., *Metabolic analysis of senescent human fibroblasts reveals a role for AMP in cellular senescence.* Biochem J, 2003. **376**(Pt 2): p. 403-11.
79. Hutter, E., et al., *Senescence-associated changes in respiration and oxidative phosphorylation in primary human fibroblasts.* Biochem J, 2004. **380**(Pt 3): p. 919-28.
80. Sitte, N., et al., *Protein oxidation and degradation during proliferative senescence of human MRC-5 fibroblasts.* Free Rad Biol Med, 2000. **28**(5): p. 701-708.
81. Sitte, N., et al., *Lipofuscin accumulation in proliferating fibroblasts in vitro: an indicator of oxidative stress.* Exp Gerontol, 2001. **36**(3): p. 475-486.
82. Liu, L., et al., *Mitochondrial dysfunction leads to telomere attrition and genomic instability.* Aging Cell, 2002. **1**(1): p. 40-6.
83. Perez, V.I., et al., *Is the oxidative stress theory of aging dead?* Biochim Biophys Acta, 2009. **1790**(10): p. 1005-14.
84. Matoba, S., et al., *p53 Regulates Mitochondrial Respiration.* Science, 2006. **312**(5780): p. 1650-1653.
85. Sahin, E., et al., *Telomere dysfunction induces metabolic and mitochondrial compromise.* Nature, 2011. **470**(7334): p. 359-65.
86. Velarde, M.C., et al., *Mitochondrial oxidative stress caused by Sod2 deficiency promotes cellular senescence and aging phenotypes in the skin.* Aging (Albany NY), 2012. **4**(1): p. 3-12.
87. Vafai, S.B. and V.K. Mootha, *Mitochondrial disorders as windows into an ancient organelle.* Nature, 2012. **491**(7424): p. 374-83.
88. Pagliarini, D.J., et al., *A mitochondrial protein compendium elucidates complex I disease biology.* Cell, 2008. **134**(1): p. 112-23.
89. Scarpulla, R.C., *Metabolic control of mitochondrial biogenesis through the PGC-1 family regulatory network.* Biochim Biophys Acta, 2011. **1813**(7): p. 1269-78.
90. Spiegelman, B.M., *Transcriptional control of mitochondrial energy metabolism through the PGC1 coactivators.* Novartis Found Symp, 2007. **287**: p. 60-3; discussion 63-9.
91. Youle, R.J. and D.P. Narendra, *Mechanisms of mitophagy.* Nat Rev Mol Cell Biol, 2011. **12**(1): p. 9-14.
92. Chan, D.C., *Fusion and fission: interlinked processes critical for mitochondrial health.* Annu Rev Genet, 2012. **46**: p. 265-87.

93. MacAskill, A.F. and J.T. Kittler, *Control of mitochondrial transport and localization in neurons.* Trends Cell Biol, 2010. **20**(2): p. 102-12.
94. Wallace, D.C., *A mitochondrial paradigm of metabolic and degenerative diseases, aging, and cancer: A dawn for evolutionary medicine.* Annual Review of Genetics, 2005. **39**: p. 359-407.
95. Wallace, D.C., *The mitochondrial genome in human adaptive radiation and disease: On the road to therapeutics and performance enhancement.* Gene, 2005. **354**: p. 169-180.
96. Lee, S., et al., *Mitochondrial fission and fusion mediators, hFis1 and OPA1, modulate cellular senescence.* J. Biol. Chem., 2007. **282**(31): p. 22977-83.
97. Kang, H.T., et al., *Autophagy impairment induces premature senescence in primary human fibroblasts.* PLoS One, 2011. **6**(8): p. e23367.
98. Tal, M.C., et al., *Absence of autophagy results in reactive oxygen species-dependent amplification of RLR signaling.* Proc Natl Acad Sci U S A, 2009. **106**(8): p. 2770-5.
99. Stephenson, L.M., et al., *Identification of Atg5-dependent transcriptional changes and increases in mitochondrial mass in Atg5-deficient T lymphocytes.* Autophagy, 2009. **5**(5): p. 625-35.
100. Young, A.R., et al., *Autophagy mediates the mitotic senescence transition.* Genes Dev, 2009. **23**(7): p. 798-803.
101. Handschin, C. and B.M. Spiegelman, *Peroxisome proliferator-activated receptor gamma coactivator 1 coactivators, energy homeostasis, and metabolism.* Endocr Rev, 2006. **27**(7): p. 728-35.
102. Xu, D. and T. Finkel, *A role for mitochondria as potential regulators of cellular life span.* Bioch Biophy Res Com, 2002. **294**(2): p. 245-248.
103. Lee, H.C., et al., *Increase in mitochondrial mass in human fibroblasts under oxidative stress and during replicative cell senescence.* J Biomed Sci, 2002. **9**(6 Pt 1): p. 517-26.
104. Hickey, F.B., et al., *IHG-1 Promotes Mitochondrial Biogenesis by Stabilizing PGC-1α.* Journal of the American Society of Nephrology, 2011. **22**(8): p. 1475-1485.
105. Lehman, J.J., et al., *Peroxisome proliferator-activated receptor {gamma} coactivator-1 promotes cardiac mitochondrial biogenesis.* J. Clin. Invest., 2000. **106**(7): p. 847-856.
106. Sawada, N., et al., *Endothelial PGC-1alpha mediates vascular dysfunction in diabetes.* Cell Metab, 2014. **19**(2): p. 246-58.
107. Hancock, C.R., et al., *Does calorie restriction induce mitochondrial biogenesis? A reevaluation.* The FASEB journal, 2011. **25**(2): p. 785-791.
108. Nisoli, E., et al., *Calorie Restriction Promotes Mitochondrial Biogenesis by Inducing the Expression of eNOS.* Science, 2005. **310**(5746): p. 314-317.
109. Price, J.C., et al., *The Effect of Long Term Calorie Restriction on in Vivo Hepatic Proteostatis: A Novel Combination of Dynamic and Quantitative Proteomics.* Molecular & Cellular Proteomics, 2012. **11**(12): p. 1801-1814.
110. Lanza, I.R., et al., *Chronic Caloric Restriction Preserves Mitochondrial Function in Senescence without Increasing Mitochondrial Biogenesis.* Cell Metabolism, 2012. **16**(6): p. 777-788.
111. Jeyapalan, J.C., et al., *Accumulation of senescent cells in mitotic tissue of aging primates.* Mech Ageing Dev, 2007. **128**(1): p. 36-44.
112. Sedelnikova, O.A., et al., *Senescing human cells and ageing mice accumulate DNA lesions with unrepairable double-strand breaks.* Nat Cell Biol, 2004. **6**(2): p. 168-170.
113. Krishnamurthy, J., et al., *Ink4a/Arf expression is a biomarker of aging.* J Clin Invest, 2004. **114**(9): p. 1299-307.
114. Herbig, U., et al., *Cellular Senescence in Aging Primates.* Science, 2006. **311**(5765): p. 1257-.

115. Wiemann, S.U., et al., *Hepatocyte telomere shortening and senescence are general markers of human liver cirrhosis.* The FASEB journal, 2002. **16**(9): p. 935-942.
116. Price, J.S., et al., *The role of chondrocyte senescence in osteoarthritis.* Aging Cell, 2002. **1**(1): p. 57-65.
117. Minamino, T. and I. Komuro, *Vascular cell senescence: contribution to atherosclerosis.* Circ Res, 2007. **100**(1): p. 15-26.
118. Williams, G.C., *Pleotropy, natural selection, and the evolution of senescence.* Evolution, 1957. **11**: p. 398-411.
119. Blasco, M.A., et al., *Telomere Shortening and Tumor Formation by Mouse Cells Lacking Telomerase RNA.* Cell, 1997. **91**(1): p. 25-34.
120. Leri, A., et al., *Ablation of telomerase and telomere loss leads to cardiac dilatation and heart failure associated with p53 upregulation.* EMBO J, 2003. **22**(1): p. 131-9.
121. Roy Choudhury, A., et al., *p21-deletion prolongs lifespan of telomere dysfunctional mice without accelerating cancer formation.* Nature genetics, 2006. **in press**.
122. Sherr, C.J. and R.A. DePinho, *Cellular senescence: mitotic clock or culture shock?* Cell, 2000. **102**(4): p. 407-10.
123. Braig, M., et al., *Oncogene-induced senescence as an initial barrier in lymphoma development.* Nature, 2005. **436**(7051): p. 660-665.
124. Collado, M., et al., *Tumour biology: Senescence in premalignant tumours.* Nature, 2005. **436**(7051): p. 642.
125. Michaloglou, C., et al., *BRAFE600-associated senescence-like cell cycle arrest of human naevi.* Nature, 2005. **436**(7051): p. 720-724.
126. Chen, Z., et al., *Crucial role of p53-dependent cellular senescence in suppression of Pten-deficient tumorigenesis.* Nature, 2005. **436**(7051): p. 725-730.
127. Gray-Schopfer, V.C., et al., *Cellular senescence in naevi and immortalisation in melanoma: a role for p16?* Br J Cancer, 2006. **95**(4): p. 496-505.
128. Munoz-Espin, D. and M. Serrano, *Cellular senescence: from physiology to pathology.* Nat Rev Mol Cell Biol, 2014. **15**(7): p. 482-496.
129. Krizhanovsky, V., et al., *Senescence of activated stellate cells limits liver fibrosis.* Cell, 2008. **134**(4): p. 657-67.
130. Jun, J.-I. and L.F. Lau, *The matricellular protein CCN1 induces fibroblast senescence and restricts fibrosis in cutaneous wound healing.* Nat Cell Biol, 2010. **12**(7): p. 676-685.
131. Kim, K.H., et al., *Matricellular protein CCN1 promotes regression of liver fibrosis through induction of cellular senescence in hepatic myofibroblasts.* Mol Cell Biol, 2013. **33**(10): p. 2078-90.
132. Lujambio, A., et al., *Non-cell-autonomous tumor suppression by p53.* Cell, 2013. **153**(2): p. 449-60.
133. Xue, W., et al., *Senescence and tumour clearance is triggered by p53 restoration in murine liver carcinomas.* Nature, 2007. **445**(7128): p. 656-60.
134. Kang, T.W., et al., *Senescence surveillance of pre-malignant hepatocytes limits liver cancer development.* Nature, 2011. **479**(7374): p. 547-51.
135. Campisi, J., *Senescent Cells, Tumor Suppression, and Organismal Aging: Good Citizens, Bad Neighbors.* Cell, 2005. **120**(4): p. 513-522.
136. Baker, D.J., et al., *Clearance of p16Ink4a-positive senescent cells delays ageing-associated disorders.* Nature, 2011. **479**(7372): p. 232-6.
137. Besancenot, R., et al., *A senescence-like cell-cycle arrest occurs during megakaryocytic maturation: implications for physiological and pathological megakaryocytic proliferation.* PLoS Biol, 2010. **8**(9).
138. Munoz-Espin, D., et al., *Programmed cell senescence during mammalian embryonic development.* Cell, 2013. **155**(5): p. 1104-18.
139. Storer, M., et al., *Senescence is a developmental mechanism that contributes to embryonic growth and patterning.* Cell, 2013. **155**(5): p. 1119-30.

140. Harrison, D.E., et al., *Rapamycin fed late in life extends lifespan in genetically heterogeneous mice.* Nature, 2009. **460**(7253): p. 392-5.
141. Zoncu, R., A. Efeyan, and D.M. Sabatini, *mTOR: from growth signal integration to cancer, diabetes and ageing.* Nat Rev Mol Cell Biol, 2011. **12**(1): p. 21-35.
142. Ma, X.M. and J. Blenis, *Molecular mechanisms of mTOR-mediated translational control.* Nat Rev Mol Cell Biol, 2009. **10**(5): p. 307-18.
143. von Manteuffel, S.R., et al., *The insulin-induced signalling pathway leading to S6 and initiation factor 4E binding protein 1 phosphorylation bifurcates at a rapamycin-sensitive point immediately upstream of p70s6k.* Mol Cell Biol, 1997. **17**(9): p. 5426-36.
144. Vezina, C., A. Kudelski, and S.N. Sehgal, *Rapamycin (AY-22,989), a new antifungal antibiotic. I. Taxonomy of the producing streptomycete and isolation of the active principle.* J Antibiot (Tokyo), 1975. **28**(10): p. 721-6.
145. Wander, S.A., B.T. Hennessy, and J.M. Slingerland, *Next-generation mTOR inhibitors in clinical oncology: how pathway complexity informs therapeutic strategy.* J Clin Invest, 2011. **121**(4): p. 1231-41.
146. Wang, X. and C.G. Proud, *mTORC1 signaling: what we still don't know.* J Mol Cell Biol, 2011. **3**(4): p. 206-20.
147. Urano, J., et al., *Point mutations in TOR confer Rheb-independent growth in fission yeast and nutrient-independent mammalian TOR signaling in mammalian cells.* Proc Natl Acad Sci U S A, 2007. **104**(9): p. 3514-9.
148. Fabrizio, P., et al., *Regulation of longevity and stress resistance by Sch9 in yeast.* Science, 2001. **292**(5515): p. 288-90.
149. Kaeberlein, M., et al., *Regulation of yeast replicative life span by TOR and Sch9 in response to nutrients.* Science, 2005. **310**(5751): p. 1193-6.
150. Jia, K., D. Chen, and D.L. Riddle, *The TOR pathway interacts with the insulin signaling pathway to regulate C. elegans larval development, metabolism and life span.* Development, 2004. **131**(16): p. 3897-906.
151. Vellai, T., et al., *Genetics: influence of TOR kinase on lifespan in C. elegans.* Nature, 2003. **426**(6967): p. 620.
152. Bjedov, I., et al., *Mechanisms of life span extension by rapamycin in the fruit fly Drosophila melanogaster.* Cell Metab, 2010. **11**(1): p. 35-46.
153. Kapahi, P., et al., *Regulation of lifespan in Drosophila by modulation of genes in the TOR signaling pathway.* Curr Biol, 2004. **14**(10): p. 885-90.
154. Liu, M., et al., *Antitumor activity of rapamycin in a transgenic mouse model of ErbB2-dependent human breast cancer.* Cancer Res, 2005. **65**(12): p. 5325-36.
155. Anisimov, V.N., et al., *Rapamycin extends maximal lifespan in cancer-prone mice.* Am J Pathol, 2010. **176**(5): p. 2092-7.
156. Anisimov, V.N., et al., *Rapamycin increases lifespan and inhibits spontaneous tumorigenesis in inbred female mice.* Cell Cycle, 2011. **10**(24): p. 4230-6.
157. Komarova, E.A., et al., *Rapamycin extends lifespan and delays tumorigenesis in heterozygous p53+/- mice.* Aging (Albany NY), 2012. **4**(10): p. 709-14.
158. Livi, C.B., et al., *Rapamycin extends life span of Rb1+/- mice by inhibiting neuroendocrine tumors.* Aging (Albany NY), 2013. **5**(2): p. 100-10.
159. Hasty, P., et al., *eRapa Restores A Normal Life Span in a FAP Mouse Model.* Cancer Prev Res (Phila), 2013.
160. Johnson, S.C., P.S. Rabinovitch, and M. Kaeberlein, *mTOR is a key modulator of ageing and age-related disease.* Nature, 2013. **493**(7432): p. 338-45.
161. Johnson, S.C., et al., *mTOR inhibition alleviates mitochondrial disease in a mouse model of Leigh syndrome.* Science, 2013. **342**(6165): p. 1524-8.
162. Inoki, K., et al., *TSC2 integrates Wnt and energy signals via a coordinated phosphorylation by AMPK and GSK3 to regulate cell growth.* Cell, 2006. **126**(5): p. 955-68.
163. Castilho, R.M., et al., *mTOR mediates Wnt-induced epidermal stem cell exhaustion and aging.* Cell Stem Cell, 2009. **5**(3): p. 279-89.

164. Chen, C., et al., *TSC-mTOR maintains quiescence and function of hematopoietic stem cells by repressing mitochondrial biogenesis and reactive oxygen species.* J Exp Med, 2008. **205**(10): p. 2397-408.
165. Pospelova, T.V., et al., *Rapamycin induces pluripotent genes associated with avoidance of replicative senescence.* Cell Cycle, 2013. **12**(24): p. 3841-51.
166. Ahmed, S., et al., *Telomerase does not counteract telomere shortening but protects mitochondrial function under oxidative stress.* J Cell Sci, 2008. **121**(7): p. 1046-1053.
167. Nelson, G., M. Buhmann, and T. von Zglinicki *DNA damage foci in mitosis are devoid of 53BP1.* Cell Cycle, 2009. **8**(20): p. 3379-83.
168. Kuma, A., et al., *The role of autophagy during the early neonatal starvation period.* Nature, 2004. **432**(7020): p. 1032-6.
169. Molenaar, C., et al., *Visualizing telomere dynamics in living mammalian cells using PNA probes.* Embo J, 2003. **22**(24): p. 6631-6641.
170. Dimri, G., et al., *A Biomarker that Identifies Senescent Human Cells in Culture and in Aging Skin in vivo.* PNAS, 1995. **92**(20): p. 9363-9367.
171. Debacq-Chainiaux, F., et al., *Protocols to detect senescence-associated beta-galactosidase (SA-betagal) activity, a biomarker of senescent cells in culture and in vivo.* Nat Protoc, 2009. **4**(12): p. 1798-806.
172. Chien, Y., et al., *Control of the senescence-associated secretory phenotype by NF-kappaB promotes senescence and enhances chemosensitivity.* Genes Dev, 2011. **25**(20): p. 2125-36.
173. d'Adda di Fagagna, F., et al., *A DNA damage checkpoint response in telomere-initiated senescence.* Nature, 2003. **426**(6963): p. 194-8.
174. Parrinello, S., et al., *Oxygen sensitivity severely limits the replicative lifespan of murine fibroblasts.* Nat Cell Biol, 2003. **5**(8): p. 741-7.
175. Kipling, D. and H.J. Cooke, *Hypervariable ultra-long telomeres in mice.* Nature, 1990. **347**(6291): p. 400-2.
176. Herbig, U., et al., *Telomere shortening triggers senescence of human cells through a pathway involving ATM, p53, and p21(CIP1), but not p16(INK4a).* Mol Cell, 2004. **14**(4): p. 501-13.
177. Cesare, A.J., et al., *Spontaneous occurrence of telomeric DNA damage response in the absence of chromosome fusions.* Nat Struct Mol Biol, 2009. **16**(12): p. 1244-1251.
178. Passos, J.F., et al., *Feedback between p21 and reactive oxygen production is necessary for cell senescence.* Mol Syst Biol, 2010. **6**: p. 347.
179. Meier, A., et al., *Spreading of mammalian DNA-damage response factors studied by ChIP-chip at damaged telomeres.* Embo J, 2007. **26**(11): p. 2707-2718.
180. de Lange, T., *How shelterin solves the telomere end-protection problem.* Cold Spring Harb Symp Quant Biol, 2010. **75**: p. 167-77.
181. Thanasoula, M., et al., *p53 Prevents Entry into Mitosis with Uncapped Telomeres.* Current Biology, 2010. **20**(6): p. 521-526.
182. de Lange, T., *Protection of mammalian telomeres.* Oncogene, 2002. **21**(4): p. 532-40.
183. Karlseder, J., A. Smogorzewska, and T. de Lange, *Senescence Induced by Altered Telomere State, Not Telomere Loss.* Science, 2002. **295**(5564): p. 2446-2449.
184. van Steensel, B., A. Smogorzewska, and T. de Lange, *TRF2 Protects Human Telomeres from End-to-End Fusions.* Cell, 1998. **92**(3): p. 401-413.
185. Ward, J.F., *DNA damage produced by ionizing radiation in mammalian cells: identities, mechanisms of formation, and reparability.* Prog Nucleic Acid Res Mol Biol, 1988. **35**: p. 95-125.
186. Henle, E., et al., *Sequence-specific DNA cleavage by Fe2+-mediated fenton reactions has possible biological implications.* J Biol Chem, 1999. **274**(2): p. 962-71

.
187. Oikawa, S., S. Tada-Oikawa, and S. Kawanishi, *Site-Specific DNA Damage at the GGG Sequence by UVA Involves Acceleration of Telomere Shortening.* Biochemistry, 2001. **40**(15): p. 4763-4768.
188. Crabbe, L., et al., *Human telomeres are tethered to the nuclear envelope during postmitotic nuclear assembly.* Cell Rep, 2012. **2**(6): p. 1521-9.
189. Giunta, S., R. Belotserkovskaya, and S.P. Jackson, *DNA damage signaling in response to double-strand breaks during mitosis.* J Cell Biol, 2010. **190**(2): p. 197-207.
190. Orthwein, A., et al., *Mitosis inhibits DNA double-strand break repair to guard against telomere fusions.* Science, 2014. **344**(6180): p. 189-93.
191. Hayashi, M.T., et al., *A telomere-dependent DNA damage checkpoint induced by prolonged mitotic arrest.* Nat Struct Mol Biol, 2012. **19**(4): p. 387-94.
192. Kruk, P.A., N.J. Rampino, and V.A. Bohr, *DNA Damage and Repair in Telomeres: Relation to Aging.* PNAS, 1995. **92**(1): p. 258-262.
193. Michelson, R.J., S. Rosenstein, and T. Weinert, *A telomeric repeat sequence adjacent to a DNA double-stranded break produces an anticheckpoint.* Genes & Development, 2005. **19**: p. 2546-2559.
194. Miller, D., et al., *Subtelomeric regions in mammalian cells are deficient in DNA double-strand break repair.* DNA Repair (Amst), 2011. **10**(5): p. 536-44.
195. Artandi, S.E., et al., *Telomere dysfunction promotes non-reciprocal translocations and epithelial cancers in mice.* Nature, 2000. **406**(6796): p. 641-5.
196. Nakamura, A.J., et al., *Both telomeric and non-telomeric DNA damage are determinants of mammalian cellular senescence.* Epigenetics Chromatin, 2008. **1**(1): p. 6.
197. Nelson, G., M. Buhmann, and T. von Zglinicki, *DNA damage foci in mitosis are devoid of 53BP1.* Cell Cycle, 2009. **8**(20): p. 3379-83.
198. Rohwer, N., et al., *The growing complexity of HIF-1alpha's role in tumorigenesis: DNA repair and beyond.* Oncogene, 2013. **32**(31): p. 3569-76.
199. Robles, S. and G. Adami, *Agents that cause DNA double strand breaks lead to p16INK4a enrichment and the premature senescence of normal fibroblasts.* Oncogene, 1998. **16**(9): p. 1113-23.
200. Wei, W. and J.M. Sedivy, *Differentiation between Senescence (M1) and Crisis (M2) in Human Fibroblast Cultures.* Experimental Cell Research, 1999. **253**(2): p. 519-522.
201. Rajavel, M., M.R. Mullins, and D.J. Taylor, *Multiple facets of TPP1 in telomere maintenance.* Biochim Biophys Acta, 2014.
202. Cesare, A.J. and J. Karlseder, *A three-state model of telomere control over human proliferative boundaries.* Curr Opin Cell Biol, 2012. **24**(6): p. 731-8.
203. Margulis, L., *Symbiosis and evolution.* Sci Am, 1971. **225**(2): p. 48-57.
204. Lane, N., *Power, sex, suicide : mitochondria and the meaning of life*. 2005, Oxford ; New York: Oxford University Press. xiii, 354 p.
205. Shen, X., et al., *Cardiac mitochondrial damage and biogenesis in a chronic model of type 1 diabetes.* Am J Physiol Endocrinol Metab, 2004. **287**(5): p. E896-905.
206. Sen, N., Y.K. Satija, and S. Das, *PGC-1alpha, a key modulator of p53, promotes cell survival upon metabolic stress.* Mol Cell, 2011. **44**(4): p. 621-34.
207. Wu, Z., et al., *Mechanisms controlling mitochondrial biogenesis and respiration through the thermogenic coactivator PGC-1.* Cell, 1999. **98**(1): p. 115-24.
208. Puigserver, P., et al., *A cold-inducible coactivator of nuclear receptors linked to adaptive thermogenesis.* Cell, 1998. **92**(6): p. 829-39.
209. Fisher, R.P., et al., *DNA wrapping and bending by a mitochondrial high mobility group-like transcriptional activator protein.* J Biol Chem, 1992. **267**(5): p. 3358-67.
210. Garesse, R. and C.G. Vallejo, *Animal mitochondrial biogenesis and function: a regulatory cross-talk between two genomes.* Gene, 2001. **263**(1-2): p. 1-16.

211. Larsson N. G., et al., *Low Levels of Mitochondrial Transcription Factor A in Mitochondrial DNA Depletion.* Biochemical and Biophysical Research Communications, 1994. **200**(3): p. 1374-1381.
212. Larsson, N.G., et al., *Mitochondrial transcription factor A is necessary for mtDNA maintenance and embryogenesis in mice.* Nat Genet, 1998. **18**(3): p. 231-6.
213. Lelliott, C.J., et al., *Ablation of PGC-1beta results in defective mitochondrial activity, thermogenesis, hepatic function, and cardiac performance.* PLoS Biol, 2006. **4**(11): p. e369.
214. Liesa, M., et al., *Mitochondrial fusion is increased by the nuclear coactivator PGC-1beta.* PLoS One, 2008. **3**(10): p. e3613.
215. Mootha, V.K., et al., *Erralpha and Gabpa/b specify PGC-1alpha-dependent oxidative phosphorylation gene expression that is altered in diabetic muscle.* Proc Natl Acad Sci U S A, 2004. **101**(17): p. 6570-5.
216. Schreiber, S.N., et al., *The estrogen-related receptor alpha (ERRalpha) functions in PPARgamma coactivator 1alpha (PGC-1alpha)-induced mitochondrial biogenesis.* Proc Natl Acad Sci U S A, 2004. **101**(17): p. 6472-7.
217. Passos, J.F., T. Von Zglinicki , and T.B. Kirkwood, *Mitochondria and ageing: winning and losing in the numbers game.* BioEssays 2007. **29**(9): p. 908-17.
218. Rubinsztein, D.C., G. Marino, and G. Kroemer, *Autophagy and aging.* Cell, 2011. **146**(5): p. 682-95.
219. Klionsky, D.J., et al., *A unified nomenclature for yeast autophagy-related genes.* Dev Cell, 2003. **5**(4): p. 539-45.
220. Janku, F., et al., *Autophagy as a target for anticancer therapy.* Nat Rev Clin Oncol, 2011. **8**(9): p. 528-39.
221. Mai, S., et al., *Decreased expression of Drp1 and Fis1 mediates mitochondrial elongation in senescent cells and enhances resistance to oxidative stress through PINK1.* J Cell Sci, 2010. **123**(Pt 6): p. 917-26.
222. Guertin, D.A., et al., *Functional genomics identifies TOR-regulated genes that control growth and division.* Curr Biol, 2006. **16**(10): p. 958-70.
223. Carroll, B., V.I. Korolchuk, and S. Sarkar, *Amino acids and autophagy: cross-talk and co-operation to control cellular homeostasis.* Amino Acids, 2014.
224. Viniegra, J.G., et al., *Full activation of PKB/Akt in response to insulin or ionizing radiation is mediated through ATM.* J Biol Chem, 2005. **280**(6): p. 4029-36.
225. Tormos, A.M., et al., *Liver-specific p38alpha deficiency causes reduced cell growth and cytokinesis failure during chronic biliary cirrhosis in mice.* Hepatology, 2013. **57**(5): p. 1950-61.
226. Jung, C.H., et al., *ULK-Atg13-FIP200 complexes mediate mTOR signaling to the autophagy machinery.* Mol Biol Cell, 2009. **20**(7): p. 1992-2003.
227. Mizushima, N., T. Yoshimori, and B. Levine, *Methods in mammalian autophagy research.* Cell, 2010. **140**(3): p. 313-26.
228. St-Pierre, J., et al., *Bioenergetic analysis of peroxisome proliferator-activated receptor gamma coactivators 1alpha and 1beta (PGC-1alpha and PGC-1beta) in muscle cells.* J Biol Chem, 2003. **278**(29): p. 26597-603.
229. Iglesias-Bartolome, R., et al., *mTOR Inhibition Prevents Epithelial Stem Cell Senescence and Protects from Radiation-Induced Mucositis.* Cell Stem Cell, 2012. **11**(3): p. 401-414.
230. Campisi, J. and F. d'Adda di Fagagna, *Cellular senescence: when bad things happen to good cells.* Nat Rev Mol Cell Biol, 2007. **8**(9): p. 729-740.
231. Hasty, P., et al., *mTORC1 and p53: clash of the gods?* Cell Cycle, 2013. **12**(1): p. 20-5.
232. Lai, K.P., et al., *S6K1 is a multifaceted regulator of Mdm2 that connects nutrient status and DNA damage response.* EMBO J, 2010. **29**(17): p. 2994-3006.
233. Zhang, H., et al., *Loss of Tsc1/Tsc2 activates mTOR and disrupts PI3K-Akt signaling through downregulation of PDGFR.* J Clin Invest, 2003. **112**(8): p. 1223-33.

234. Menon, S., et al., *Chronic activation of mTOR complex 1 is sufficient to cause hepatocellular carcinoma in mice.* Sci Signal, 2012. **5**(217): p. ra24.
235. Ellisen, L.W., et al., *REDD1, a developmentally regulated transcriptional target of p63 and p53, links p63 to regulation of reactive oxygen species.* Mol Cell, 2002. **10**(5): p. 995-1005.
236. Li, X.H., et al., *REDD1 protects osteoblast cells from gamma radiation-induced premature senescence.* PLoS One, 2012. **7**(5): p. e36604.
237. Sofer, A., et al., *Regulation of mTOR and cell growth in response to energy stress by REDD1.* Mol Cell Biol, 2005. **25**(14): p. 5834-45.
238. Alexander, A., et al., *ATM signals to TSC2 in the cytoplasm to regulate mTORC1 in response to ROS.* Proc Natl Acad Sci U S A, 2010. **107**(9): p. 4153-8.
239. !!! INVALID CITATION !!!
240. Bakkenist, C.J. and M.B. Kastan, *DNA damage activates ATM through intermolecular autophosphorylation and dimer dissociation.* Nature, 2003. **421**(6922): p. 499-506.
241. Jiang, H. and P.K. Vogt, *Constitutively active Rheb induces oncogenic transformation.* Oncogene, 2008. **27**(43): p. 5729-40.
242. Nardella, C., et al., *Aberrant Rheb-mediated mTORC1 activation and Pten haploinsufficiency are cooperative oncogenic events.* Genes Dev, 2008. **22**(16): p. 2172-7.
243. Sahin, E. and R.A. DePinho, *Axis of ageing: telomeres, p53 and mitochondria.* Nat Rev Mol Cell Biol, 2012. **13**(6): p. 397-404.
244. Wu, H., et al., *Regulation of mitochondrial biogenesis in skeletal muscle by CaMK.* Science, 2002. **296**(5566): p. 349-52.
245. Jain, S.S., et al., *High-Fat Diet-Induced Mitochondrial Biogenesis Is Regulated by Mitochondrial-Derived Reactive Oxygen Species Activation of CaMKII.* Diabetes, 2014. **63**(6): p. 1907-13.
246. Ventura-Clapier, R., A. Garnier, and V. Veksler, *Transcriptional control of mitochondrial biogenesis: the central role of PGC-1alpha.* Cardiovasc Res, 2008. **79**(2): p. 208-17.
247. Kelly, D.P. and R.C. Scarpulla, *Transcriptional regulatory circuits controlling mitochondrial biogenesis and function.* Genes Dev., 2004. **18**(4): p. 357-368.
248. Hatch, G.M., *Cell biology of cardiac mitochondrial phospholipids.* Biochem Cell Biol, 2004. **82**(1): p. 99-112.
249. Gomes, L.C., G. Di Benedetto, and L. Scorrano, *During autophagy mitochondria elongate, are spared from degradation and sustain cell viability.* Nat Cell Biol, 2011. **13**(5): p. 589-98.
250. Yoon, Y.S., et al., *Formation of elongated giant mitochondria in DFO-induced cellular senescence: involvement of enhanced fusion process through modulation of Fis1.* J Cell Physiol, 2006. **209**(2): p. 468-80.
251. Lelliott, C.J., et al., *Ablation of PGC-1β Results in Defective Mitochondrial Activity, Thermogenesis, Hepatic Function, and Cardiac Performance.* PLoS Biol, 2006. **4**(11): p. e369.
252. St-Pierre, J., et al., *Suppression of Reactive Oxygen Species and Neurodegeneration by the PGC-1 Transcriptional Coactivators.* Cell, 2006. **127**(2): p. 397-408.
253. Bartoletti-Stella, A., et al., *Gamma rays induce a p53-independent mitochondrial biogenesis that is counter-regulated by HIF1alpha.* Cell Death Dis, 2013. **4**: p. e663.
254. Yecies, J.L. and B.D. Manning, *Transcriptional control of cellular metabolism by mTOR signaling.* Cancer Res, 2011. **71**(8): p. 2815-20.
255. Goo, C.K., et al., *PTEN/Akt signaling controls mitochondrial respiratory capacity through 4E-BP1.* PLoS One, 2012. **7**(9): p. e45806.
256. Morita, M., et al., *mTORC1 controls mitochondrial activity and biogenesis through 4E-BP-dependent translational regulation.* Cell Metab, 2013. **18**(5): p. 698-711.

257. Sarbassov, D.D., et al., *Rictor, a novel binding partner of mTOR, defines a rapamycin-insensitive and raptor-independent pathway that regulates the cytoskeleton.* Curr Biol, 2004. **14**(14): p. 1296-302.
258. Li, Y., et al., *Phosphatase and tensin homolog deleted on chromosome 10 (PTEN) signaling regulates mitochondrial biogenesis and respiration via estrogen-related receptor alpha (ERRalpha).* J Biol Chem, 2013. **288**(35): p. 25007-24.
259. Cook, S.A., et al., *Transcriptional effects of chronic Akt activation in the heart.* J Biol Chem, 2002. **277**(25): p. 22528-33.
260. Schieke, S.M., et al., *The mammalian target of rapamycin (mTOR) pathway regulates mitochondrial oxygen consumption and oxidative capacity.* J Biol Chem, 2006. **281**(37): p. 27643-52.
261. Chen, C., Y. Liu, and P. Zheng, *mTOR regulation and therapeutic rejuvenation of aging hematopoietic stem cells.* Sci Signal, 2009. **2**(98): p. ra75.
262. Zong, H., et al., *AMP kinase is required for mitochondrial biogenesis in skeletal muscle in response to chronic energy deprivation.* Proc Natl Acad Sci U S A, 2002. **99**(25): p. 15983-7.
263. Hervouet, E., et al., *A new role for the von Hippel-Lindau tumor suppressor protein: stimulation of mitochondrial oxidative phosphorylation complex biogenesis.* Carcinogenesis, 2005. **26**(3): p. 531-9.
264. Welford, S.M., et al., *HIF1alpha delays premature senescence through the activation of MIF.* Genes Dev, 2006. **20**(24): p. 3366-71.
265. Zhang, H., et al., *HIF-1 Inhibits Mitochondrial Biogenesis and Cellular Respiration in VHL-Deficient Renal Cell Carcinoma by Repression of C-MYC Activity.* Cancer Cell, 2007. **11**(5): p. 407-420.
266. Li, F., et al., *Myc stimulates nuclearly encoded mitochondrial genes and mitochondrial biogenesis.* Mol Cell Biol, 2005. **25**(14): p. 6225-34.
267. Mills, C.N., S.S. Joshi, and R.M. Niles, *Expression and function of hypoxia inducible factor-1 alpha in human melanoma under non-hypoxic conditions.* Mol Cancer, 2009. **8**: p. 104.
268. Romanino, K., et al., *Myopathy caused by mammalian target of rapamycin complex 1 (mTORC1) inactivation is not reversed by restoring mitochondrial function.* Proc Natl Acad Sci U S A, 2011. **108**(51): p. 20808-13.
269. Risson, V., et al., *Muscle inactivation of mTOR causes metabolic and dystrophin defects leading to severe myopathy.* J Cell Biol, 2009. **187**(6): p. 859-74.
270. Polak, P., et al., *Adipose-specific knockout of raptor results in lean mice with enhanced mitochondrial respiration.* Cell Metab, 2008. **8**(5): p. 399-410.
271. Barreto, P., et al., *Overexpression of UCP1 in tobacco induces mitochondrial biogenesis and amplifies a broad stress response.* BMC Plant Biol, 2014. **14**: p. 144.
272. Cunningham, J.T., et al., *mTOR controls mitochondrial oxidative function through a YY1-PGC-1alpha transcriptional complex.* Nature, 2007. **450**(7170): p. 736-40.
273. Um, S.H., et al., *Absence of S6K1 protects against age- and diet-induced obesity while enhancing insulin sensitivity.* Nature, 2004. **431**(7005): p. 200-5.
274. Aguilar, V., et al., *S6 kinase deletion suppresses muscle growth adaptations to nutrient availability by activating AMP kinase.* Cell Metab, 2007. **5**(6): p. 476-87.
275. Lustig, Y., et al., *Separation of the gluconeogenic and mitochondrial functions of PGC-1{alpha} through S6 kinase.* Genes Dev, 2011. **25**(12): p. 1232-44.
276. Duvel, K., et al., *Activation of a metabolic gene regulatory network downstream of mTOR complex 1.* Mol Cell, 2010. **39**(2): p. 171-83.
277. Zhang, S., et al., *Constitutive reductions in mTOR alter cell size, immune cell development, and antibody production.* Blood, 2011. **117**(4): p. 1228-38.
278. Wu, J.J., et al., *Increased mammalian lifespan and a segmental and tissue-specific slowing of aging after genetic reduction of mTOR expression.* Cell Rep, 2013. **4**(5): p. 913-20.

279. Selman, C., et al., *Ribosomal protein S6 kinase 1 signaling regulates mammalian life span.* Science, 2009. **326**(5949): p. 140-4.
280. Wenz, T., et al., *Increased muscle PGC-1alpha expression protects from sarcopenia and metabolic disease during aging.* Proc Natl Acad Sci U S A, 2009. **106**(48): p. 20405-10.
281. Ruas, J.L., et al., *A PGC-1alpha Isoform Induced by Resistance Training Regulates Skeletal Muscle Hypertrophy.* Cell, 2012. **151**(6): p. 1319-31.
282. Wang, L., et al., *Apoptosis induced by PGC-1beta in breast cancer cells is mediated by the mTOR pathway.* Oncol Rep, 2013. **30**(4): p. 1631-8.
283. Iglesias-Bartolome, R., et al., *mTOR inhibition prevents epithelial stem cell senescence and protects from radiation-induced mucositis.* Cell Stem Cell, 2012. **11**(3): p. 401-14.
284. Kaplon, J., et al., *A key role for mitochondrial gatekeeper pyruvate dehydrogenase in oncogene-induced senescence.* Nature, 2013. **498**(7452): p. 109-112.
285. Wilson, L., et al., *Pyruvate induces mitochondrial biogenesis by a PGC-1 alpha-independent mechanism.* Am J Physiol Cell Physiol, 2007. **292**(5): p. C1599-605.
286. Philp, A., et al., *Pyruvate suppresses PGC1alpha expression and substrate utilization despite increased respiratory chain content in C2C12 myotubes.* Am J Physiol Cell Physiol, 2010. **299**(2): p. C240-50.
287. Roche, T.E. and Y. Hiromasa, *Pyruvate dehydrogenase kinase regulatory mechanisms and inhibition in treating diabetes, heart ischemia, and cancer.* Cell Mol Life Sci, 2007. **64**(7-8): p. 830-49.
288. Olenchock, B.A. and M.G. Vander Heiden, *Pyruvate as a pivot point for oncogene-induced senescence.* Cell, 2013. **153**(7): p. 1429-30.
289. Vredeveld, L.C., *Abrogation of BRAFV600E-induced senescence by PI3K pathway activation contributes to melanomagenesis.* Genes Dev., 2012. **26**: p. 1055-1069.
290. Kirkwood, T.B., *Understanding the odd science of aging.* Cell, 2005. **120**(4): p. 437-47.
291. Barzilai, N., et al., *The place of genetics in ageing research.* Nat Rev Genet, 2012. **13**(8): p. 589-94.
292. Kenyon, C., *The plasticity of aging: Insights from long-lived mutants.* Cell, 2005. **120**(4): p. 449-460.
293. Partridge, L., et al., *Ageing in Drosophila: The role of the insulin/Igf and TOR signalling network.* Experimental Gerontology, 2011. **46**(5): p. 376-381.
294. Selman, C., et al., *Evidence for lifespan extension and delayed age-related biomarkers in insulin receptor substrate 1 null mice.* Faseb Journal, 2008. **22**(3): p. 807-818.
295. Selman, C., L. Partridge, and D.J. Withers, *Replication of Extended Lifespan Phenotype in Mice with Deletion of Insulin Receptor Substrate 1.* Plos One, 2011. **6**(1).
296. Stipp, D., *A New Path to Longevity.* Scientific American, 2012. **306**(1): p. 32-39.
297. Cao, K., et al., *Rapamycin Reverses Cellular Phenotypes and Enhances Mutant Protein Clearance in Hutchinson-Gilford Progeria Syndrome Cells.* Science Translational Medicine, 2011. **3**(89).
298. Blagosklonny, M.V., *Aging: ROS or TOR.* Cell Cycle, 2008. **7**(21): p. 3344-54.
299. Bartoletti-Stella, A., et al., *Gamma rays induce a p53-independent mitochondrial biogenesis that is counter-regulated by HIF1 alpha.* Cell Death & Disease, 2013. **4**.
300. Risson, V., et al., *Muscle inactivation of mTOR causes metabolic and dystrophin defects leading to severe myopathy.* Journal of Cell Biology, 2009. **187**(6): p. 859-874.
301. Sonoda, J., et al., *Nuclear receptor ERR alpha and coactivator PGC-1 beta are effectors of IFN-gamma-induced host defense.* Genes Dev, 2007. **21**(15): p. 1909-20.

302. Lelliott, C.J. and A. Vidal-Puig, *PGC-1beta: a co-activator that sets the tone for both basal and stress-stimulated mitochondrial activity.* Adv Exp Med Biol, 2009. **646**: p. 133-9.
303. Ungar, L., et al., *Tor complex 1 controls telomere length by affecting the level of Ku.* Curr Biol, 2011. **21**(24): p. 2115-20.
304. Schonbrun, M., et al., *TOR complex 2 controls gene silencing, telomere length maintenance, and survival under DNA-damaging conditions.* Mol Cell Biol, 2009. **29**(16): p. 4584-94.
305. Schieke, S.M., J.P. McCoy, Jr., and T. Finkel, *Coordination of mitochondrial bioenergetics with G1 phase cell cycle progression.* Cell Cycle, 2008. **7**(12): p. 1782-7.
306. Houtkooper, R.H., et al., *Mitonuclear protein imbalance as a conserved longevity mechanism.* Nature, 2013. **497**(7450): p. 451-7.
307. Fok, W.C., et al., *Mice fed rapamycin have an increase in lifespan associated with major changes in the liver transcriptome.* PLoS One, 2014. **9**(1): p. e83988.
308. Lamming, D.W. and D.M. Sabatini, *A Central role for mTOR in lipid homeostasis.* Cell Metab, 2013. **18**(4): p. 465-9.
309. Yecies, J.L., et al., *Akt stimulates hepatic SREBP1c and lipogenesis through parallel mTORC1-dependent and independent pathways.* Cell Metab, 2011. **14**(1): p. 21-32.
310. Umemura, A., et al., *Liver damage, inflammation, and enhanced tumorigenesis after persistent mTORC1 inhibition.* Cell Metab, 2014. **20**(1): p. 133-44.
311. Suram, A., et al., *Oncogene-induced telomere dysfunction enforces cellular senescence in human cancer precursor lesions.* Embo J, 2012. **31**(13): p. 2839-2851.
312. Vazquez, F., et al., *PGC1alpha expression defines a subset of human melanoma tumors with increased mitochondrial capacity and resistance to oxidative stress.* Cancer Cell, 2013. **23**(3): p. 287-301.
313. Bhalla, K., et al., *PGC1alpha promotes tumor growth by inducing gene expression programs supporting lipogenesis.* Cancer Res, 2011. **71**(21): p. 6888-98.

## CONTRIBUTIONS

| FIGURE | | DESCRIPTION |
|---|---|---|
| **3.1** | | FM |
| **3.2** | **a-e** | GH |
| | **f-g** | FM prepared the samples, JM conducted ChIP |
| **3.3** | **a-d** | FM prepared the samples |
| | **a-c** | GH conducted Immuno-FISH |
| | **d** | RA conducted Ki67 staining and Sen-β-Gal assay |
| **3.4** | **a-f** | FM prepared, conducted and analysed jointly with JP life-cell imaging experiment (d-f) |
| | **a-c** | GH conducted Immuno-FISH |
| **3.5** | | DJ conducted Immuno-FISH in liver and gut, FM imaged Immuno-FISH and analysed together with JP, DJ and CM Immuno-FISH experiment. |
| **4.1** | | FM |
| **4.2** | **a** | FM prepared the WB samples, GH ran the WB |
| | **b-e** | FM |
| **4.3** | | FM |
| **4.4** | | FM |
| **4.5** | **a** | FM transfected and analysed cell size |
| | **b** | BC prepared samples and ran WB |
| | **c** | FM transfected cells, did and analysed Ki67 staining |
| | **d** | BC prepared samples and ran WB |

| | | |
|---|---|---|
| | **e** | FM transfected cells, did and analysed 53BP1 staining |
| | **f** | FM transfected cells, did and analysed Sen-β-Gal |
| **4.6** | | FM |
| **4.7** | **a** | FM cultured and NAO stained the majority of the cell lines depicted. GH cultured Hela and did NAO staining. RA treated MRC5 with $H_2O_2$, NCS and Etoposite and did NAO staining. FM and JP ran all samples by Flow Cytometry. |
| | **b** | RA |
| | **c** | FM |
| | **d** | MC conducted TEM, JP analysed experiment |
| | **e** | FM |
| | **f** | JP |
| **4.8** | **a** | as stated in 4.7a |
| | **b** | FM |
| | **c** | as stated in 5.1d |
| | **d** | FM prepared samples, LG ran RT-PCR |
| | **e** | FM |
| | **f** | FM |
| | **g** | FM |
| **4.9** | | FM |
| **4.10** | **a** | VK conducted WB, GH did LC-3 staining |
| | **b-c** | FM |

| | | |
|---|---|---|
| **4.11** | **a** | FM prepared and ran WB (right), MC did RT-PCR (left) |
| | **b** | FM |
| | **c** | MC did RT-PCR |
| **4.12** | **a-b** | FM |
| | **c** | FM prepared samples, CM ran RT-PCR |
| **4.13** | | FM |
| **4.14** | **a-b** | FM |
| | **c** | FM prepared samples, DJ ran RT-PCR |
| **4.15** | | FM |
| **4.16** | | FM |
| **4.17** | | FM |
| **4.18** | | FM |
| | **a** | FM prepared sample, BC ran WB |
| **5.1** | | FM designed, co-conducted and supervised TS in all experimental procedures |
| **5.2** | | |
| **5.3** | | |
| **6.1** | **a** | FM |
| | **b** | FM |
| | **c** | FM |
| | **d** | FM and VK |
| | **e** | FM (Sen-β-Gal assay and p21 WB on livers treated with rapamycin), CM p21 WB on 3 and 12 months old mice |

| | | |
|---|---|---|
| | **f** | CM did Immuno-FISH in liver, FM imaged al Immuno-FISH, FM and CM analysed Immuno-FISH |
| | **g** | SM did respiration assay, CM prepared TEM, FM analysed all TEM and RA ran mtDNA copy number assay |
| | **h** | FM ran WB on PGC-1β on liver from rapamycin fed animals, CM ran WB on 3 and 12 months old mice and MnSOD on mice treated with rapamycin |
| **6.2** | **a** | FM and SRC |
| | **b** | FM and SRC |
| | **c** | FM obtained the samples, RA ran mtDNA copy number assay |
| | **d** | FM obtained the samples, CM performed staning |
| | **e** | FM obtained the samples and CM performed Immuno-FISH, FM imaged and analysed all Imunno-FISH |
| | **f** | CM |
| | **g** | CM |
| | **h** | RA |
| | **i** | DJ |
| **6.3** | **a** | CM performed TEM; FM analysed lipid vesicles within hepatocytes |
| | **b** | FM |

FM – Francisco Marques, GH – Graeme Hewitt, RA – Rhys Anderson, CM – Clara Melo, BC – Bernadette Carroll, TS – Thanet Sornda, MC – Michelle Charles, DJ – Diana Jurk, SM – Satomi Miwa, SRC – Sergio Rodriguez-Cuenca, JM – Jelena Mann, LG – Laura Greaves, VK – Viktor Korolchuk, JP – João Passos

## ANEXES

## ANNEX 1.

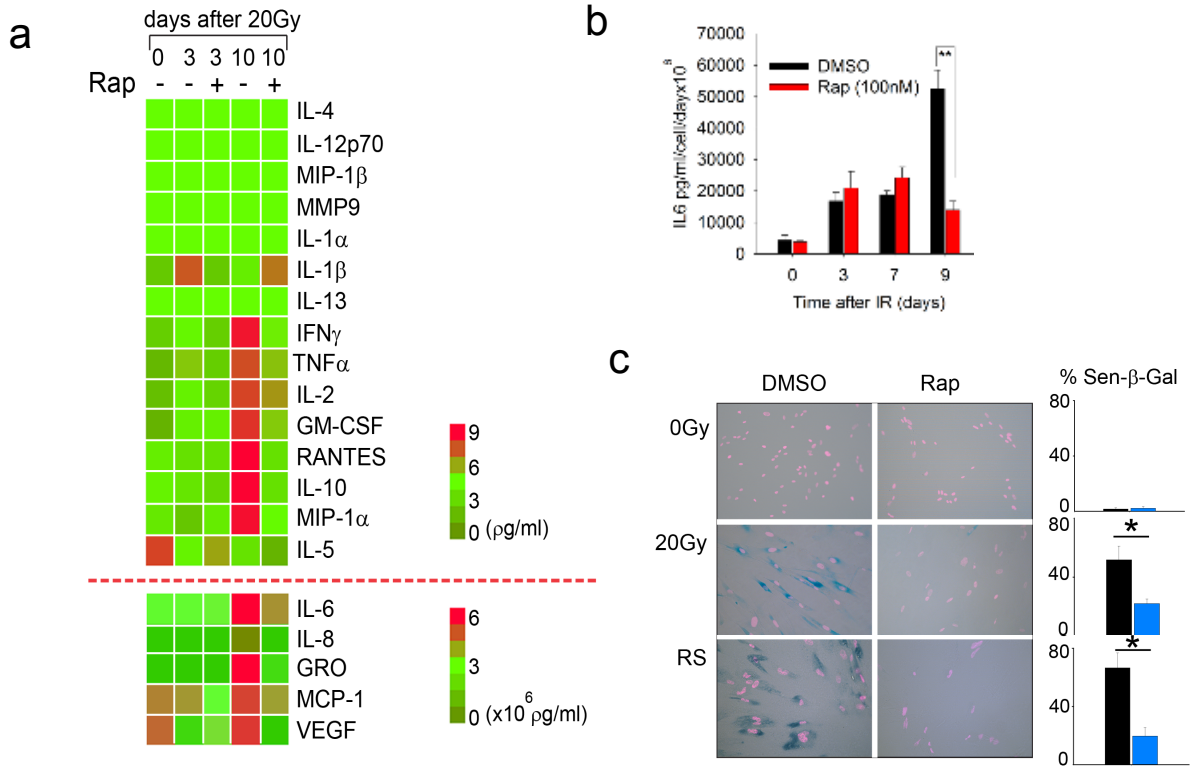


**a)** secreted protein array of a variety of SASP components following X-ray induced senescence with or without rapamycin treatment in MRC5 fibroblasts (3 and 10 days after 20Gy). Data are mean of 3 independent experiments**;**

**b)** inflammatory IL-6 protein levels measured by ELISA on stress-induced senescent MRC5 cells. Levels were 5-fold decreased after nine days upon rapamycin treatment;

**c)** representative images of Sen-β-Gal activity (Sen-β-Gal–cytoplasmic blue; nucleus-pink) with or without rapamycin treatment in MRC5 fibroblast induced to senescence using X-ray irradiation and replicatively senescent MRC5 (RS) (scale bar=40mm), (right) quantification of Sen-β-Gal positive cells. Data are mean±S.E.M, n=10 randomly analysed fields (at least 150 cells were analysed per condition); Data generated by Rhys Anderson, Alina Merz and Clara Melo.

d

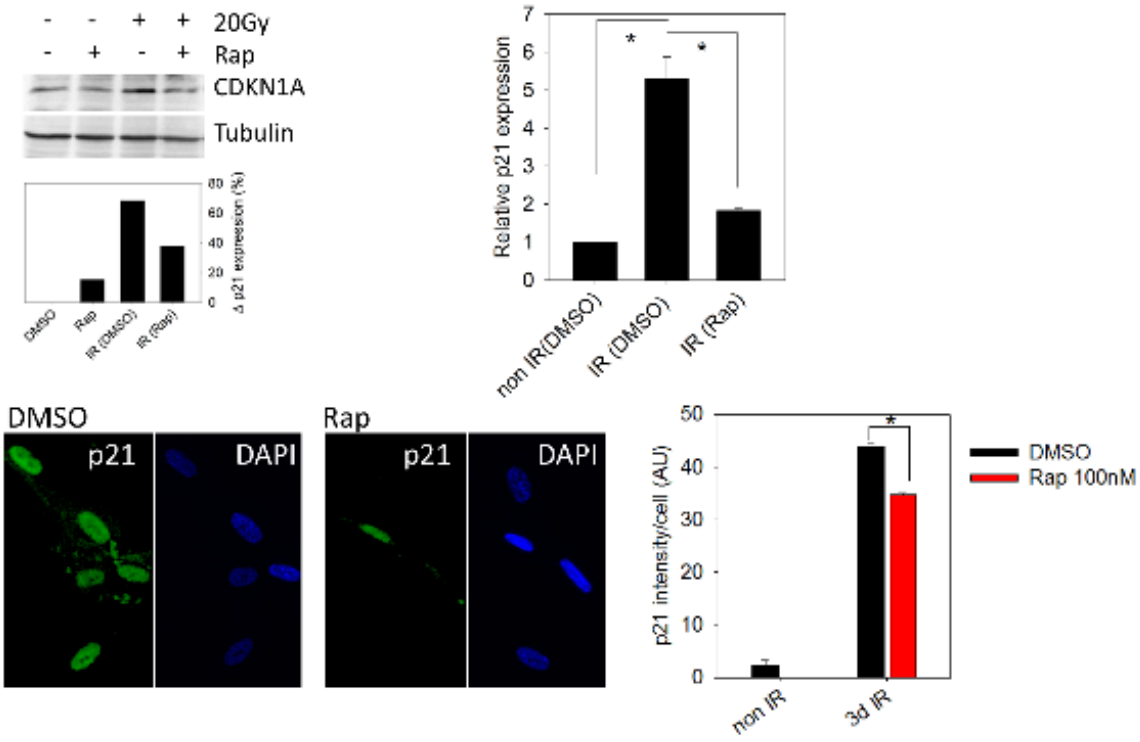


**d)** p21 protein levels on MRC5 fibroblasts 3 days after 20Gy treated with rapamycin (top left); p21 mRNA levels on MRC5 fibroblasts 3 days after 20Gy treated with rapamycin (top right); representative images and quantification of p21 IF staining (green) on MRC5 fibroblasts 3 days after 20Gy treated with or without rapamycin. Data generated by Alina Merz.

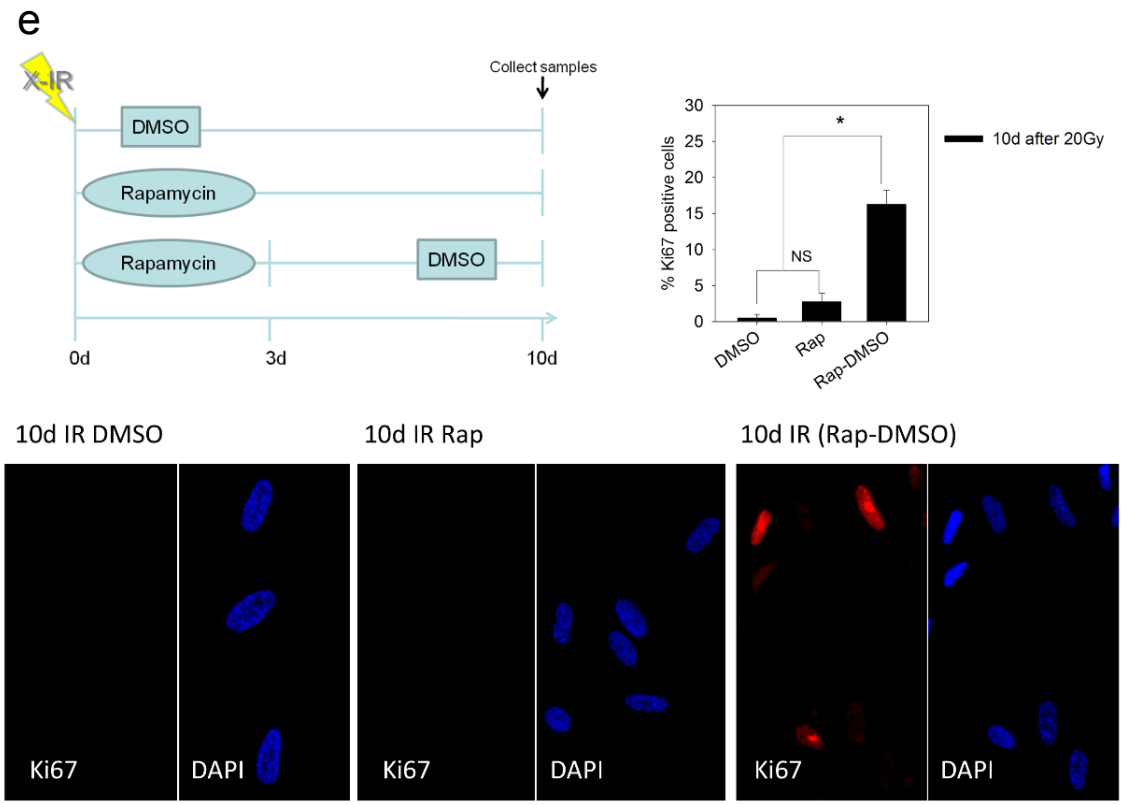


**e)** Experimental design (top left) - MRC5 were X-ray irradiated with 20Gy were treated with or without rapamycin. Cells under DMSO for 10 days were used as negative control. Two rapamycin treatments were performed: in the first rapamycin was kept and replaced daily until sample collection at day 10; the second in which rapamycin was kept for the first three days following X-ray irradiation and then media was replaced by DMSO until day of collection. Cellular proliferation (Ki7 staining) quantification and representative images (top right and below). Short-term mTOR inhibition by rapamycin and consequent release leads either to a prevention of cell cycle arrest or, allows cells to resume proliferation post 20Gy. This might indicate that inhibition of mTOR immediately after senescence induction by X-ray radiation may control initial events that lead to a permanent cell cycle arrest. Data generated by Alina Merz.

## ANNEX 2.

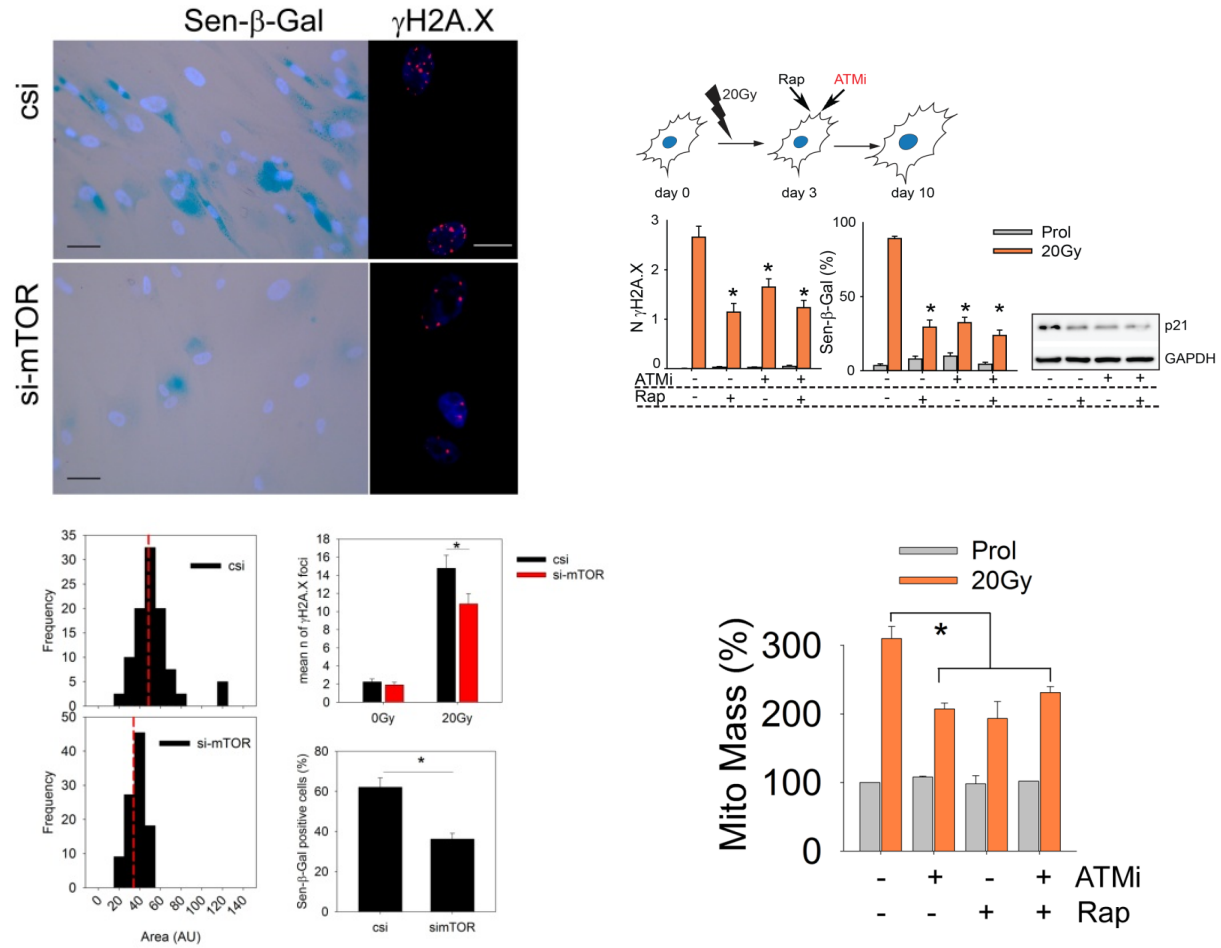


(left) MRC5 in which the mTOR kinase was silenced by siRNA have reduced γH2A.X damage foci and only a small fraction of cells are positive for Sen-β-Gal activity when compared to control siRNA (csi). Cells were analysed 10 days post 20Gy X-ray radiation. Additionally, mTOR siRNA treated MRC5 are smaller than control siRNA treated cells; (right) ATM inhibitor 10μM (Ku55933) and rapamycin (100nM) had non-additive effects on mean number of DNA damage foci, p21 expression and induction of Sen-β-Gal on MRC5 irradiated with 20Gy; (bottom right) mitochondrial mass measured by NAO staining is reduced in MRC5 cells treated with rapamycin or ATM inhibitor. No cumulative effects were observed when both drugs are used suggestion that mitochondrial mass is being controlled by this pathway in a non-cumulative manner. Data generated by Rhys Anderson.

## ACHIEVEMETNS DURING THE PhD

### TEACHING

Demonstrator - Faculty of Medical Sciences - Newcastle University, Newcastle upon Tyne, United Kingdom
2011 - 2014

### PEER-REVIEWED PUBLICATIONS

1. Graeme Hewitt*, Diana Jurk*, **Francisco D.M. Marques***, Clara Correia-Melo, Timothy Hardy, Agata Gackowska, Rhys Anderson, Morgan Taschuk, Jelena Mann & João F. Passos, ***Telomeres are favoured targets of a persistent DNA damage response in ageing and stress-induced senescence***. *Nature Commun.* 3, 708 (2012) - *First co-author. Impact Factor =10.02; total citations [between 34-44, May 2014].

2. Clara Correia-Melo, **Francisco D.M. Marques**, Rhys Anderson, Graeme Hewitt, Alina Merz, Michael D. Rushton, Bernadette M. Carroll, Michelle Charles, Diana Jurk, Stephen W.G. Tait, Glyn Nelson, James Wordsworth, Satomi Miwa, Antje Thien, Kathrin Thedieck, Fiona Oakley, Rafal Czapiewski, Jodie Birch, Mohammad Bohlooly-Y, Antonio Vidal-Puig, Sergio Rodriguez-Cuenca, Derek Mann, Gabriele Saretzki, Thomas von Zglinicki, Viktor I. Korolchuk and João F. Passos, ***Mitochondria are required for the induction of the senescent phenotype*****.** Under revision on Cell Metabolism, Impact Factor = 16.747

3. Jodie Birch, Rhys K. Anderson, Clara Correia-Melo, Diana Jurk, Graeme Hewitt, **Francisco Madeira Marques**, Nicola J. Green, Elizabeth Moisey, Mark A. Birrell, Maria G. Belvisi, Fiona Black, John J. Taylor, Andrew J. Fisher, Anthony De Soyza, João F. Passos. ***DNA damage response at telomeres contributes to lung ageing and chronic obstructive pulmonary disease***. Under revision in *Thorax.* Impact Factor =8.562

4. **Francisco D.M. Marques**, João F. Passos. ***Mitochondria and the DDR: a moTOR of senescence?*** Review (under preparation).

**CONFERENCES, MEETINGS, SYMPOSIUMS, WORKSHOPS AND RESEARCH SEMINARS**

- "Applying for Fellowships" workshop - Faculty of Medical Sciences Graduate School – Newcastle University, Newcastle upon Tyne, UK, 16th May 2014
- Institute of Ageing & Health and Northern Institute of Cancer Research (IAH/NICR) Joint Postgraduate Research Day, Newcastle University, Newcastle upon Tyne, UK, 7th March 2014
- 4th Alliance for Healthy Aging Symposium – Molecular mechanisms of Age-related multi Morbidity, Groningen, The Netherlands, 7th-9th November 2013
- "Introduction to Learning and Teaching in Higher Education – ITLHE part A course" – Staff Development Unit – Newcastle University, Newcastle upon Tyne, UK, 29th and 30th October 2013
- Faculty of Medical Sciences Research Symposium on the Biology of Ageing, Newcastle University, Newcastle upon Tyne UK, 5th and 6th September 2013
- Cell Senescence in Cancer and Ageing - Wellcome Trust Scientific Conference, Cambridge, UK, 20th-23th July 2013
- Biochemical Society Focused Meeting: Talks about TORCs: recent advances in target of rapamycin signalling, Charles Darwin House, London, UK, 14th and 15th March 2013
- Institute of Ageing & Health and Institute of Genetic Medicine (IAH/IGM) Joint Postgraduate Research Day, Newcastle University, Newcastle upon Tyne, UK, 25th January 2013
- Ageing and Basic Bioscience Conference (ABBC), Babraham Institute, Babraham Research Campus, Cambridge University, Cambridge, UK, 20th and 21st September 2012
- Gordon Research Conference (GRC) on Biology of Aging, Ventura, California, USA, 12th-17th February 2012
- Gordon Research Seminar (GRS) on Biology of Aging, Ventura, California, USA, 11th and 12th February 2012
- Institute of Ageing & Health and Institute of Health & Society (IAH/IHS) Joint Postgraduate Research Day, Newcastle University, Newcastle upon Tyne, UK, 27th January 2012

**POSTER PRESENTATION**

- "Increased mitochondrial density drives and maintains cellular senescence *in vivo* and *in vitro*" - Institute of Ageing & Health and Northern Institute of Cancer Research (IAH/NICR) Joint Postgraduate Research Day, Newcastle University, Newcastle upon Tyne, UK, 7th March 2014
- "Increased mitochondrial density drives and maintains cellular senescence *in vivo* and *in vitro*" - 4e Alliance for Healthy Aging Symposium – Molecular mechanisms of Age-related multi Morbidity, Groningen, The Netherlands, 7th-9th November 2013
- "*mTOR-dependent mitochondrial biogenesis drives the senescent phenotype*" - Biochemical Society Focused Meeting: Talks about TORCs: recent advances in target of rapamycin signalling - Charles Darwin House, London, UK, 14th and 15th March 2013
- "*mTOR-dependent mitochondrial biogenesis drives the senescent phenotype*" - Ageing and Basic Bioscience Conference (ABBC), Babraham Institute, Babraham Research Campus, Cambridge University, Cambridge, UK, 20th and 21st September 2012
- "*Telomeres are favoured targets of a persistent DNA damage response in ageing and stress-induced senescence*" - Gordon Research Conference (GRC) on Biology of Aging, Ventura, California, USA, 12th-17th February 2012
- "*Telomeres are favoured targets of a persistent DNA damage response in ageing and stress-induced senescence*" - Gordon Research Seminar (GRS) on Biology of Aging, Ventura, California, USA, 11th and 12th February 2012

**ORAL PRESENTATION**

*"Increased mitochondrial density drives and maintains cellular senescence in vivo and in vitro"* - Senescence Symposium 2014 – Blizard Institute – Barts and the London School of Medicine and Dentistry - Queen Mary university, London, UK, 30th October 2014

- Research seminar on the "Biology of Ageing" (BMS2014) module – Faculty of Medical Sciences – School of Biomedical Sciences, Newcastle upon Tyne UK, 25th March 2014
- *"Mitochondrial hypertrophy drives and sustains a DNA damage response during senescence"* - Faculty of Medical Sciences Research Symposium on the Biology of Ageing, Newcastle University, Newcastle upon Tyne UK, 5th and 6th

September 2013

- *"Increased mitochondrial density drives and maintains cellular senescence in vivo and in vitro"* - Cell Senescence in Cancer and Ageing - Wellcome Trust Scientific Conference, Cambridge, UK, 20th-23th July 2013
- *"mTOR-dependent mitochondrial biogenesis drives the senescent phenotype"* - Institute of Ageing & Health and Institute of Genetic Medicine (IAH-IGM) Joint Postgraduate Research Day, Newcastle University, Newcastle upon Tyne, UK, 25th January 2013
- "*Only telomeres trigger a persistent DNA damage response in stress-induced senescence and during ageing*" - Institute of Ageing & Health and Institute of Health & Society (IAH-IAS) Joint Postgraduate Research Day, Newcastle University, Newcastle upon Tyne, UK, 27th January 2012

**AWARDS AND BURSARIES**

- Biochemical Society Student Bursary - "*mTOR-dependent mitochondrial biogenesis drives the senescent phenotype*" - Biochemical Society Focused Meeting: Talks about TORCs: recent advances in target of rapamycin signalling, Charles Darwin House, London, UK, 14th and 15th March 2013
- Best Oral Presentation prize: *"mTOR-dependent mitochondrial biogenesis drives the senescent phenotype"* - Institute of Ageing & Health and Institute of Genetic Medicine (IAH-IGM) Joint Postgraduate Research Day, Newcastle University, Newcastle upon Tyne, UK, 25th January 2013
- Faculty of Medical Sciences – Newcastle University Travel Grant – 2012

**SUPERVISION**

- Master Research student: Mr. Thanet Sornda – 'Does pyruvate induce cellular senescence via mitochondrial dysfunction, ROS and the mTOR pathway?' - February - August 2013 – MRes poster prize and current PhD student at Dr. David Gems lab at UCL, UK
- Undergraduate student: Miss Ellen Milner – 'The Potential role of OGG1 in DNA single stranded break repair in senescence' - January - March 2012

**PROFESSIONAL MEMBERSHIPS**

Member, Biochemical Society 2012- present

Member, International Cell Senescence Association 2013 - present